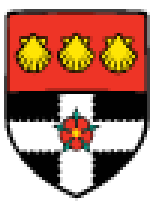

University of Reading

Production of nanoparticles with Beta lactoglobulin and whey proteins for the encapsulation of food ingredients

A thesis submitted as a partial fulfilment of the degree of Doctor of Philosophy

Yuchen Guo

Department of Food and Nutritional Science

Reading, UK

August 2017

To my parents

Declaration of original authorship

I confirm that this is my own work and the use of all material from other sources has been properly and fully acknowledged.

Yuchen GUO
Reading, UK
August 2017

ABSTRACT

Nutraceuticals face significant challenges in delivery due to poor solubility of some bioactives, and instability during processing. The major whey protein in bovine milk, ß-lactoglobulin (ß-Lg), has versatile properties and the potential for the development of novel delivery vehicles for bioactives. The aim of this study is to develop a solid and reproducible method to produce ß-Lg nanoparticles and investigate their application to the encapsulation of bioactives. Temperature and pH were found to be the key operating parameters to produce and control the size of nanoparticles. Monodisperse and spherical ß-Lg nanoparticles in the size range of 200-300 nm were produced at optimum conditions of pH (6.0) and heat load (heating incubation 75 °C for 45 mins). ß-Lg nanoparticles exhibited high colloidal stability (zeta potential: -37.42 mV) and high yield of aggregation (93%). The hydrogen bonding and hydrophobic interactions played a predominant role in the microstructure of these nanoparticles. Caffeine was bound to these nanoparticles with 13.54% as maximum encapsulation efficiency at 50:1 molecular ratio and the binding followed a Langmuir type isotherm. Only partial release of caffeine happened at gastric conditions (about 36%) whilst total release happened at intestinal conditions. Also, resveratrol-ß-Lg nanoparticles were produced at 181.8 nm using this method. Heat degradation and isomerisation of resveratrol occurred when heating at 75°C which led to reduced antioxidant activity. Resveratrol-beta-lactoglobulin nanoparticles exhibited an ability to improve antioxidant activity at this temperature and at pasteurisation condition. Lastly, whey protein nanoparticles could be produced following the same method with smaller size and lower yield of aggregation. Further

studies should be carried out to explore other applications of ß-Lg/whey protein nanoparticles as a novel nanovehicle of bioactives in food products.

ACKNOWLEDGEMENT

At this moment, I would like to thank many people who help me to go through the tough time and finish my PhD and this Thesis

First and foremost, I would like to express my gratitude and appreciation to my supervisor, Dr Paula Jauregi for her guidance, patience, and encouragement throughout the completion of my PhD. It is my honour to be a member of her research group. I found motivation and inspiration in discussions and meetings with her throughout this study. Moreover, I am very thankful for her care and concern about my life. She helps me to build confidence to live in the UK as for foreigner.

I would like to thank Professor Lorenzo, Professor Dimitris Charalampopoulos and Dr Qiaofen Cheng for their help and encouragement and Chris for his teaching and support of HPLC.

I would like to thank Dr Peter Harris and Amanpreet Kaur for their assistance in use of the Environmental Scanning Electron Microscopy. Their patience and guidance helped me to finish my work.

I would like to thank my dear colleagues Esereosa Dilenu Ama Otiwa Omoarukhe, and Nurmahani Binti MohdMaidin. You two accompany me for the whole PhD life, and you are like two older sisters who are always there to support me. Also, I appreciate Dr.Olatujoye Jumoke Bukola, Dr Khairul Paee, Cristiano, Natalia, Ignacio and all other friends in the department.

I would like to thank my dear friends: Xuan Wei, Haokun Wang, Xi Rui Zhou, Qianting

Sun, Fei Xu, Yaoqi Fu, Fei Lu, and Ning Wei. You are amazing.

Lastly, I would like to express my appreciation to my entire family for their love and care. With their support, I can finish this work. I would like to thank my older brother Rui Ren and her wife Yi Ru for their companionship and love. Above all, I would like to thank my parents for their care and education.

CONTENTS

LIST OF FIGURES

LIST OF TABLES

PUBLICATION

1. Guo, Y., Harris, P., Kaur, A., Pastrana, L., & Jauregi, P. (2017). Characterisation of ß-lactoglobulin nanoparticles and their binding to caffeine. *Food Chemistry, 71*(2017), 85-93.

CHAPTER ONE

Introduction and Literature reviews

1.1. Introduction

Whey is the main by-product of cheese manufacturing and the dispose of whey as food waste contributes to a high volume high Chemical Oxygen Demand (COD) and Biochemical Oxygen Demand (BOD) values, hence it has a potentially harmful environmental effect (Brião & Tavares, 2007; Siso, 1996; Worldbankgroup, 2007). However, whey contains 20% of the total protein of bovine milk, and it is an essential food ingredient, which provides versatile nutritional value and functional properties. Therefore, whey and whey proteins are widely used as food ingredient including formulated milk powder, animal feed and agricultural fertiliser (Ramos et al., 2017; Siso, 1996). Main proteins in whey are ß-lactoglobulin, α-Lactalbumin, Bovine Serum Albumin (BSA), Lactoferrin, and Immunoglobulin (IgG). ß-lactoglobulin accounts for over 50% and as a member of lipocalin family, the core function of ß-lactoglobulin is to transport the retinol molecules, and other hydrophobic compounds (Yoav D. Livney, 2010) and this function has attracted the attention of food scientists among others. Since the start of the 21st century, ß-lactoglobulin and whey proteins have been widely studied as carrier or vehicles of bioactive compounds, and numerous candidates of nutraceuticals including vitamins, fatty acids, carotenoids, polyphenols and some antimicrobial and other functional bioactives have been investigated. (Castroa et al., 2017; Jia, Dumontn, & Orsat, 2016; Yoav D. Livney, 2010; Nicolai, Britten, & Schmitt, 2011; Shafaei et al., 2017).

There are different approaches delivering selected bioactives including gels, emulsions and microparticles. With the development of technology, the nanostructures of whey proteins including nanofibrils, nanoparticles, nanotubes are interesting emerging approaches for the delivery of bioactives (Tavares et al., 2014). These nanostructures can offer advantages in the improvement of solubility, bioavailability, and control release of nutraceuticals at specific points in the gastric-intestinal tract. (GI-tract) (Chen, Remondetto, & Subirade, 2006; Kontopidis, Holt, & Sawyer, 2004; Shpigelman, Israeli, & Livney, 2010b). Therefore, it is interesting to establish an easy and reproducible method to produce ß-lactoglobulin nanoparticles and to study their application for encapsulation of selected bioactives.

In previous work carried out by our group, the heat-induced denaturation method was preliminarily investigated to produce ß-lactoglobulin nanoparticles. This was continued in the present work in order to achieve a robust and reproducible method to produce ß-lactoglobulin nanoparticles. In chapter two, the investigation focused on the identification of the key parameters to produce ß-lactoglobulin nanoparticles and their influence on size; these parameters were: pH, temperature and the heating incubation time.

The characteristics of the nanoparticles were determined by a range of methods. Then, caffeine, as the model molecule was chosen to be encapsulated by ß-lactoglobulin nanoparticles to study the encapsulation efficiency and their stability to simulated gastrointestinal conditions. In chapter three, resveratrol, a natural antioxidant, was chosen to be encapsulated to investigate the protective function of ß-lactoglobulin

nanoparticles. It is important to explore the interactions between ß-lactoglobulin and these bioactive molecules, the properties of these complexes and their effect on solubility, stability, bioavailability or control release of these bioactives. Moreover, in chapter four, the stability of ß-lactoglobulin nanoparticles under different types of processing conditions was investigated. Furthermore, the method developed here to produce nanoparticles with ß-lactoglobulin was applied to whey. In chapter five, the conclusion of this study and the suggestions for future work has been made.

1.2. Literature review

1.2.1. Nutraceuticals and food applications

In 1989, the definition of “Nutraceutical” was given by DeFelice, the chairman of Foundation for Innovation in Medicine. It was defined as hybrid or contraction of nutrition and pharmaceutical. Since then, food manufacturers and the scientific community were interested in the relationship between diet and health. Nutraceutical was defined in detail in 1994 as “any substance that may be considered a food or part of a food and provides medical or health benefits, including the prevention and treatment of disease. Such products may range from isolated nutrients, dietary, supplements and diets to genetically engineered “designer” foods, herbal products and processed foods such as cereals, soup and beverage” (DeFelice, 1994). Partly due to advances in technology and the internet, “nutraceutical” becomes a high-frequency word in articles, journals, and web pages and therefore reaches the public life. As chronical diseases including obesity, heart diseases, cancers and arthritis start to affect a large fraction of the ageing population, people start paying attention to functional foods which may have the ability to prevent disease and bring health benefits through diet (Wildman & Kelley, 2006). However, the fact is that in 1992, the American market of nutraceutical was only around $10 billion which accounted for a small fraction of the retail food market ($504 billion) (DeFelice, 1994). In 2010, this figure reached $140.1 billion, and the annual average growth rate was 14.3% which was double this number in 1999 (FICCI, 2010).

Over last two decades, a large number of food products with added nutraceuticals have been developed such as calcium-enriched bread, fortified cereals, and β-carotene-

enriched rice and soybean. Most of the nutraceuticals are found the origin to treat or prevent various diseases in the plant since many plants produce the constituents to defend themselves from infection. These constituents may have the same function to human infection (Rajat, Manisha, Robin, & Sunil, 2012)

Common nutraceuticals include antioxidants, phenolic compounds, polyunsaturated fatty acid and probiotics and prebiotics. Some nutraceuticals suffer the limitation of intake. This is partly due to poor effectiveness of oral administration of antioxidants and polyunsaturated fatty acids. Some may be influenced by the low pH in the stomach and gastrointestinal conditions. In general, a small portion of these nutraceuticals can achieve high bioavailability in the human body (Chen *et al,* 2006). Flavour aspect is another limitation since some nutraceuticals may bring unpleasant flavour to the product. For example, caffeine brings bitter flavour sometimes unpleasant mouth feeling when the concentration is over 0.5 mmol/L (Drewnowski, 2001).

1.2.2. Encapsulation and Nanotechnology in Food Science

Due to the limitations above, the idea of “protection” of nutraceutical is necessary to be studied to improve stability, solubility, bioavailability or other health benefit properties of nutraceutical. Over last several decades, encapsulation has become one of the options. Encapsulation can be explained as coating one compound with another. At the molecular level, it can be understood as the confinement of small molecule within a larger molecule or smaller particles adhering to the larger particles. Capsules in pharmaceutical applications were the first developments in encapsulation, and it has over hundred

year's history. Most of the capsules are gelatins or polymers from cellulose. Other options are the use of hydrogel, which is a water-swollen network of hydrophilic polymer. When it comes to food, capsules are not a good choice. Low nutrition value is one of the weaknesses, and these capsules do not meet the food safety requirement known as Generally Recognized as Safe (GRAS) as defined by U.S. food and drug administration (Burdock, Carabin, & Griffiths, 2006). For food applications, it is necessary to investigate alternative encapsulants and methods, which meet the GRAS classification, and it will be another health benefit if encapsulants have some nutritional values.

In food science, encapsulation is a process to entrap one substance (active compounds) in another, which may be called carrier material, matrix, wall material, coating, shell or a membrane (Augustin & Oliver, 2012; Nedovic, Kalusevic, Manojlovic, Levic, & Bugarski, 2011). Different encapsulation methods have been extensively researched and been used in the food industry including spray drying/ chilling extrusion, fluidised bed cocrystallization *etc.* (Tavares et al., 2014). Based on the materials and procedures, it has a simple structure (homogeneous) or complex structure (heterogeneous) which are schematically described in Figure 1.1 (McClements, 2012).

Figure 1.1: Examples of different kinds of structural organisation of possible encapsulation within delivery systems (The combination represents using both core-shell and dispersion approaches).(McClements, 2012).

Polysaccharides like starch, cellulose and their derivate and plant exudates and extracts are the most widely used encapsulants in the food industry (Nedovic et al., 2011) and protein is also considered as a good option, especially milk proteins, which have high nutritional value and are generally recognised as safe (Dickinson, 2003; Wang, Bamdad, Song, & Chen, 2012). Many studies have been conducted with milk proteins including casein micelle and whey proteins such as, β-lactoglobulin and α-lactalbumin. Also, lipids can be utilised as encapsulants and for transportation of nutraceutical. Some combinations of biopolymers have also been investigated such as chitosan/β-lactoglobulin core-shell (Lingyun Chen & Muriel Subirade, 2005), and alginate–milk microspheres (Shi et al., 2013).

Nanomaterials are defined by food and drug administration of the USA as particles with dimensions less than micrometre scale that exhibit unique properties (FDA, 2006). The same recommendation from Science and Technology committee in 2010 pointed out that rather than size limitation of 100nm, all materials with a dimension under 1000nm are considered especially in novel food regulation (Science and Technology Committee,

2010), but there is an emphasis on size (400nm) of nano-size carries, which can act as nano-capsule (Ghalandari, Divsalar, Sabour, & Parivar, 2015). Some food materials can build up nanoscale structure naturally. Like some globular proteins, casein micelle and calcium phosphate from milk, which consist of self-assembled nanostructures in the range of 40nm-600nm (Kruif, 1998). However, most of the biopolymers need to be manipulated to control the size of the particle within the range of nano size. Thus there are two concepts to produce nanostructure: 'top-down structuring', 'bottom-up structuring'. 'Top-down' approach is to break down bulk materials by employing size reduction processes, while the 'bottom up' is basically formation by molecular the self-assembly (Augustin & Oliver, 2012; Chen et al., 2006). These two approaches are shown in Figure 1.2. In detail, homogenization and wet milling are the typical examples of 'top-down' methods and 'bottom-up' procedures use physical phenomena like precipitation or phase separation to form the nano-dispersion (Thies, 2012a, 2012b). The advantages of nanostructure has been emphasised by Chen et al. (2006) and Ramos et al. (2017): 1) improving the bioavailability of poor-soluble nutraceutical compounds; 2) prolonging the residence time in GI-tract, thus, increasing the surface availability of interactions with biological support; 3) Deep penetration into tissues even cells to finish control release. Indeed, there are some concerns from customers about the nanotechnology applications in food products (Kessler, 2011; Siegrist, Cousin, Kastenholz, & Wiek, 2007), therefore, numerous regulations have been established all over the world and some new requirements including new labelling system and safety information, risk assessment are underway (Chau, Wu, & Yen, 2007).

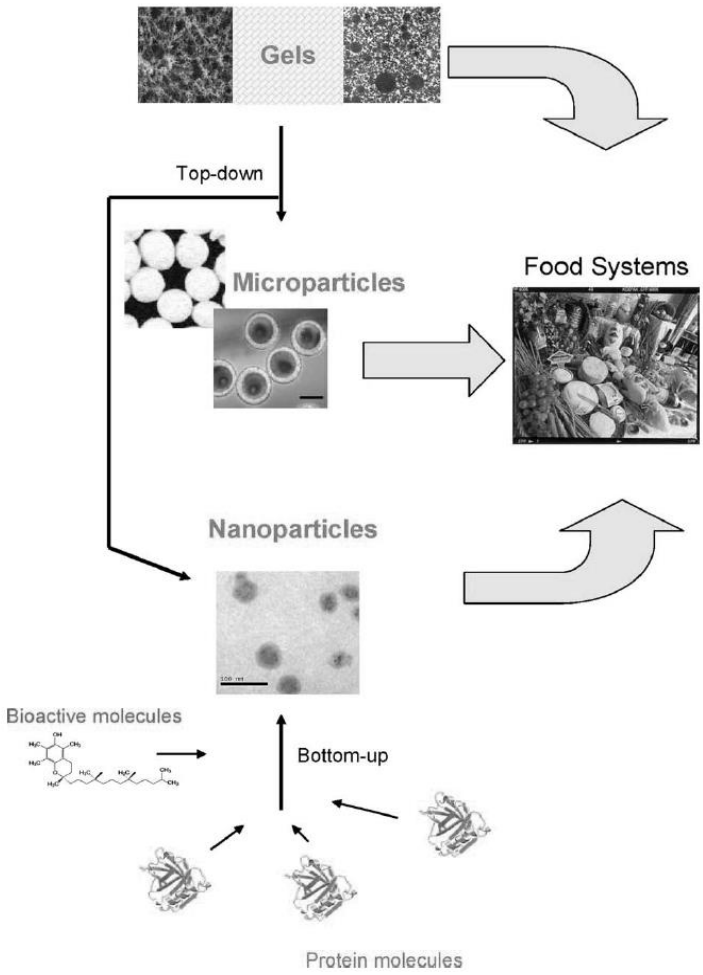

Figure 1.2: Schematic representation of food-protein-based materials as nutraceutical delivery systems (Chen et al., 2006).

Therefore, according to the basic understanding, the theory of encapsulation and methods to build nanostructure, whey protein can be a good candidate for both “Top down” and “bottom up” approaches. The next section will introduce whey protein and β–Lactoglobulin.

1.2.3. Whey protein: composition and functions

After centrifugally separating the cream from milk by traditional fractionation, whey proteins are included in the serum. It is the by-product of cheese making and it remains

in the supernatant after the isoelectric precipitation of the caseins (cheese curd) from skim milk at pH 4.6. Similarly, sweet whey is the by-product of rennet or natural enzyme-produced cheese manufacture at higher pH 6.7 (Yoav D. Livney, 2010). Whey protein concentrates (WPC) are obtained from whey by ultrafiltration, and whey protein isolates (WPI) by subsequent diafiltration or ion exchange, then drying (>85% protein) (Singh & Ye, 2014). Whey protein contributes 20% of milk protein, and the remaining 80% is in casein. Briefly, whey proteins mainly including β–Lactoglobulin (β-Lg), α–Lactalbumin (α-La), Bovine serum albumin (BSA), Immunoglobulin G (IgG) and Lactoferrin (Lf) are shown in Table 1.1.

Table 1.1: The main proteins in milk (Tavares et al., 2014).

Origin	Proteins		Concentration in milk (g/kg)	Molecular weight (kDa)	Isoelectric point
Synthesised in the mammary gland	Casein micelle		26	≈10^5 (100-500nm)	4.6
	Casein fractions	α_{S1}	10.7	23.6	4.9
		α_{S1}	2.8	25.2	5.2
		β	8.6	24	5.4
		K	3.1	19	5.6
From blood	Whey protein	β-Lactoglobulin	3.2	18.3	5.2
		α-Lactalbumin	1.2	14.2	4.3-4.7
		BSA	0.4	66.3	5
		Lactoferrin	0.1	83	8.5

Whey proteins have essential nutritional value and health benefits. First of all, an important role played by whey proteins is that it contains an abundant amount of all

nine essential amino acids. Especially, cysteines present in β–Lactoglobulin are key amino acids for stimulation of glutathione synthase in the liver. Also, a review paper (Markus, Olivier, & Haan, 2002) mentioned that α-Lactalbumin is an abundant source of essential amino acids tryptophan and cysteine. They are the precursors of serotonin and glutathion, which improve the ability to reduce the depressive mood. Similarly, β-Lactoglobulin is the precursor of bioactive peptides with a variety of bioactivities like antihypertensive, antimicrobial, antioxidative, anticarcinogenic etcetera (Castroa et al., 2017; Korhonen, 2009). For example, several studies suggest that bioactive peptides from β-Lactoglobulin have an ability as angiotensin I-converting enzyme (ACE) inhibitor (Chatterton, Smithers, Roupas, & Brodkor, 2006; Ortiz-Chao et al., 2009; Pihlanto-Leppälä, 2001). Table 1.2 shows the major bioactive peptides from the whey protein and their bioactivities.

Table 1.2: The summary of whey protein- derived bioactive peptides (Meisel & Bockelmann, 1999).

Bioactive peptides	Protein precursor	Bioactivity
α-lactorphin	α-Lactalbumin	Opioid against
β-lactorphin	β-Lactoglobulin	Opioid against
Lactoferroxins	Lactoferrin	Opioid antagonist
Lactokinins	α-lactalbumin,β-lactoglobulin, serum albumin	ACE-inhibitory
Lactoferricin	Lactoferrin	Antimicrobial

Unlike intrinsically unstructured casein, whey proteins are typically globular proteins and have various biological functions (Tavares et al., 2014). β-Lactoglobulin, has a structure similar to retinol-binding proteins, which can bind hydrophobic ligands like fatty acids

and vitamins, even though the biological functions of β-Lactoglobulin still remain unclear (L. Sawyer, 2013), but some of the publications indicate that β-Lactoglobulin inhibits the hydrolysis of phosphate by phosphoprotein phosphatases in the spleen (H. M. Farrell & Thompson, 1990). In contrast, α-Lactalbumin has specific functions to the regulatory protein of lactose synthase enzyme system (Brew, 2013). Other minor whey proteins like blood serum albumin (BSA) acts as minerals and hydrophobic molecules transportation role in blood plasma (Gelamo, Silva, Imasato, & Tabak, 2002). Lactoferrin (LF) is an iron-binding glycoprotein which exists not only in milk but other body secretions. Another important role of Lactoferrin is that it can impede iron utilisation by bacteria, thus it has a bacteriostasis function (Lönnerdal & Suzuki, 2013).

1.2.4. Beta-lactoglobulin

As the major whey protein, beta-lactoglobulin is chosen as the main encapsulant in this work. Comprehensive understanding of the molecular structure and conformation of β-lactoglobulin would lead to better choices of processing conditions of nanoparticle preparation and the binding ligands selection. Beta-lactoglobulin is abundant in bovine milk at a concentration 0.2-0.3 g/100 ml (Bell & Mckenzie, 1964; J.Cerbulis & H.M.FarrellJr., 1975; Lindsay Sawyer & Kontopidis, 2000), while it is rare in human milk. It is a member of lipocalin family, which has a similar common structure and exhibits high affinity and selectivity for hydrophobic molecules, especially act as the transporters of retinol (Flower, 1996; Flower, North, & Attwood, 1993; Ganfornina Álvarez, Sánchez Romero, Greene, & Flower, 2006; Kontopidis et al., 2004). Beta-lactoglobulin contains

162 amino acids residues with molecular weight 18.3 kDa including two disulphide bonds (Cys 66–Cys 160 and Cys 106–Cys 119) and a free thiol (Cys 121). There are two genetic variants A and B, which is different in two amino acid residues; Asp 64 and Val 118 in variant A are replaced by Gly and Ala in variant B, respectively (Zsila, Bikádi, & Simonyi, 2002). The structure of beta-lactoglobulin has been one of the important targets of molecular biological science and protein science due to:

1) Large molecular size, so it is a good example to understand the principles of denaturation and aggregation of proteins in this size.

2) Binding ligands, especially small hydrophobic molecules, is another attractive characteristic of beta-lactoglobulin. (Sakurai, Konuma, Yagi, & Goto, 2009)

The schematic graph illustrates the three-dimensional structure and amino acid sequence of beta-lactoglobulin in Figure 1.3 (A) and (B). Several groups use X-ray crystallography and solution nuclear magnetic resonance to carry out the structure studies. Briefly, like other lipocalin, it is made of eight strands of antiparallel β-sheet (A-H blue strands) to wrap round to the central calyx or β-barrel, which is flanked with a three-turn α-helix (between H and G strands) (Edwards, Creamer, & Jameson, 2009; Kontopidis et al., 2004; Papiz et al., 1986; Sakurai et al., 2009). The ninth strand (I strand) plays an important role of the dimer interface at neutral pH (Bewley, Qin, Jameson, Sawyer, & Baker, 1997).

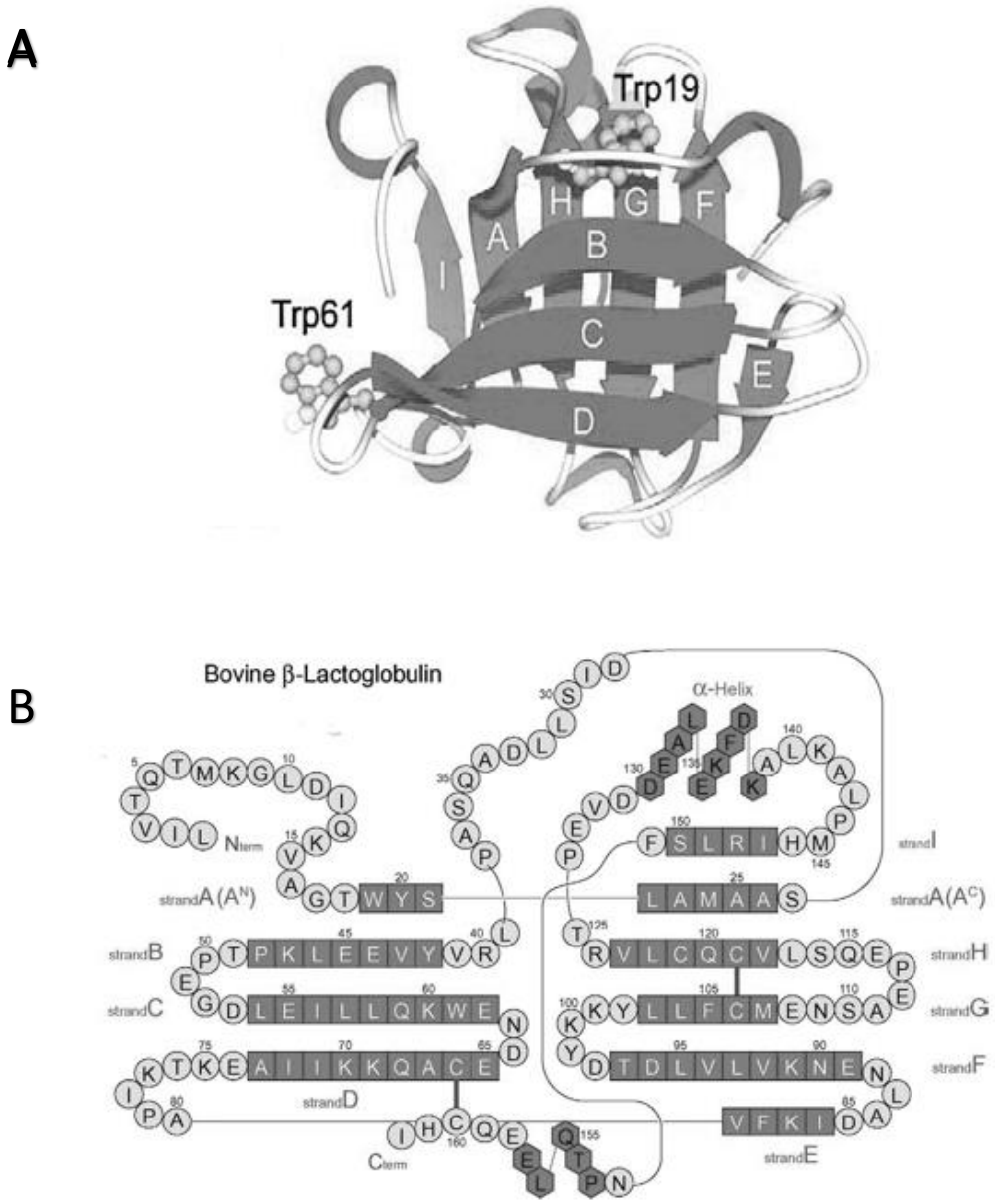

Figure 1.3: The 3D structure and amino acid sequence of bovine beta-lactoglobulin (Sakurai et al., 2009). A: The 3D structure of bovine beta-lactoglobulin, B: the amino acid of bovine β-lactoglobulin.

The connections between open ends AB, CD, EF, and GH is longer and more flexible than closed BC, DE, and FG (Sakurai, 2009). The central calyx surrounded by hydrophobic

residues is the principal main ligand-binding site (Lange, Kothari, Patel, & Patel, 1998; Narayan & Berliner, 1997). Alternatively, some studies suggest that there may be some more binding points at the surface of beta-lactoglobulin but not sufficient proofs of crystallographic data (the second point is located at Trp19, Tyr20, Tyr42, Gln44, Gln59, Gln68, Leu156, Glu157, Glu158 and His161 and third point is located at Tyr102, Leu104, and Asp129) (Shafaei et al., 2017; Yang et al., 2008; Zhang, Liu, Subirade, Zhou, & Liang, 2014; Zsila et al., 2002).

Among various factors influencing the structure of β-lactoglobulin, temperature and pH are the most important parameters that may affect the cross-linking and network among protein molecules.

At neutral conditions, it is believed that β-lactoglobulin exists as a dimer in the aqueous solution. Actually, it can be understood that the native β-lactoglobulin present as an equilibrium of monomers and dimers (J.N.deWit, 2009; Bin Y. Qin et al., 1998; Taulier & Chalikian, 2001). When heating the beta-lactoglobulin solution, the dimer changes to a monomer at elevated temperature (50°C). Continuing heating beta-lactoglobulin will result in an exposure of previous hidden hydrophobic residues and thiol groups. Also, the conformation of native beta-lactoglobulin will change to a “molten-globule state” (de Wit，2009 and Sawyer, 2013). That is the start of the irreversible modifications between 60 and 70 °C. Further heating (65-75°C) will cause some oligomers due to exposure of thiol groups and thiol/thiol oxidation reactions. The large aggregation occurs via disulphide bond and hydrophobic force when the temperature reaches 75°C but below the 100°C. The schematic graph is illustrated in Figure 1.4.

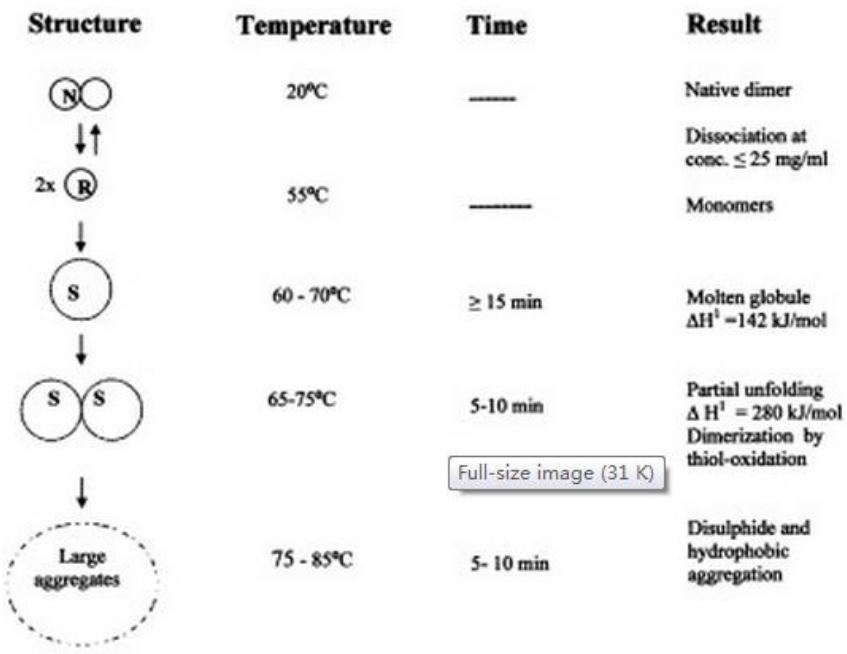

Figure 1.4: The structural changes of β-lactoglobulin by the temperature increasing at neutral pH. (J.N.deWit, 2009).

Moreover, pH is another important factor will affect the conformation and structure of β-lactoglobulin. The isoelectric point (pI) of β-lactoglobulin is around 4.7-5.1 (Edwards et al., 2009; Kontopidis et al., 2004; Sakurai et al., 2009). This is an important pH at which no electrical charge at the surface of the protein. Hence, the closer to its pI, the lower electrical repulsion force. The most famous conformational change is the Tanford transition presented by Tanford, Bunville, and Nozaki (1959), which propose EF-loop close the hydrophobic cavity of the β-barrel of the β-Lg molecule below pH 7 and open the cavity above pH 7 (Sakurai & Goto, 2006). Moreover, a three-step mechanism for the Tanford transition is suggested at pH 6.2, 7.1 and 8.2 due to open or closure E-F loops. Meanwhile, a widely pH study by Taulier and Chalikian (2001) shows more complex structural changes in the range of pH 1 to pH 13: five pH-dependent structural

states including pH 2 transition (pH<2), dimer-to-monomer transition (pH 2.5- pH 4.0), pH 5 transition (pH 4.5- pH 6.0, native form to acidic form), the Tanford transition (pH 6.0- pH 8.0), the base-induced denature (pH>9.0). To emphasise, only pH 5 transition has no significant alteration in the secondary structure of beta-lactoglobulin.

Except for these two factors above, there are still some other factors including the concentration of β-Lg, which determines the total number of disulphide bonds and the chance of protein-protein interactions, and the Ionic strength, which relates more to the types of salt added and addition methods. When producing nanoparticles to encapsulate nutraceutical or bioactive food ingredients, all of these factors are under consideration. Therefore, under different conditions, various structure and conformation changes will result in a complex three-dimensional network of aggregation.

1.2.5. Encapsulation applications of whey protein and ß-lactoglobulin

Whey protein has been considered as an encapsulation matrix to deliver nutraceuticals by using the different structures including hydrogel, emulsions, supra-molecular structures, microparticles and nanoparticles. There are two main strategies to achieve the nanoparticles: heat-induced aggregation and desolvation.

The typical desolvation reagents include ethanol and acetone. Sanghoon Ko and Sundaram Gunasekaran (2006) prepared sub-100nm beta-lactoglobulin nanoparticles with acetone in the range of 131±8 nm and 59±5 nm at pH 9, without preheating and with preheating (60°C for 30 min) respectively. They found that preheating had a

function of lowering particle size and improving the uniformity at the alkaline conditions. Gülseren, Fang, and Corredig (2012) were also able to produce nanoparticles of whey protein with a diameter <100 nm by using ethanol as the desolvation buffer. They found that this type of nanoparticles was not stable at neutral pH, and acidification to pH 3 was necessary to stabilize the particle size. On the other hand, they observed that heating led to stable nanoparticles but enhancement in size. At the same time, they used this nanoparticle to encapsulate the Zinc and achieved high encapsulation efficiency (over 80%) (Gülserena, Fang, & Corredig, 2012). These two examples indicated that the interactions to form nanoparticles were different depending on the desolvation reagent. In most cases, the influence on the binding properties by organic reagent remains unclear (Chen et al., 2006), and adding organic solvents for food applications is highly questionable as it is not generally recognised as safe. Therefore, there were some limitations using the desolvation method for food products. Moreover, ethanol as desolvation buffer would definitely influence the groups of customers due to the alcoholic content.

Alternatively, there are numerous studies among several groups using the heat-induced aggregation to produce nanoparticle. Giroux, Houde, and Britten (2010) conducted an experiment with the heating denatured whey protein following the pH cycling method. After heating at 80°C for 15 min, nanoparticles around 50 nm were produced, and then an acidification (5.0, 5.5, 6.0) ageing step, as well as the addition of Calcium (0, 2.5, 5 mM), was introduced to promote aggregation. They found that the nanoparticles were mainly cross-linked by disulphide bonds, while hydrogen bonds and hydrophobic also

contributed to internal structure. Calcium promoted protein aggregation, but it was not required to maintain the stability. Phan-Xuan et al. (2014) produced beta-lactoglobulin microgels around 260-440 nm in the range of pH 5.8-7.2 with Calcium (0.1M, 0.5M) by heating at 85°C for 15 hours. Calcium promoted the aggregation of microgels, and the net charge of native protein was the crucial parameter for the formation of microgels, which can be controlled by adding calcium or the pH adjustment. Similar particle size (50-300nm) was reported under mildly acidic conditions (pH 5.7-5.9) with 1.0 % β-Lg and heating at 70°C for 24 hours and 85°C 8 hours respectively (Laurence Donato, Christophe Schmitt, Lionel Bovetto, & Martine Rouvet, 2009). They proposed a model of β-Lg microgel aggregation pathway and emphasized the importance of pH in this pathway. Oancea et al. (2017) achieved that 98-192 nm nanoparticles of β-Lg by heating 0.2% protein solution in pH 7.7 Tris-HCl buffer at 70^{o}C for 20 mins. Among of all these studies, whey protein or β-Lg solution was heated at similar pH range but with different heat-load.

On the other hand, the application of nanoparticles has been investigated widely. Available binding ligands with native β-Lg have been explored since the middle of last century with SDS as the first binding ligand (Davis & Dubos, 1947). There is a good summary by L. Sawyer (2013). Briefly, the fatty acid, vitamins, and retinol and numerous hydrophobic compounds have been bound to beta-lactoglobulin. The scientific society makes great efforts to use β-Lg/ whey nanoparticles as encapsulants to deliver bioactives. Patricia Zimet and Yoav D. Livney (2009) achieved encapsulation of low-water soluble

ω-3 fatty acids (166 times higher) in β-Lg nanoparticles (~100 nm) and proved its effectiveness of protection against oxidation. Shpigelman et al. (2010b) and Avi Shpigelman, Yifat Cohen, and Yoav D. Livney (2012) continued to work on the thermally-induced beta-lactoglobulin-EGCG nanocomplexes and achieved high encapsulation (60-70%) and protection functions (33-fold lower initial degradation rate and control release in the intestine. Madalena et al. (2016) produced beta-lactoglobulin nanoparticles (172 nm) at pH 6, 80 °C for 10 min and achieved encapsulation of riboflavin (26% association efficiency) and control release in the small intestine. Stability of beta-lactoglobulin nanoparticles over 14 days in stimulant conditions (yoghurt, pH 3.45) was achieved.

Despite all this work being done on the formation of nanoparticles with β-lactoglobulin and their application to encapsulation of bioactives, there is a need to establish a robust and reproducible method to produce β-Lg nanoparticles which can be applied to the encapsulation of bioactives.

1.3. Aims and objectives

Beta-lactoglobulin, the major whey protein, has interesting binding ligand properties and a potential to be a delivery system for bioactive compounds. There are still some challenges to develop an approach to use beta-lactoglobulin as bioactives carrier in food products. The aim of this work was to explore the feasibility and operability to produce β-Lg nanoparticles as a novel delivery vehicle for nutraceuticals and try to apply these nanoparticles to the encapsulation of some interesting molecules. Also, if given a consideration to practical and economical aspects, it is worth trying to produce whey protein nanoparticles using the same method. Therefore the specific objectives of this research were :

1. To investigate the main operating parameters to produce β-Lg nanoparticles and their influence on the size of nanoparticles in order to establish a robust and reproducible method to produce β-Lg nanoparticles.
2. To characterise these nanoparticles including size, shape, charge and main interactions responsible for the stabilisation of these nanoparticles.
3. To produce caffeine-loaded β-Lg nanoparticles and examine the encapsulation efficiency, the caffeine release under simulated gastric fluid and intestinal conditions and to elucidate the mechanism of encapsulation.
4. To produce resveratrol-β-Lg nanocomplexes and investigate the effect of these nanoparticles and native β-lactoglobulin on the solubility and stability of resveratrol under different thermal processing conditions.
5. To study the stability of β-Lg nanoparticles under various processes/conditions

including ethanol concentration, different speed of centrifugation and freeze drying.

6. To produce whey protein nanoparticles using the same method as for β-Lg and make a comparison between β-Lg nanoparticles and whey protein nanoparticles.
7. To evaluate the production of nanoparticles with β-lactoglobulin and whey proteins in the context of industrial applications for encapsulation of food ingredients.

References

Augustin, M. A., & Oliver, C. M. (2012). An overview of the development and applications of nanoscale materials in the food industry. In Q. Huang (Ed.), *Nanotechnology in the Food, Beverage and Nutraceutical Industries* (Vol. Woodhead Publishing Limited, pp. 3-39).

Bell, K., & Mckenzie, H. A. (1964). β-Lactoglobulins. *Nature, 204*, 1275-1279.

Bewley, M. C., Qin, B. Y., Jameson, G. B., Sawyer, L., & Baker, E. N. (1997). β-Lactoglobulin and its variants: A three-dimensional structural perspective. In J. P. Hill & M. Boland (Eds.), *Milk Protein Polymorphism Special Issue 9702* (pp. 100-109). Brussels, Belgium: Int. Dairy Fed.

Brew, K. (2013). α-Lactalbumin. In P. L. H. McSweeney & P. F. Fox (Eds.), *Advanced Dairy Chemistry 4th Edition* (Vol. Volume 1A, pp. 261-273). New York: Springer Science+Business Media.

Brião, V. B., & Tavares, C. R. G. (2007). Effluent generation by the dairy industry: Preventive attitudes and opportunities. *Brazilian Journal of Chemical Engineering 24*(4), 487-497.

Burdock, G. A., Carabin, I. G., & Griffiths, J. C. (2006). The importance of GRAS to the functional food and nutraceutical industries. *Toxicology, 221*(1), 17-27.

Castroa, R. J. S. d., Domingues, M. A. F., Ohara, A., Okuro, P. K., Santos, J. G. d., Brexó, R. P., & Sato, H. H. (2017). Whey protein as a key component in food systems: Physicochemical properties, production technologies and applications. *Food Structure.*

Retrieved from http://www.sciencedirect.com/science/article/pii/S2213329116300922

Chatterton, D. E. W., Smithers, G., Roupas, P., & Brodkor, A. (2006). Bioactivity of β-lactoglobulin and α-lactalbumin—Technological implications for processing. *International Dairy Journal, 16*(11), 1229-1240.

Chau, C.-F., Wu, S.-H., & Yen, G.-C. (2007). The development of regulations for food nanotechnology. *Trends in Food Science & Technology, 18*(5), 269-280.

Chen, L., Remondetto, G. E., & Subirade, M. (2006). Food protein-based materials as nutraceutical delivery systems. *Trends in Food Science & Technology, 17*(5), 272-283.

Chen, L., & Subirade, M. (2005). Chitosan/β-lactoglobulin core–shell nanoparticles as nutraceutical carriers. *Biomaterials, 26*(30), 6041-6053.

Davis, B. D., & Dubos, R. J. (1947). The binding of fatty acids by serum albumin, a protective growth factor in bacteriological media. *The Journal of Experimental Medicine, 86*(3), 215-228.

DeFelice, S. L. (1994). What is a true nutraceutical and what is the nature & size of the U.S. nutraceutical market? Retrieved from http://www.fimdefelice.org/p2462.html

Dickinson, E. (2003). Colloidal aggregation: Mechanism and implications. In E. Dickinson & T. v. Vliet (Eds.), *Food Colloids, Biopolymers and Materials* (pp. 68-83). Cambridge: The Royal Society of Chemistry.

Donato, L., Schmitt, C., Bovetto, L., & Rouvet, M. (2009). Mechanism of formation of stable heat-induced β-lactoglobulin microgels. *International Dairy Journal 19*(5), 295-306.

Drewnowski, A. (2001). The Science and Complexity of Bitter Taste. *Nutrition Reviews, 59*(6), 163-169.

Edwards, P. B., Creamer, L. K., & Jameson, G. B. (2009). Structure and stability of whey proteins In H. Singh, MikeBoland, & A. Thompson (Eds.), *Milk Proteins: From Expression to Food* Elsevier.

FDA. (2006). *Nomination and review of toxicological literature*. Retrieved from https://ntp.niehs.nih.gov/ntp/htdocs/chem_background/exsumpdf/nanoscale_materials_508.pdf.

FICCI. (2010). Global nutraceutical industry: investing in health living. Retrieved from http://www.frost.com/prod/servlet/cio/236145272

Flower, D. r. (1996). The lipocalin protein family: structure and function. *Biochemistry Journal, 318*(1), 1-14.

Flower, D. R., North, A. C. T., & Attwood, T. K. (1993). Structure and sequence relationships the lipocalins and related proteins. *Protein Science, 2*, 753-761.

Ganfornina Álvarez, M. D., Sánchez Romero, D., Greene, L. H., & Flower, D. R. (2006). The lipocalin protein family: protein sequence, structure and relationship to the Calycin superfamily. In B. Åkerström, N. Borregaard, D. R. Flower, & J.-P. Salier (Eds.), *Lipocalins* (pp. 1-11): Landes Bioscience.

Gelamo, E. L., Silva, C. H. T. P., Imasato, H., & Tabak, M. (2002). Interaction of bovine (BSA) and human (HSA) serum albumins with ionic surfactants: spectroscopy and modelling. *Biochimica et Biophysica Acta, 1594*(1), 84-99.

Ghalandari, B., Divsalar, A., Sabour, A., & Parivar, K. (2015). β-Lactoglobulin nanoparticle as a chemotherapy agent carrier for oral drug delivery system. *Journal of the Iranian Chemical Society, 12*(4), 613-619.

Giroux, H. J., Houde, J., & Britten, M. (2010). Preparation of nanoparticles from denatured whey protein by pH-cycling treatment. *Food Hydrocolloids, 24*(4), 341-346.

Gülseren, I., Fang, Y., & Corredig, M. (2012). Whey protein nanoparticles prepared with desolvation with ethanol: Characterization, thermal stability and interfacial behavior. *Food Hydrocolloids 29*(2), 258-264.

Gülserena, İ., Fang, Y., & Corredig, M. (2012). Zinc incorporation capacity of whey protein nanoparticles prepared with desolvation with ethanol. *Food Chemistry, 135*(2), 770-774.

H. M. Farrell, J., & Thompson, M. P. (1990). β-Lactoglobulin and α-lactalbumin as potential modulators of mammary cellular activity. *Protoplasma, 159*(2-3), 157-167.

J.Cerbulis, & H.M.FarrellJr. (1975). Composition of Milks of Dairy Cattle. I. Protein, Lactose, and Fat Contents and Distribution of Protein Fraction. *Journal of Dairy Science, 58*(6), 817-827.

J.N.deWit. (2009). Thermal behaviour of bovine β-lactoglobulin at temperatures up to 150 °C. A review. *Trends in Food Science & Technology, 20*(1), 27-34.

Jia, Z., Dumontn, M.-J., & Orsat, V. (2016). Encapsulation of phenolic compounds present in plants using protein matrices. *Food Bioscience, 15*, 87-104.

Kessler, R. (2011). Engineered Nanoparticles in Consumer Products: Understanding a New Ingredient. *Environmental health perspectives, 119*(3), A120-A125.

Ko, S., & Gunasekaran, S. (2006). Preparation of sub-100-nm β-lactoglobulin (BLG) nanoparticles. *Journal of Microencapsulation, 23*(8), 887-898.

Kontopidis, G., Holt, C., & Sawyer, L. (2004). Invited Review: β-Lactoglobulin: Binding Properties, Structure, and Function. *Journal of Dairy Science 87*(4), 785-796.

Korhonen, H. J. (2009). Bioactive Components in Bovine Milk In Y. W. Park (Ed.), *Bioactive Components in Milk and Dairy Products* (pp. 15-42). Oxford: Wiley-Blackwell.

Kruif, C. G. d. (1998). Supra-aggregates of Casein Micelles as a Prelude to Coagulation. *Journal of Dairy Science, 81*(11), 3019-3028.

Lange, D. C., Kothari, R., Patel, R. C., & Patel, S. C. (1998). Retinol and retinoic acid bind to a surface cleft in bovine β-lactoglobulin: a method of binding site determination using fluorescence resonance energy transfer. *Biophysical ChemistrY, 74*(1), 45-51.

Livney, Y. D. (2010). Milk proteins as vehicles for bioactives. *Current Opinion in Colloid & Interface Science, 15*, 73-83.

Lönnerdal, B., & Suzuki, Y. A. (2013). Lactoferrin. In P. L. H. McSweeney & P. F. Fox (Eds.), *Advanced Dairy Chemistry 4th Edition* (Vol. 1A, pp. 295-315). New York: Springer Science+Business Media.

Madalena, D. A., Ramos, O. L., Pereira, R. N., Bourbon, A. I., Pinheiro, A. C., Malcata, F. X., . . . Vicente, A. A. (2016). In vitro digestion and stability assessment of β-lactoglobulin/riboflavin nanostructures. *Food Hydrocolloids, 58*, 89-97.

Markus, C. R., Olivier, B., & Haan, E. H. d. (2002). Whey protein rich in alpha-lactalbumin increases the ratio of plasma tryptophan to the sum of the other large neutral amino acids and improves cognitive performance in stress-vulnerable subjects. *The American Journal of Clinical Nutrition, 75*(6), 1051-1056.

McClements, D. J. (2012). Requirements for food ingredient and nutraceutical delivery systems. In N. Garti & D. J. McClements (Eds.), *Encapsulation Technologies and Delivery Systems for Food Ingredients and Nutraceuticals* (pp. 3-18). Oxford Cambridge Philadelphia New Delhi: Woodhead Publishing Limited.

Meisel, H., & Bockelmann, W. (1999). Bioactive peptides encrypted in milk proteins: proteolytic activation and thropho-functional properties. *Antonie van Leeuwenhoek, 76*(1-4), 207-215.

Narayan, M., & Berliner, L. J. (1997). Fatty Acids and Retinoids Bind Independently and Simultaneously to β-Lactoglobulin. *Biochemistry 36*(7), 1906-1911.

Nedovic, V., Kalusevic, A., Manojlovic, V., Levic, S., & Bugarski, B. (2011). An overview of encapsulation technologies for food applications *Procedia Food Science, 1*, 1806-1815.

Nicolai, T., Britten, M., & Schmitt, C. (2011). ß-Lactoglobulin and WPI aggregates: Formation, structure and applications. *Food Hydrocolloids, 25*(8), 1945-1962.

Oancea, A.-M., Aprodu, I., Ghinea, I. O., Barbu, V., Ioniţă, E., Bahrim, G., . . . Stănciuc, N. (2017). A bottom-up approach for encapsulation of sour cherries anthocyanins by using ß-lactoglobulin as matrices. *Journal of Food Engineering, 210*, 83-90.

Ortiz-Chao, P., Go´mez-Ruiz, J. A., Rastall, R. A., Mills, D., Cramer, R., Pihlanto, A., . . . Jauregi, P. (2009). Production of novel ACE inhibitory peptides from β-lactoglobulin using Protease N Amano. *International Dairy Journal, 19*(2), 69-76.

Papiz, M. Z., Sawyer, L., Eliopoulos, E. E., North, A. C. T., J. B. C. Findlay, Sivaprasadarao, R., . . . Kraulis£, P. J. (1986). The structure of β-lactoglobulin and its similarity to plasma retinol-binding protein. *Nature, 324*, 383-385.

Phan-Xuan, T., Durand, D., Nicolai, T., Donato, L., Schmitt, C., & Bovetto, L. (2014). Heat induced formation of beta-lactoglobulin microgels driven by addition of calcium ions. *Food Hydrocolloids, 34*, 227-235.

Pihlanto-Leppälä, A. (2001). Bioactive peptides derived from bovine whey proteins: Opioid and ace-inhibitory peptides. *Trends in Food Science & Technology, 11*(9-10), 347-356.

Qin, B. Y., Bewley, M. C., Creamer, L. K., Baker, H. M., Baker, E. N., & Jameson, G. B. (1998). Structural Basis of the Tanford Transition of Bovine β-Lactoglobulin. *Biochemistry, 37*(40), 14014–14023.

Rajat, S., Manisha, S., Robin, S., & Sunil, K. (2012). Nutraceuticals: a review. *International research journal of pharmacy, 3*(4), 95-99.

Ramos, O. L., Pereira, R. N., Martins, A., Rodrigues, R., Fucinos, C., Teixeira, J. A., . . . Vicente, A. A. (2017). Design of whey protein nanostructures for incorporation and release of nutraceutical compounds in food. *Food science and nutrition, 57*(7), 1377-1393.

Sakurai, K., & Goto, Y. (2006). Dynamics and Mechanism of the Tanford Transition of Bovine ß-Lactoglobulin Studied using Heteronuclear NMR Spectroscopy. *Journal of Molecular Biology, 356*(2), 483-496.

Sakurai, K., Konuma, T., Yagi, M., & Goto, Y. (2009). Structural dynamics and folding of β-lactoglobulin probed by heteronuclear NMR. *Biochimica et Biophysica Acta, 1790*(6), 527-537.

Sawyer, L. (2013). β-Lactoglobulin. In P. L. H. McSweeney & P. F. Fox (Eds.), *Advanced dairy chemistry 4th Edition* (Vol. Volume 1A: Proteins: Basic Aspects, pp. 211-260). New York: Springer Science+Business Media.

Sawyer, L., & Kontopidis, G. (2000). The core lipocalin, bovine β-lactoglobulin. *Biochimica et Biophysica Acta, 1482*(1-2), 136-148.

Science and Technology Committee. (2010). *Nanotechnologies and Food* Retrieved from London: https://www.publications.parliament.uk/pa/ld200910/ldselect/ldsctech/22/22i.pdf

Shafaei, Z., Ghalandari, B., Vaseghi, A., Divsalar, A., Haertlé, T., Saboury, A. A., & Sawyer, L. (2017). β-Lactoglobulin: An efficient nanocarrier for advanced delivery systems. *Nanomedicine: Nanotechnology, Biology and Medicine, 13*(5), 1685-1692.

Shi, L.-E., Li, Z.-H., Li, D.-T., Xu, M., Chen, H.-Y., Zhang, Z.-L., & Tang, Z.-X. (2013). Encapsulation of probiotic Lactobacillus bulgaricus in alginate–milk microspheres and evaluation of the survival in simulated gastrointestinal conditions. *Journal of Food Engineering, 117*(1), 99-104.

Shpigelman, A., Cohen, Y., & Livney, Y. D. (2012). Thermally-induced ß-lactoglobulin-EGCG nanovehicles: Loading, stability, sensory and digestive-release study. *Food Hydrocolloids, 29*, 57-67.

Shpigelman, A., Israeli, G., & Livney, Y. D. (2010). Thermally-induced protein-polyphenol co–assemblies: beta lactoglobulin-based nanocomplexes as protective nanovehicles for EGCG. *Food Hydrocolloids, 24*, 735-743.

Siegrist, M., Cousin, M.-E., Kastenholz, H., & Wiek, A. (2007). Public acceptance of nanotechnology foods and food packaging: The influence of affect and trust. *Appetite, 49*(2), 459-466.

Singh, H., & Ye, A. (2014). Interactions and Functionality of Milk Proteins in Food Emulsions. In M. Boland, H. Singh, & A. Thompson (Eds.), *Milk Proteins (Second Edition)* (pp. 359-386): Elsevier Inc.

Siso, M. I. G. (1996). The biotechnological utilization of cheese whey: A review *Bioresource Technology, 57*(1), 1-11.

Tanford, C., Bunville, L. G., & Nozaki, Y. (1959). The Reversible Transformation of β-Lactoglobulin at pH 7.5. *Journal of the American Chemical Society, 81*(15), 4032-4036.

Taulier, N., & Chalikian, T. V. (2001). Characterization of pH-induced Transitions of β-Lactoglobulin: Ultrasonic, Densimetric, and Spectroscopic Studies. *Journal of Molecular Biology, 314*(4), 873-889.

Tavares, G. M., Croguenne, T., Carvalho, A. F., & Bouhallab, S. ı. (2014). Milk proteins as encapsulation devices and delivery vehicles: Applications and trends. *Trends in Food Science & Technology, 37*, 5-20.

Thies, C. (2012a). Microencapsulation methods based on biopolymer phase separation and gelation phenomena in aqueous media. In N. Garti & D. J. McClements (Eds.), *Encapsulation Technologies and Delivery Systems for Food Ingredients and Nutraceuticals* (pp. 177-207). Oxford Cambridge Philadelphia New Delhi: Woodhead Publishing Limited.

Thies, C. (2012b). Nanocapsules as delivery systems in the food, beverage and nutraceutical industries. In Q. Huang (Ed.), *Nanotechnology in the Food, Beverage and Nutraceutical Industries* (pp. 208-256). Oxford Cambridge Philadelphia New Delhi: Woodhead Publishing Limited.

Wang, Y., Bamdad, F., Song, Y., & Chen, L. (2012). Hydrogel particles and other novel protein-based methods for food ingredient and nutraceutical delivery systems. In N. Garti & D. J. McClements (Eds.), *Encapsulation Technologies and Delivery Systems for Food Ingredients and Nutraceuticals* (pp. 412-450). Oxford Cambridge Philadelphia New Delhi: Woodhead Publishing Limited.

Wildman, R., & Kelley, M. (2006). Nutraceuticals and Functional Foods. In R. E. C. Wildman (Ed.), *Handbook of Nutraceuticals and Functional Foods, Second Edition* (2nd ed., pp. 1). London New York Boca Raton: CRC Press

Worldbankgroup. (2007). *Environmental, Health, and Safety Guidelines for Dairy Processing*. Retrieved from http://www.fpeac.org/dairy/EnvironmentalHealthSafety-DairyProcessing.pdf

Yang, M.-C., Guan, H.-H., Liu, M.-Y., Lin, Y.-H., Yang, J.-M., Chen, W.-L., . . . Mao, S. J. T. (2008). Crystal structure of a secondary vitamin D3 binding site of milk ß-lactoglobulin. *Proteins, 71*(3), 1197-1210.

Zhang, J., Liu, X., Subirade, M., Zhou, P., & Liang, L. (2014). A study of multi-ligand beta-lactoglobulin complex formation. *Food Chemistry, 15*, 256-261.

Zimet, P., & Livney, Y. D. (2009). Beta-lactoglobulin and its nanocomplexes with pectin as vehicles for u-3 polyunsaturated fatty acids. *Food Hydrocolloids, 23*(4), 1120-1126.

Zsila, F., Bikádi, Z., & Simonyi, M. (2002). Retinoic acid binding properties of the lipocalin member β-lactoglobulin studied by circular dichroism, electronic absorption spectroscopy and molecular modelling methods. *Biochemical Pharmacology, 64*(11), 1651-1660.

CHAPTER TWO

Characterisation of β-Lactoglobulin nanoparticles and their binding to caffeine

[1]Yuchen Guo [2]Peter Harris, [3]Lorenzo Pastrana,[1]*Paula Jauregi

[1]Department of Food and Nutritional Sciences. University of Reading, Whiteknights, Reading, RG6 6AP, United Kingdom.

[2]Centre for Advanced Microscopy, University of Reading, Whiteknights, Reading, RG6 6AP, United Kingdom

[3]INL - International Iberian Nanotechnology Laboratory, Av. Mestre José Veiga s/n, 4715-330 Braga Portugal

*Corresponding author.

E-mail address: p.jauregi@reading.ac.uk (P.Jauregi)

Address: Department of Food and Nutritional Sciences. University of Reading, Whiteknights, Reading, RG6 6AP, United Kingdom.

Telephone: +44(0)1183788728

Keywords: Caffeine; Nanoparticles; β-Lactoglobulin; Simulated digestion, Encapsulation.

ABSTRACT

The production of β-Lg nanoparticles by a simple heat-induced denaturation method without the need to add chemicals was performed at different conditions of pH, and temperature of denaturation. Optimum conditions were set as 0.2 % w/v β-Lg, pH 6 and simply heating in water bath at 75°C for 45 minutes. At these conditions, a monodisperse solution with colloidal stability was obtained, and the yield of aggregation was over 90%. Shape and size of nanoparticles were determined by Dynamic Light Scattering technique and by electron microscopy. A monodisperse particle size distribution of spherical shape particles (200nm-300nmin) diameter was obtained. The stability of the aggregates towards various types of dissociating buffers was studied. Sodium dodecyl sulphate (SDS) and urea had a strong effect on the size of the nanoparticles, while 2-Mercaptoethanol and Dithiothreitol (DTT) had no significant effect. Therefore hydrogen bonding and hydrophobic interactions were the predominant interactions responsible for the microstructure. Maximum yield of caffeine encapsulation of 13.54% was obtained at caffeine to the β-Lg molar ratio of 50:1. Rapid nanoparticle degradation and increase of polydispersity during the incubation of β-Lg nanoparticles at simulating stomach conditions time was observed due to enzymatic attack. Nevertheless, little release of entrapped caffeine was noted. Total release was achieved at intestinal conditions. Finally, the adsorption of caffeine to both native and denatured β-Lg followed a Langmuir adsorption isotherm model, and caffeine had three times more affinity for partially denatured β-Lg in nanoparticles than for native protein.

2.1. Introduction

Whey is the principal by-product of cheese manufacturing, and it represents 85-95% of the initial volume of processed milk with high Chemical oxygen demand (COD) and Biochemical oxygen demand (BOD) values hence its disposal would have a negative environmental impact. The total world production of liquid cheese whey in 2008 was in the region of 187 million metric tons and of this 3.2 million metric tons were industrially utilised and processed into higher added value products such as, whey powder, whey proteins concentrate and whey protein fractions (Afferstsholt & Palmer, 2009; C. Baldasso , T.C. Barros, & Tessaro, 2011); the remaining whey is used for animal feed, fertilisers, baby milk powder and some it is just dumped. Whey is a valuable source of proteins (about 0.8-0.9% protein) with high nutritional value and additional biological properties as well as numerous functional properties such as gelation, emulsifying and foaming properties (Jauregi & Welderufael, 2010). The major whey protein, beta-lactoglobulin (β-Lg) which comprises 51 % (w/w) of total protein has very interesting aggregation properties which have been exploited for its application as an encapsulant (Chen et al., 2006; H. J. Giroux, J. Houde, & M. Britten, 2010; Jones, Lesmes, Dubin, & McClements, 2010). This protein is predominantly dimeric under physiological conditions, but dissociates to a monomer at about pH 3 (Tauliera & Chalikiana, 2001); its isoelectric point (pI) is 5.13. Four out of its five cysteine residues form two disulfide bridges leaving a free reactive thiol group that appears to be responsible for the formation of covalent aggregates upon heating (L. Sawyer, 2002). Also β-Lg possess a hydrophobic pocket that when exposed by, for example, heat denaturation forms

aggregates by hydrophobic interactions. These aggregation properties can be manipulated by changing temperature, pH, and ionic strength. Under prolonged heating at low pH and low ionic strength, a transparent `fine-stranded' gel is formed, in which the protein molecules assemble into long stiff fibers and also can produce nanoparticles (S. Ko & S. Gunasekaran, 2006).

Food protein-based nanoparticles are of great interest because they are Generally Recognised as Safe (GRAS), easy to prepare, no need for chemical cross-linking agents during preparation, better control over size distributions (Chen et al., 2006; Gunasekaran, Ko, & Xiao, 2006). β-Lg is able to aggregate forming nanoparticles that have some technological advantages as an encapsulant for bioactives; among others: inexpensive, food grade and non-toxic material, capable of solubilizing and protecting hydrophobic biologically active molecules in aqueous media as well as capable of retaining sensory qualities, and promote bioavailability of hydrophobic biologically active molecules. In this sense, when electrically charged, β-Lg is also able to ion binding and electrostatic complex formation, self and co-assembly and covalent conjugation (Y. D. Livney, 2010).

In previous works, β-Lg nanoparticles have been applied as carriers for a range of nutraceutical products such as, polysaccharides, pectin, carageenan or chitosan (L. Chen & M. Subirade, 2005; Jones et al., 2010; Ron, Zimet, Bargarum, & Livney, 2010; P. Zimet & Y. D. Livney, 2009) where β-Lg forms complexes with each of these products. The complexity of method and materials used for the production of such complexes hinders the possibility of scaling up production. On the other hand, simple production steps such as desolvation with ethanol can produce nanoparticles without application of heat, thus

making it very feasible for heat-labile bioactive components (Gulseren, Fang, & Corredig, 2012). Nonetheless, usage of organic solvents for food application is still the major drawback for this method (Nicolai et al., 2011).

Caffeine is an amphiphilic alkaloid drug that has a strong bioactivity acting as a stimulant drug of the central nervous system. For this reason is considered the most popular legal stimulant consumed in the world, mainly in the form of coffee and tea infusion (Gilbert, 1984). In the last years, several energy drinks containing caffeine have been launched to the market having a great success and customer acceptation (Somogyi, 2010). Unfortunately, caffeine has very bitter taste and unpleasant aftertaste limiting or even excluding their use from many foods and drink formulations. Encapsulation of caffeine enables bitterness masking, and it can be easily added to food and drink products without changing the flavour or increasing the bitterness level. In addition, encapsulation could provide protection against harsh processing conditions and controlled release.

The aim of this study is to investigate the production of β-Lg nanoparticles by a simple heat-induced denaturation method without the need to add chemicals and/or other reagents and to investigate their application to the encapsulation of caffeine. Particles were characterised in terms of size by Dynamic Light Scattering technique, fluorescence and by electron microscopy. Stability to buffers was examined as an indirect measurement of the internal forces responsible for the molecular network within the particles. This led to an improved understanding of the mechanism of aggregate formation and their interaction with caffeine.

2.2. Materials and Methods

2.2.1. Materials

β-lactoglobulin (β-Lg) from bovine milk, ≥90% PAGE lyophilised powder was purchased from Sigma-Aldrich (United Kingdom) for all the experiments. The material used for encapsulation was caffeine (99% purity) also obtained from Sigma-Aldrich (United Kingdom).

2.2.2. Methods

2.2.2.1. Preparation of β-lactoglobulin nanoparticle

The β-Lg powder was dispersed in deionized water to make 50 ml 0.2 % w/v β-Lg stock solution and it was stirred magnetically for about 2 h at room temperature. This stock solution was stored in a 50ml Falcon tube (VWR International, 525-0403, USA) at 4°C over the whole night to complete hydration. In order to prevent the growth of microorganisms, 200 ppm sodium azide was added.

A 5 ml sample from the β-Lg stock solution was added into 15ml a Falcon tube (VWR International, 5250401, USA) and after warming the sample up to room temperature, the pH was measured. Then the pH of the sample was adjusted to 6.0 (except when the pH effect was investigated) using a pH meter (Mettler Toledo, Switzerland) with 0.1M HCl and 0.1M NaOH. After this, the Falcon tube containing the sample was introduced into a water bath (Grant Instrument Ltd., Cambridge, United Kingdom) that had been previously heated at 75 °C. The sample was left for 45 minutes at this temperature except when the effect of heat load was investigated. The temperature of the sample was

monitored, and it took about 12-14 minutes for the temperature in the samples to reach the water temperature (75 °C). After the set heating time, samples were moved to an ice bath for 10 minutes to terminate incubation, and the pH of the sample was measured.

For experiments where pH effect (5.7-6.2) was investigated, nanoparticles were produced following procedure described above but initial pH of sample was changed. For experiments where temperature effect was investigated, samples were heated at 60 °C and 75°C; all other conditions were kept constant (0.2 % w/v of β-Lg, pH 6 and heating time 45 minutes). For experiments where the heating time (heat load) effect was investigated, nanoparticles were produced following procedure described at 0.2 % w/v of β-Lg, pH 6 and 75°C but at varying heating incubation time: 15, 25, 35, 45, 55, 65, and 75 min.

2.2.2.2. Preparation of caffeine encapsulated β-lactoglobulin nanoparticles

The experiment on the encapsulation of caffeine was conducted only with 0.2% (w/v) dispersions. Caffeine (99% purity) was added to the β-Lg dispersions prior to pH adjustment to obtain 10:1, 20:1, 50:1, 100:1, 200:1 caffeine to β-Lg molar ratios. A certain volume of stock caffeine solution (10mg/ml) was mixed with protein samples to achieve 10:1, 20:1 caffeine to β-Lg molar ratios, respectively. The final protein concentration after pH adjustment and caffeine addition was 0.2 % (w/v). Caffeine powder was added into samples to obtain 50:1, 100:1, 200:1 caffeine to β-Lg molar ratios, respectively. Once caffeine was added to the β-Lg solution, the encapsulation method proceeded in the same way as the nanoparticle formation procedure described in

section 2.2.2.1.

2.2.2.3. Particle size distribution

The Z-average hydrodynamic diameter of β-Lg nanoparticles was measured by dynamic light scattering technique using Zetasizer Nano Z (Malvern Instruments Inc., Malvern, United Kingdom) at 25 ± 0.1°C and five measurements were taken for each sample. The measurement was determined by considering the refractive index of β-Lg as 1.45 and that of the dispersant medium (deionized water) as 1.33. The z-average mean was calculated from the intensity of light scattered from the nanoparticles, based on Stokes-Einstein equation, which assumes that all particles are spherical. Each sample was measured five times and the mean and standard deviation was determined. In some case samples were diluted in order to operate at concentrations appropriate for DLS (as indicated by machine). When samples were incubated with different dissociating buffers, the refractive index of these buffers was taken into account: (i) 10M urea, refractive index 1.370 (Warren & Gordon, 1966) (ii) 0.1M Mercaptoethanol, refractive index 1.500 (Sigma-Aldrich, 2017), (iii) 1.0 % (w/v) SDS, refractive index 1.334 (Tumolo, Angnes, & Baptista, 2004), (v) 0.1 M DTT, refractive index 1.576 (ChemBK, 2017).

2.2.2.4. β-lactoglobulin aggregation

The degree of thermal aggregation for β-Lg was determined by separation of denatured β-Lg nanoparticles from native β-Lg using centrifugal ultrafiltration Vivaspin® 20 (Sartorius Stedim Biotech, Germany) with 50 kDa molecular weight cut-off membrane. To quantify the amount of native and aggregated β-Lg, 5ml of the heated β-Lg solution

following the method described in section 2.2.2.1 was centrifuged at 2000 rpm for 15 minutes to collect the retentate as well as the permeate; the retentate and permeate volumes were determined by weight. The concentration of the native β-Lg remained in permeate was determined by bicinchoninic acid (BCA) method. In brief, 0.1 ml of the permeate solution was added to 2 ml of BCA working reagent (bicinchoninic acid and copper (II) sulphate pentahydrate), followed by incubation at 37°C for 30 min. The reaction solution was measured at 562 nm in an Ultrospec ® 1100 Pro UV-vis spectrophotometer (United Kingdom). The percentage of protein aggregated was determined by measuring the total protein in the permeate followed by mass balance on protein.

2.2.2.5. Microscopy Method.

Environmental Scanning Electron Microscopy (ESEM) image was carried out on samples produced at the optimum conditions - 0.2 % β-lactoglobulin, pH 6.0, at 75 °C for 45 min. The microscope used was an FEI Quanta 600, operated in environmental mode with a water vapour pressure of 822.46Pa, and a specimen temperature of 5°C. The accelerating voltage was 20 kV. One drop of β-lactoglobulin nanoparticles sample was dispersed at the surface of the metal stub of the microscope and was dry at the room temperature to achieve the evaporation of some moisture content, which ensured that nanoparticles images were easier to be captured.

2.2.2.6. Fluorescence measurement of protein solutions

The degree of β-Lg conformational changes on fluorescence emission of tryptophan (Trp)

was accessed by fluorescence spectrophotometer with temperature controller (Varian Cary Eclipse, United Kingdom). Fluorescence spectra were obtained after excitation at 280 nm, scanning an emission wavelength range between 290 nm to 510 nm, using 5nm excitation and emission slits wavelength. The data was collected by Cary Eclipse software version 2 (Varian Cary Eclipse, United Kingdom). Samples of native β-Lg, heated β-Lg nanoparticles, and caffeine loaded β-Lg nanoparticles were analysed in duplicate at a constant temperature of 20°C.

2.2.2.7. Stability against dissociating buffers

All samples and buffers were filtered by 0.45 μm filters before the incubation with dissociation buffers. β-Lg nanoparticle dispersions were mixed with equal volume of various dissociating buffers: (i)10M urea (ii) 0.1M mercaptoethanol, (iii) 1% (w/v) SDS, (v) 0.1 M DTT. Dispersions were incubated for 60 min with each buffer, and the particle size was measured following the method described in section 2.2.2.3.

2.2.2.8. Zeta potential

Zeta potential of the sample was measured by Dynamic light scattering technique using Zetasizer Nano Z in Electrophoretic Light Scattering mode (Malvern Instruments Inc., Malvern, United Kingdom) at 25 ± 0.1°C and five measurements were taken for each sample. A folded capillary cell (DTS1070) was used to measure the zeta potential. The cell was washed with ethanol and deionized water before each measurement.

2.2.2.9. Caffeine determination by HPLC

An isocratic Reversed phase High-Performance Liquid Chromatography (RP-HPLC) equipped with Gilson Model 302 Pump, CE212 Variable wavelength ultraviolet detector and Hewlett Packard 3396A integrator was used to quantify the caffeine concentration contained in permeate. The column used was Ace 5 C18, 25cm × 4.6mm (Hinchhrom Limited, United Kingdom), operated at 25 ± 1°C, the flow rate was 1.0 mL/min, with 50 µL injection volume, while mobile phase comprised of methanol/water (50/50). Absorption wavelength was selected at 273 nm, which is the maximum wavelength for caffeine. Standard solution of caffeine was prepared in deionized water in the range of concentrations from 0.001% to 0.01% (w/v). A standard calibration plot for was prepared by plotting concentration versus area from which the concentration of caffeine was determined in a range of samples.

2.2.2.10. Encapsulation efficiency

To study the encapsulation efficiency of caffeine into β-Lg nanoparticles, the caffeine encapsulated by the β-Lg particles was separated from free caffeine by centrifugal ultrafiltration membranes of 50 KDa MWCO, Vivaspin® 20 (Sartorius Stedim Biotech, Germany). To quantify the amount of free and entrapped caffeine, 5 ml of protein and caffeine solution prepared according to section 2.2.2.2 was sampled and centrifuged for 30 min at 2000 rpm. The retentate was removed carefully by pipette for further analysis while the permeate was used for determination of free caffeine using RP-HPLC. The amount of the entrapped caffeine was determined based on the determination of free

caffeine in the permeate and by applying a mass balance. The entrapment efficiency of caffeine was calculated based on the following equations (Eq. (1)):

$$Entrapment\ efficiency\ (\%) = \frac{mass\ of\ caffeine\ entrapped}{original\ mass\ of\ caffeine} \times 100 \quad \textbf{(1)}$$

2.2.2.11. In-vitro gastrointestinal digestion

2.2.2.11.1. Gastric digestion. The *in-vitro* gastric model protocol was adapted from Zeese, Huppertz, and Kelly (2008) and Sarkar, Goh, Singh, and Singh (2009) with some modifications introduced here. Simulated gastric fluid (SGF) containing 2g of NaCl and 7 mL of HCl, without the addition of pepsin was diluted to 1 L and pH adjusted to 1.2 using 1.0M HCl. Afterwards, 14.93 mg of pepsin enzyme was added to 7 ml of SGF and held at 37°C with continuous shaking at 95 rpm in a temperature-controlled water bath (Grant OLS 200, Grant Instrument, United Kingdom) to mimic the conditions in the stomach. The pH and temperature were continuously monitored and controlled.

Caffeine-loaded β-Lg nanoparticles and pure β-Lg nanoparticles separated from 14 mL suspensions by Ultrafiltration (UF) (as described in section 2.2.2.11) were re-dispersed in 14 mL of SGF. Then, 7 mL of SGF containing pepsin was added to the mixture to make up a final volume of 21 mL (protein: enzyme ratio 1.87:1 w/w). The mixture was then incubated at 37°C for up to 2h and samples were withdrawn at different time intervals for particle size measurement and RP-HPLC analysis. The pH of the mixture was maintained at 1.5 using 1M HCl. The digestion reaction was terminated by raising the pH to 8 with 0.1M NaOH prior to any analysis.

2.2.2.11.2 Gastrointestinal digestion. This method was based on a digestion protocol according to D. J. S. Mills et al. (2008) and Maccaferri et al. (2012) with some modifications. 15ml solution sample containing nanoparticles with and without caffeine was adjusted to pH 2 by using HCl (6M) and mixed with 2.5ml 0.1 M HCl which contained 0.27g pepsin (protein: pepsin ratio 1:9 w/w). The solution was incubated in the 37 ℃ water bath and on a shaker with 95 rpm for 2 h. A 0.1 ml sample was taken for analysis of released caffeine by HPLC. Then the rest of the sample was mixed with 12.5ml $NaHCO_3$ in which 56mg pancreatin (protein: pancreatin ratio 1.07:2 w/w) (P3292, Sigma; 4UPS) and 0.35g bile (protein: bile ratio 1:11.7 w/w) (B 8631, Sigma) was dissolved and pH of the sample was adjusted to 7 using NaOH (6M). Samples were incubated for 3 h. After small intestinal phase incubation, samples were filtered through 0.45um filtration unit and analysed by HPLC to determine the caffeine release.

2.2.2.12. Caffeine adsorption isotherm

To describe the caffeine adsorption process to β-Lg nanoparticles and native protein, the experimental data were fitted to Langmuir adsorption model (Eq. (2)):

$$\boldsymbol{Cad = \frac{Cadmax \times k \times C}{1 + k \times C}} \quad \textbf{(2)}$$

Where, $\boldsymbol{Cad}$ is the caffeine adsorbed to β-Lg per protein at equilibrium (mg mg^{-1} protein), $\boldsymbol{Cad_{max} \times k}$ is the maximum amount of caffeine absorbed to β-Lg (mg mg^{-1} protein), $\boldsymbol{C}$ is the concentration of caffeine free in solution at equilibrium (mg ml^{-1}) and $\boldsymbol{k}$ is the adsorption constant (ml mg^{-1})

2.2.2.13. Calculations and Statistical Analysis

Calculation of the net charge of β-Lg at different values of pH was performed with the online "protein calculator v3.4" software (http://protcalc.sourceforge.net) using the sequence of β-Lg. The results were statistically analysed by analysis of variance using IBM® SPSS® Statistics version 20.0. Means and standard deviations from at least three measurements carried out on two freshly prepared β-Lg nanoparticles were repeated. The significance level was set at 0.05. Data fitting of experimental data to models was performed with Solver from Excel MS Office 2013 (Microsoft Corporation, Redmond, WA, USA)

2.3. Results and Discussion

2.3.1. Effect of pH, temperature and heating incubation time on β-Lg nanoparticles

Native and heated β-Lactoglobulin (β-Lg) solutions were prepared 0.2% (w/v) and pH adjusted near to their isoelectric point (pH 6.0). All samples appeared to be transparent initially. Also there was only slight turbidity after pH adjustment in agreement with observation previously reported (Chanasattru, Jones, Decker, & McClements, 2009; Mehalebi, Nicolai, & Durand, 2008; Nicolai et al., 2011; P. Zimet & Y. D. Livney, 2009). High turbidity after heating at 75°C for 45 min appeared to provide a rough quantitative indication of protein aggregation in the system. A monodisperse particle size distribution was obtained consistently with particles of an average diameter of 200 nm to 300 nm. (See Fig. 2.1.).

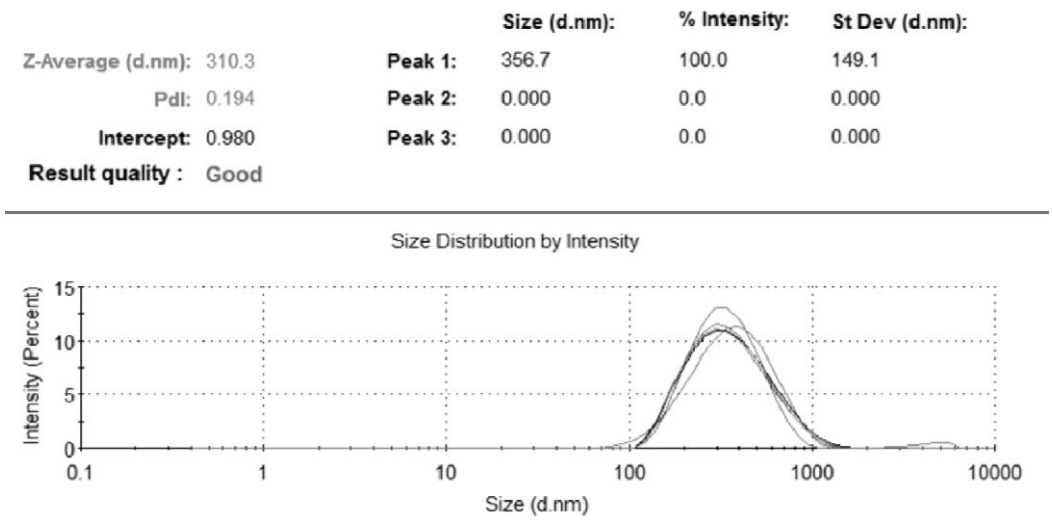

Figure 2.1: An example of particle size result by DLS for nanoparticle produced under conditions pH 6, heating at 75 °C for 45 mins.

2.3.1.1. Effect of pH

Near the isoelectric point (pI) of the protein the overall charge is close to zero, therefore, repulsive electrostatic interactions between protein molecules will be minimised and their aggregation will be promoted. In particular, β-Lg aggregation close to its pI and under denaturing conditions was reported to produce particulate gels, which were composed of spherical particles (Donald, 2007).

Here we studied the effect of a range of pH's near and above the pI on the particle size. The pH of the aqueous β-Lg solution (0.2 % w/v) before pH adjustment was 6.8 ± 0.3. At this pH, a clear solution was obtained even after heating. This pH was further away from the pI therefore, strong electrostatic repulsive interactions between proteins molecules hindered their self-aggregation which resulted in reduced turbidity. To test the effect of pH on protein aggregation and formation of nanoparticles samples were incubated at pH close to the pI in the range of 5.7 to 6.2 (see Figure 2.2). At pH 5.7, the largest particle size, about 600nm, was recorded and clearly, particle size decreased with an increase in pH. This indicated that when the pH was close to pI, and the repulsive electrostatic forces between molecules were minimised, large particles could be formed. Conversely, when the pH was far from the pI, the repulsive electrostatic forces were too strong to promote aggregation, and consequently smaller particles were produced. Moreover, according to Tauliera and Chalikian (2001), within pH 5.7-6.2 only a slight change in its tertiary structure occurred but no alteration in secondary structure. Therefore, the hidden hydrophobic parts of β-Lg were exposed upon pH adjustment.

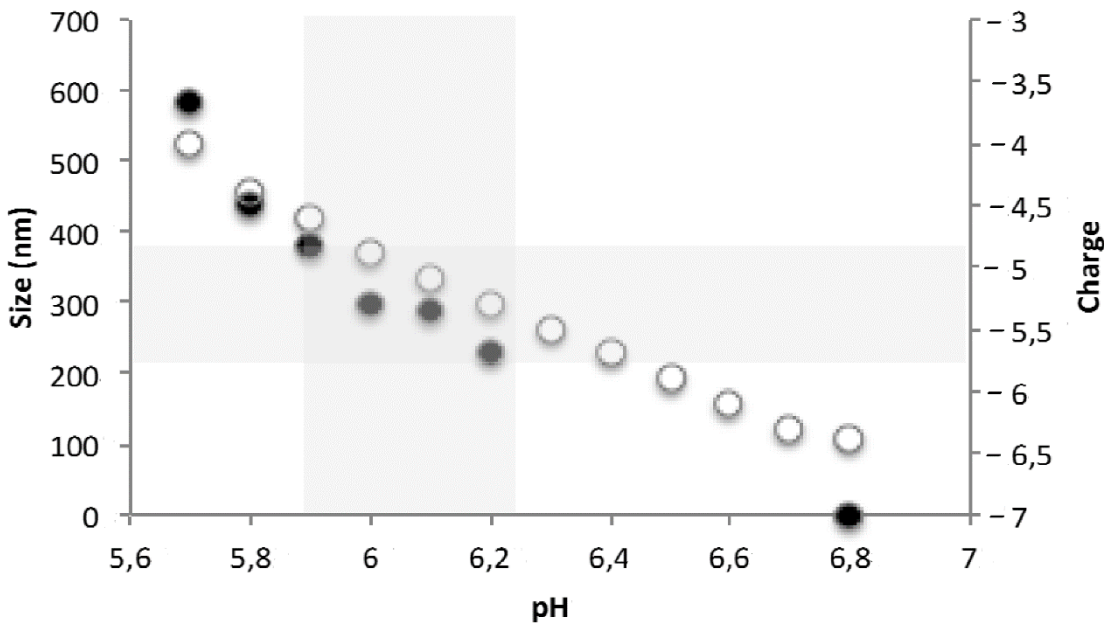

Figure 2.2: Effect of pH on the size and the net charge of protein nanoparticles. Size: black circles; protein charge: white circles (predicted by "protein calculator v3.4" software http://protcalc.sourceforge.net. Experiments were carried out in duplicates and mean standard deviations were 0.6-9.1 nm).

Figure 2.2 shows the relationship between pH and particle size and protein's net charge. It was concluded that to form nanoparticles with size in the range of 200 nm-350 nm, the pH should be strictly controlled at 5.9 to 6.2 and protein's net charge between -5.8 to -4.8. Small changes in pH outside this range led to small changes in the protein charge but dramatic changes in particle size. So these results highlighted the effect of a narrow range of pH close to the protein's pI on the particle size.

2.3.1.2. Effect of temperature

The heating temperature was also found to have a significant effect on particle size at

constant protein concentration. The turbidity of β-Lg solution heated at 50-60 °C remained relatively low but increased steeply from 60-75 °C. Reproducible size measurements were difficult to obtain at 65 °C, and a bimodal distribution was obtained. For instance, the peak of the first distribution produced with 0.2% (w/v) β-Lg was recorded at 3.81 nm, and the sub-population was found at 145 nm. The first population was conjectured to be native β-Lg which is known to have a hydrodynamic radius of around 2.5 nm (Mehalebi et al., 2008). The possible reason for obtaining such population as explained by Bauer, Carrotta, Rischel, and Ogendal (2000) was that early aggregation of β-Lg is initiated only at 67.5°C. Significantly larger nanoparticles were formed at 75 °C than at 65 °C. This suggests that 65°C was not sufficient to induce complete β-Lg chain unfolding to produce nanoparticles in a consistent manner. On the other hand, at 75°C, a monodisperse particle size distribution was obtained consistently with particles of an average diameter about 200 nm-300 nm.

The findings were in agreement with those by Mehalebi et al. (2008) and Gulseren et al. (2012), who found that elevated temperature could accelerate the rate of aggregation to produce larger nanoparticles. Overall the particle sizes reported here were in agreement with those reported by L. Donato, C. Schmitt, L. Bovetto, and M. Rouvet (2009), who had observed elongated compact aggregates smaller than 200 nm upon heating of 1% (w/v) β-Lg (pH 5.9) at 75°C. Also, Jones et al. (2010) had produced β-Lg particles (d<300 nm) with good stability to sedimentation as in this study under similar conditions. Giroux and Britten (2011) reported whey protein nanoparticles in the range of 194 nm produced at pH 5.0 using pH-cycling treatment. According to Jones et al. (2010)

optimal conditions for production of β-Lg nanoparticles occurred when the system was heated above thermal denaturation temperature of β-Lg and at a pH close to its pI which is in agreement with the above findings; these nanoparticles were reported to be irreversible protein aggregates and generally stable towards storage and pH changes.

2.3.1.3. Heating incubation time

Besides temperature, the heating time is another factor which has a significant effect on the particle size. Previous studies suggested that long heating incubation time promotes the formation of large aggregates. This was confirmed in the experiments carried out at varying heating times (15 to 75 minutes) but constant temperature, 75 °C (Figure 2.3); Note that although the water bath was at 75 °C, it took about 12-14 mins for the temperature in the dispersion to reach 75 °C.

Particle size increased from 218 nm to 327 nm in the studied heating time range. The conformation structure changes might happen including the hidden hydrophobic groups at the central cavity and disulphate bonds exposing to the environment, and the particles were produced. The polydispersion index (PDI) decreased and had a minimum value at 45mins. As shown by the low PDI number at this heating incubation time, a monodispersion was obtained.

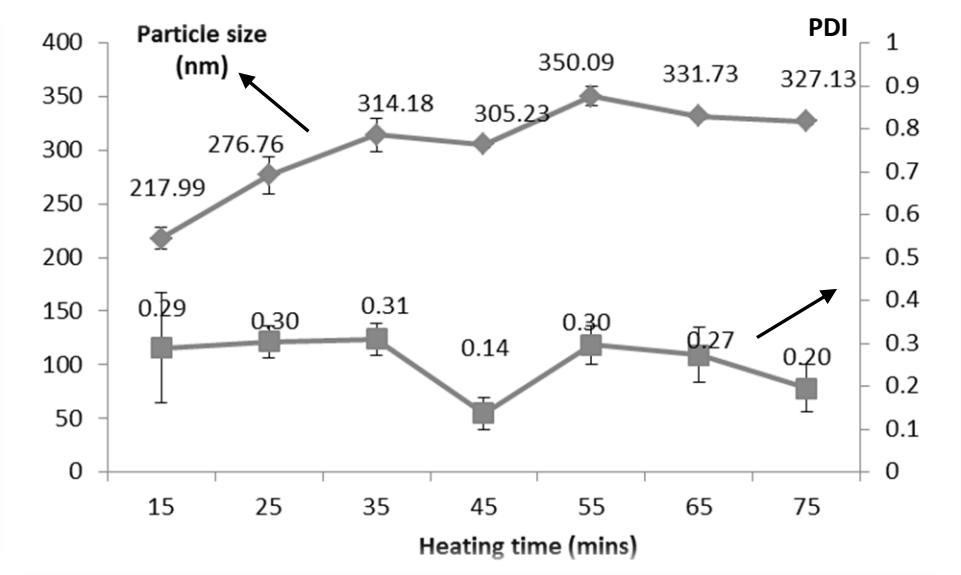

Figure 2.3: β-Lg nanoparticle size for continuing heating incubation (15minutes-75mintues). ◆The β-Lg nanoparticles size; ■ PDI of nanoparticles.

In summary, both heat load (combination of temperature and time) and pH were found to be the key operating parameters at constant protein concentration in the production of nanoparticles of a given size. The β-Lg nanoparticles in the range of 200-300 nm were obtained in a consistent and reproducible manner by inducing heat denaturation and aggregation of the protein in an aqueous solution at 0.2%, pH 6.0 and 75 °C for 45 minutes. At these conditions, a monodisperse size distribution was obtained and with good reproducibility.

Protein aggregation may occur due to covalent and non-covalent interactions between unfolded protein molecules. As protein denatures, it will unfold to expose the hydrophobic groups as well as the reactive thiol group at Cys 121, which leads to protein molecules interacting via non-covalent interactions (hydrophobic interaction, hydrogen bonding) and covalent interactions (disulphide bonds) to form particles of a given microstructure.(L. Donato et al., 2009; Havea, Singh, & L.K., 2001) In order to obtain an

insight into the physical characteristics of the nanoparticles and their microstructure, the following characterisation study was carried out.

2.3.2. Characterisation of β-Lg nanoparticles

2.3.2.1 Stability to dissociating buffers

In order to get an insight into the type of the microstructure formed and the main interactions governing its formation, the stability of the particles to several buffers was investigated. All samples were filtered by 0.45 µm filter before the incubation with dissociation buffers. The effect of dissociating buffers was determined based on changes in particle size (Table 2.1).

Table 2.1: Effect of dissociating buffers on nanoparticle diameter (nm). The incubation time with dissociating buffers was 60 minutes.

Treatment	Before incubation	10M Urea	1%(W/V) SDS	0.1 M 2-Mercap-toethanol	0.1 M DTT
Particle size	173.0±12.5 [a]	234.2±1.9[b]	17.41±8.8[c]	176.5±0.6[a]	186.1±1.5 [a]

Experiments were carried out in duplicate, mean values with different superscript letters are significantly different at $p < 0.05$, the particle size before incubation is lower than 200 nm due to the filtration of 0.45 mm filter.

Sodium dodecyl sulphate (SDS) interacts with proteins via electrostatic interactions and hydrophobic interactions while keeping covalent bonds intact (Reynolds & Tanford, 1970; Roy, Kumar, & Gurusubramanian, 2012). A significant reduction in particle size was observed which demonstrates that hydrophobic interactions are essential to the stabilisation of the microstructure of these particles.

Urea is a very powerful protein denaturant with the ability to break hydrogen bonds. It

is considered that urea acts by breaking down protein hydrogen bonds as it interacts with peptide groups in unfolded proteins by hydrogen bonding. Interestingly, most β-Lg nanoparticles were not disrupted by urea. On the contrary, the particle size increased significantly as demonstrated. The swelling of the nanoparticles could be due to the formation of hydrogen bonds with the water molecules within the particles (Huppertz & de Kruif, 2008). These results demonstrated the presence of hydrogen bonds within the internal structure of β-Lg nanoparticles.

2-Mercaptoethanol was added to β-Lg nanoparticle dispersions to cleave disulphide bonds. Interestingly, 2-Mercaptoethanol had no significant effect on the size of the nanoparticles, therefore, disulphide bonds were not responsible for the microstructure formation. In order to confirm the above results, another dissociating buffer, 0.1 M Dithiothreitol (DTT), was used. DTT is a dissociating buffer, which disrupts disulphide bonds. The nanoparticles were stable during incubation with DTT for 60 min and even after one day (data not shown here). These results confirmed that disulphide bonds were not mainly responsible for the microstructure formation. Various authors (Alting, Hamer, de Kruif, Paques, & Visschers, 2003; H. J. Giroux et al., 2010; S. Ko & S. Gunasekaran, 2006; Mudgal, Daubert, & Foegeding, 2011; Nicolai et al., 2011) have demonstrated the significant role of thiol-disulphide reactions in β-Lg aggregation but the reaction was shown to be favoured at neutral to alkaline pHs. In addition, Alting *et al.* (Alting et al., 2003) had further ascertained the fact that disulphide bonds did not significantly contribute to the acid-induced aggregation of diluted solutions of whey protein in the initial stage of aggregation. However, partially cross-linked disulphide bonds were found

in protein gels kept for a period of time, namely ageing period (Alting et al., 2003; H. J. Giroux et al., 2010; Nicolai et al., 2011). Alting et al. (2003) demonstrated that the formation of disulphide cross-linking was strongly affected by the pH (at pH 5 only 1:3160 sulphur groups is deprotonated and able to initiate thiol/disulphide exchange reactions) and protein concentration (4.5% initial protein concentration was identified as the critical value below which no significant crosslinking may occur). Since the β-Lg nanoparticles produced in this study did not undergo the aforementioned ageing period and the pH and protein concentrations were not favourable to disulphide cross-linking, it is reasonable to conclude that disulphide bonds did not actively participate in the formation of the microstructure of the nanoparticles produced in the current study.

In summary, the predominant interactions responsible for the microstructure of the nanoparticles were found to be hydrogen bonding and hydrophobic interactions. Increased hydrogen bonding induces the formation of β-sheets in a protein which, is commonly found in aggregates (Gunasekaran et al., 2006). Hydrophobic interactions also played a major role in the aggregation process of β-Lg as expected since this protein has significant portions of hydrophobic patches, with the exact effective hydrophobicity reported to be 12.2 (Gunasekaran et al., 2006; Hansted, Wejse, Bertelsen, & Otzen, 2011; S. Ko & S. Gunasekaran, 2006) and upon denaturation this area will be further exposed.

2.3.2.2. Microscope image of nanoparticle

To further characterise the microstructure of β-Lg nanoparticles, environmental scanning electron microscopy was carried out on samples produced at the optimum

conditions (described in 2.2.2.5.).

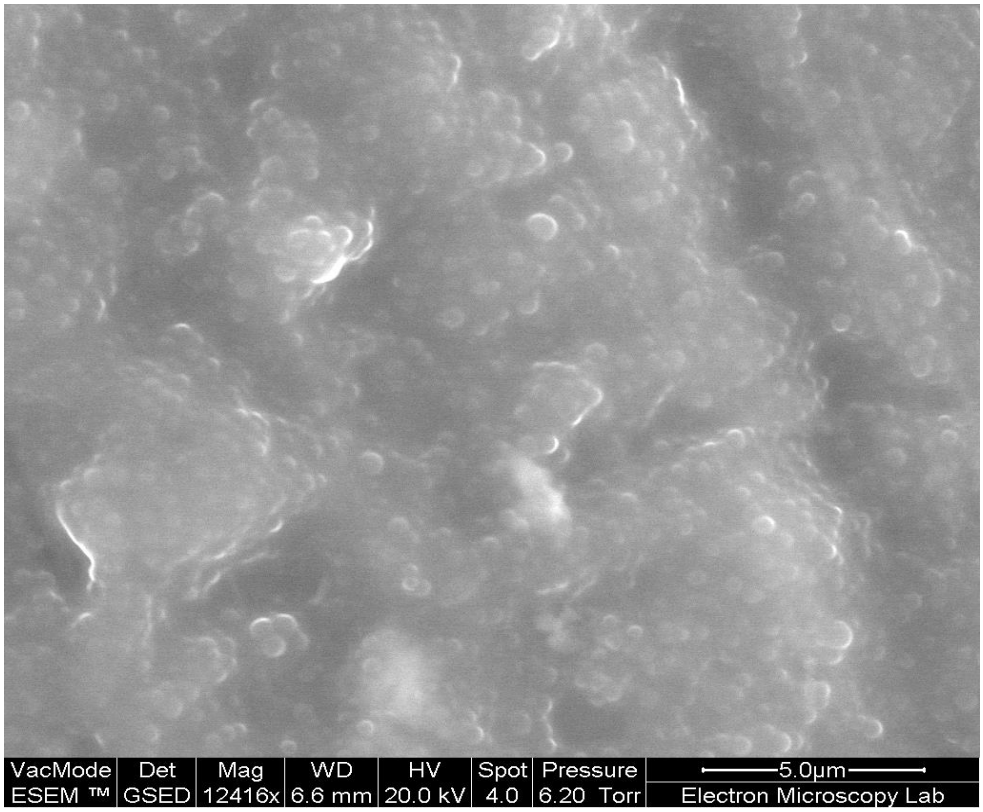

Figure 2.4: The ESEM image of β-Lg nanoparticles.

The ESEM image in Figure 2.4 showed spherical aggregates and in the range of sizes of those measured by DLS. This was in agreement with Krebs et al (Krebs, Devlin, & Donald, 2009) who reported the formation of spherical aggregates at the pH close to protein's pI. Moreover, the zeta potential of these nanoparticles was determined as the key indicator of the stability of colloidal dispersions. The zeta potential of the β-Lg dispersion was -37.42±2.93 mV, which indicated a moderate stable colloidal system.

2.3.2.3 Yield of aggregation of β-Lg

In preliminary filtration experiments with an aqueous solution of β-Lg and a 50 KDa ultrafiltration membrane, it was shown that any non-aggregated β-Lg permeated

through the ultrafiltration membrane and thus the aggregation yield was determined based on the determination of protein concentration in the permeate by using bicinchoninic acid (BCA) method as described in 2.2.2.4. Nearly 93% of β-Lg aggregated when heated at 75 °C for 45 min. These aggregation yields were similar to those reported by others at higher heat loads (L. Donato et al., 2009; H. J. Giroux et al., 2010; Moitzi et al., 2011; Mudgal et al., 2011; Schokker, Singh, Pinder, & Creamer, 2000); Giroux *et al.* (H. J. Giroux et al., 2010) reported an aggregation yield of 97.3% after heating 1% (w/v) whey protein dispersion at 80°C for 15 min.

2.3.2.4. β-lactoglobulin conformational changes by fluorescence spectroscopy

The β-Lg contains two Trp residues, Trp^{19} and Trp^{61}: Trp^{19} is within the cavity of β-Lg whereas Trp^{61} is located at the surface of the protein molecule and is close to the Cys^{66}-Cys^{160} disulfide bridge (B. Y. Qin, M. C. Bewley, et al., 1998; Qin, Creamer, Baker, & Jameson, 1998). The X-ray crystallographic image also illustrated that Trp^{19} is located in the interior of the β-Lg molecule, which is the major binding point of β-Lg (L. Sawyer, 2002). A mutant β-Lg molecule study helped to prove that Trp^{19} was a major fluorophore of β-Lg in the non-polar environment (Creamer, 1995). By the influence of heat, the conformation changed at about 50 °C, one of the tryptophan was transferred to a more polar environment accessible to solvent and above 70°C the second tryptophan residue became exposed to solvent. But even at 90°C, the second one was partially buried (O. E. Mills, 1976). Therefore in order to investigate conformational changes in β-Lg after heat denaturation and after caffeine encapsulation, the fluorescence emission spectra of

tryptophan was measured (Figure 2.5). An increase in the fluorescence intensity was observed for β-Lg nanoparticles and a fluorescence quenching effect by the caffeine upon binding to the nanoparticles. The increase in fluorescence intensity can be explained based on the exposure of previously buried Trp groups upon heating induced conformational changes in the protein.

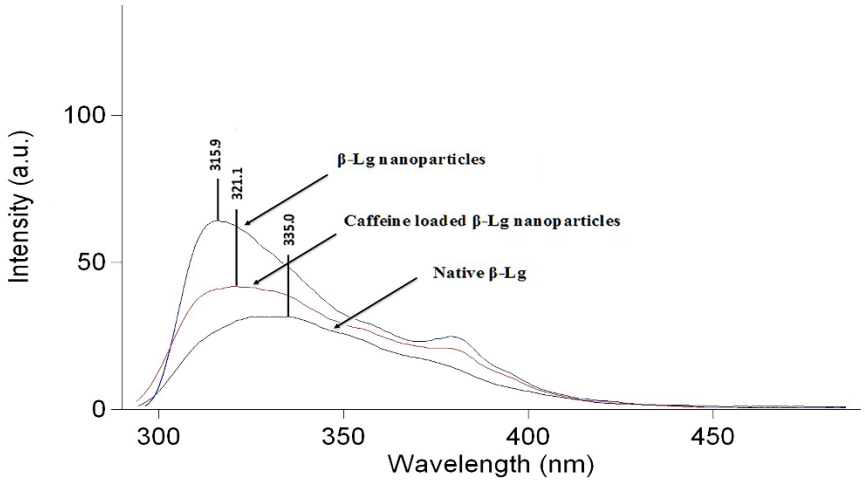

Figure 2.5: The fluorescence emission changes of native β-Lg, β-Lg nanoparticles and caffeine-loaded β-Lg nanoparticles.

2.3.2.5. Mechanism of nanoparticle formation

Based on previous studies on β-Lg and our observations above the following mechanism of nanoparticle formation is proposed. At neutral pH, β-Lg exists as dimer in aqueous solution. Upon pH adjustment (to pH 6) and heating the dimer dissociates and denatures to reactive monomers. Protein molecules start to unfold, and hydrophobic groups are exposed (as shown by fluorescence measurements) which promote intermolecular non-covalent interactions (hydrophobic interactions, and hydrogen bonding) to form

particles of a given microstructure as demonstrated by the stability to buffers. Although at these denaturing conditions, the reactive thiol group in the protein would get exposed the pH and protein concentration conditions (and lack of ageing time) used in this study did not lead to the formation of disulphide bonds and subsequent cross-linked gel-like structure. Moreover, the spherical aggregates (as visualised by ESEM) had a good colloidal stability which was supported by an overall strong negative charge (-37.42±2.93 mV) measured as zeta-potential.

2.3.3. Yield of caffeine encapsulation

The yield of caffeine encapsulation increased when caffeine to β-Lg molar ratio increased reaching a maximum 13.54% at a molar ratio of 50 (mass ratio caffeine to ß-Lg 1:2) (Table 2.2). Above this maximum, a slow reduction of the percentage of caffeine encapsulation was observed for higher caffeine to β-Lg molar ratio values. In addition, caffeine-loaded particles were significantly larger than those without caffeine (over 350 nm). Li *et al.* (B. Li, Du, Jin, & Du, 2012) and Shpingelman *et al.* (A. Shpigelman, Y. Cohen, & Y. D. Livney, 2012) had also found a similar trend for their EGCG (epigallocathechin-3-gal-late)-loaded β-Lg nanoparticles.

Table 2.2: Caffeine encapsulation by β-Lg nanoparticles. (All the encapsulation efficiency results are the average of three replicates)

Caffeine to β-Lg molecular ratio	*10:1*	*20:1*	*50:1*	*100:1*	*200:1*
Encapsulation efficiency (%)	*10.25±1.2^{b}*	*11.68±3.0^{a}*	*13.54±3.3^{a}*	*10.07±2.0^{c}*	*9.73±0.2^{d}*
Particle size (nm)	*374.1±5.1^{a}*	*366.5±4.7^{b}*	*381.7±1.7^{c}*	*359.6±3.0^{d}*	*356.0±2.6^{d}*

Experiments were carried out in triplicate, mean values with different superscript letters are significantly different at $p < 0.05$

The same results were plotted as an adsorption isotherm (Figure 2.6) as it was hypothesised that caffeine bound (adsorbed) the exterior of the nanoparticles up to reaching equilibrium concentration. Interestingly it was found that the equilibrium concentrations of caffeine bound (measured as caffeine mass per protein mass) and caffeine free in solution followed a Langmuir type isotherm. Parameters of adjustment of experimental data to Langmuir model were shown in Table 2.3

Table 2.3: Adjustment of caffeine adsorption to Langmuir model.

	Native β-Lg	***β-Lg nanoparticles***
Cad $_{max}$	0.103 mg/mg protein	0.263 mg/mg protein
k	1.194 ml/mg	0.423 ml/mg
r^2	0.96332	0.96244

In the case of nanoparticles, a maximum binding capacity of 0.205 mg caffeine per mg β-Lg was found which means 19.4 molecules of caffeine per protein. However, when the same experiments were conducted with native β-Lg the maximum binding capacity was

only 0.084 mg caffeine per mg protein. Additionally, caffeine showed three times more affinity for partially denatured β-Lg in nanoparticles than for native protein.

This clearly showed that the conformational change induced in the protein due to heat denaturation led to an increase in binding capacity.

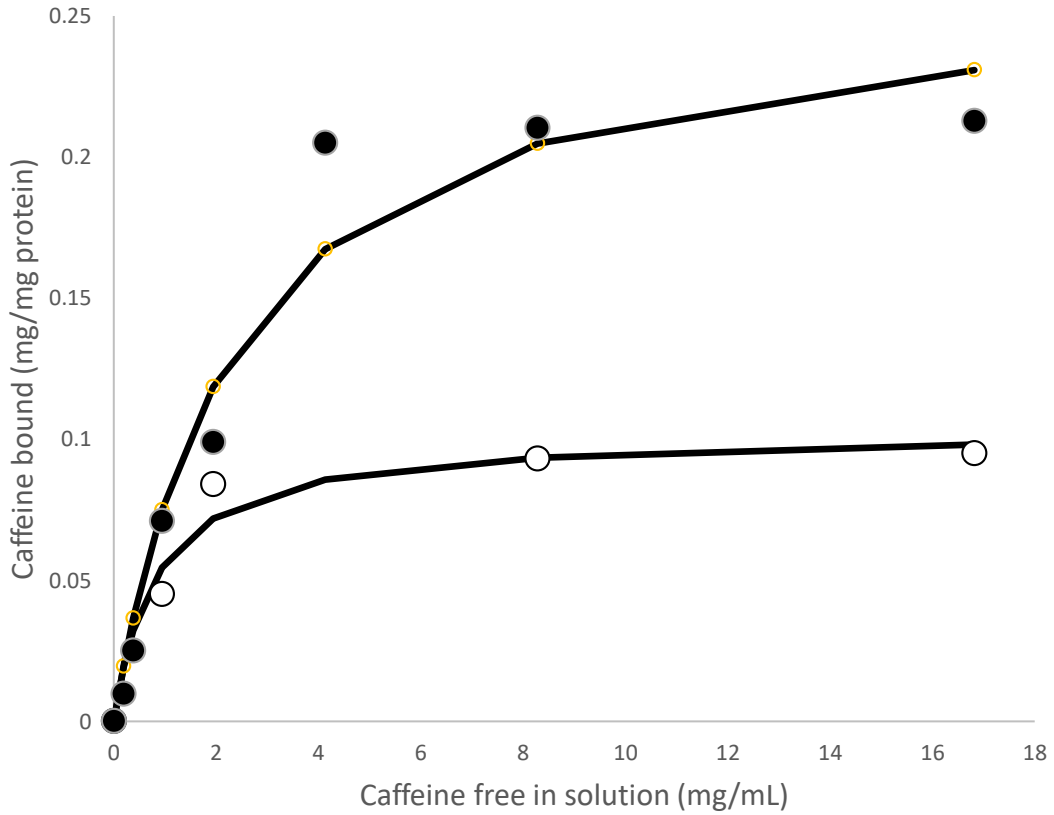

Figure 2.6: Isotherm of caffeine encapsulation of native β-Lg (white circles) and the β-Lg nanoparticles (black circles). Lines represent adjustment to Langmuir model.(. Each of these experiments did in duplicate. For β-Lg nanoparticles (black circles), Standard deviations of Caffeine bound was 0.000116-0.000915 mg/mg protein. Standard deviations of Caffeine free in solution was 0.000466-0.010735mg/ml. For native β-Lg (white circles), Standard deviations of Caffeine bound was 0.001437-0.017185 mg/mg protein. Standard deviations for Caffeine free in solution was 0.001437-0.0017185 mg/ml).

2.3.4. Simulated gastric digestion

The in-vitro experiment was carried out by suspending the nanoparticles containing caffeine in simulated gastric fluid (SGF) with pepsin for 120 min under continuous shaking at 37°C. Conditions of temperature and pH were set equivalent to the normal gastric digestion conditions (A. Shpigelman et al., 2012). The protein: enzyme ratio (1.875:1) used here was similar ratio to that reported in other works (L. Chen & M. Subirade, 2005; Sarkar et al., 2009; A. Shpigelman et al., 2012; Zeese et al., 2008). It is important to note that optimal ratio that suits the exact physiological secretion in humans was extremely hard to establish due to the variation in gastric secretions in different individual's health conditions and food choice (Sarkar et al., 2009). Various protein: enzyme ratio had been proposed by Kibatake and Kinekawa (1998), Zeese et al. (2008), Sarkar et al. (2009), and A. Shpigelman et al. (2012), but all the authors claimed that complete hydrolysis of β-Lg was not achievable at any given pepsin concentration. Therefore, this ratio was chosen here to expose β-Lg nanoparticles to more extreme gastric conditions.

Upon addition to SGF, the pH of the β-Lg dispersions dropped immediately to around ~1.5 to mimic the empty stomach pH and to provide the optimum conditions for hydrolysis by pepsin. Rapid decay of particle size was observed (Figure 2.7) and during the incubation period polydispersity increased which can be a consequence of the unspecific action of pepsin on the peptide bonds.

So particle degradation happened in the first 2 minutes. At this time particle size reduced to 5 nm which corresponds to the average size of a protein dimer (Nicolai et al., 2011;

Sakurai, Oobatake, & Goto, 2001) and the size remained to less than 10 nm with no significant difference for 60 minutes (Figure 2.7).

High Burst effect was observed in the kinetics of caffeine release revealing a common problem in the development of controlled release formulations when low molecular weight compounds are loaded into nanoparticles. This Burst effect seems related to the rapid nanoparticle degradation. In spite of this, high amounts of caffeine were retained in the nanoparticle (68.14% at 2 minutes) and slow and little release of entrapped caffeine was noted, even at the end of incubation (36.40%).

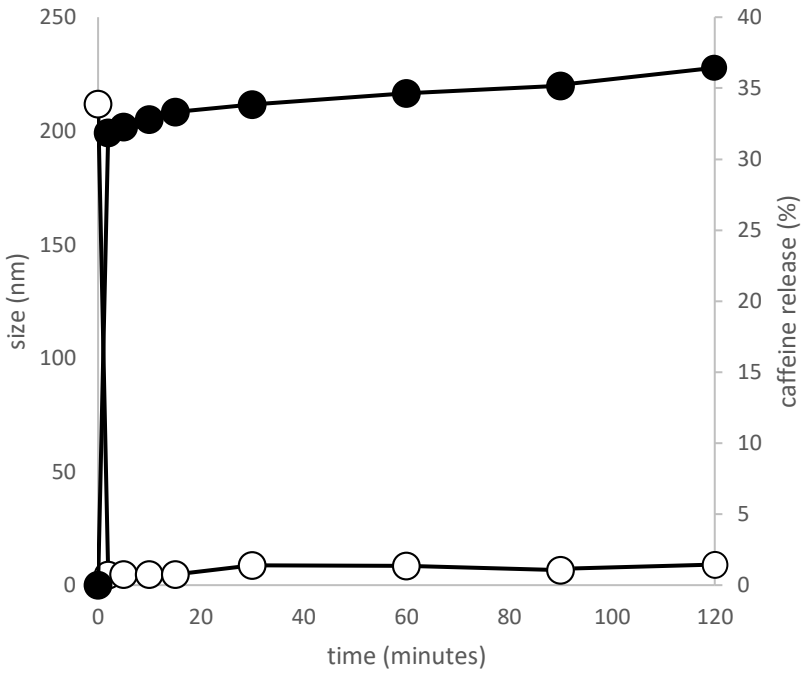

Figure 2.7: The release of caffeine and changes of nanoparticles size under SGF. Black circles: Caffeine release percentage under SGF condition. White circles: Stability of β-Lg nanoparticles SGF condition. (Each of these experiments did in duplicate with standard deviations 2.21-3.19% for release and for size 0.80-2.33 nm).

Moreover, the gastric digestion applied in the gastrointestinal digestion experiments, where lower protein to pepsin ratio was used (1:9) than in the gastric digestion experiments (1.87:1) (see Methods), led to similar results, 36.71% caffeine released. Furthermore, almost all the caffeine was released after the small intestinal digestion phase (99.22%). Our results agreed with those of A. Shpigelman et al. (2012) as their β-Lg-EGCG complex managed to preserve 79% of their contents after 180 min of incubation in 1:20 pepsin: protein ratio solution.

The fact that most of the caffeine was still bound to the protein after the microstructure has been destroyed indicates that the binding of the caffeine to protein was not so dependent on the microstructure but on the protein conformation and the establishment of interactions (most probably hydrophobic and hydrogen bonds) between the protein molecule and the caffeine.

2.4. Conclusion

One of the main outcomes of this study is that we have developed a simple method that relies on the heat denaturation of β-Lg and leads to the consistent production of nanoparticles of given size (average diameter 200-300 nm) and characteristics with colloidal stability and high yield of aggregation (>93%) at the optimum conditions of pH (6.0) and heat load (heating at 75 °C for 45 mins), which were found to be the key operating parameters. The characterisation of the nanoparticles by a range of techniques including fluorescence, DLS, and microscopy in combination with the measurement of their stability to buffers led to an improved insight of their formation and their microstructure at the optimum conditions. In summary, heat denaturation led to the protein unfolding, exposure of hydrophobic regions and subsequent formation of protein aggregates by non-covalent intermolecular interactions.

Maximum encapsulation efficiency of caffeine was 13.54% at 50:1 caffeine to β-Lg molar ratio. Caffeine-β-Lg nanoparticles (~350 nm) were found significantly larger than pure β-Lg nanoparticles (~250 nm). Heating of β-Lg unfolded the non-polar region in the protein and led to an increase in binding of caffeine as compared to native β-Lg. Interestingly，the binding of caffeine to protein followed a Langmuir type isotherm. Both pure β-Lg and caffeine loaded β-Lg nanoparticles exhibited rapid peptic degradation, but only 36.4% caffeine was released under these conditions and complete release at intestinal conditions, hence suggesting improved enteric delivery. Furthermore, both the fitting of the experimental results to a binding isotherm and the low release of caffeine even when complete disruption of the microstructure occurred suggest that caffeine binds to the

unfolded protein molecule at a maximum ratio of 19 molecules of caffeine per molecule of protein. Overall the encapsulation efficiency was slightly better than that obtained with liposomes nanoparticles (3.8% to 9.7%) produced by Pham, Jaafar-Maalej, Charcosset, and Fessi (2012) utilising phospholipid and cholesterol and less than that obtained with niosomes particles produced from cholesterol and surfactant (30.4%) by Khazaeli, Pardakhty, and Shoorabi (2007) but with significantly larger vesicle sizes (6-22μm). Spontaneous binding of caffeine to β-Lg nanoparticles could open the opportunity for the application of this milk protein as a molecular nano-vehicle to manufacture products fortified with caffeine without intense bitterness that may interfere with the original product flavour. Other potential applications include the binding of bioactives to improve their solubility and/or bioavailability.

Conflict of interest statement

The author declares that there are no conflicts of interest.

Acknowledgements

Special thanks to Thong Thong Choo who initiated part of this work as an MSc project which formed the basis of the current project.

References

Afferstsholt, T., & Palmer, S. (2009). Whey proteins: continued market growth despite economic crisis. *NUTRAfoods, 8*, 56-58.

Alting, A. C., Hamer, R. J., de Kruif, C. G., Paques, M., & Visschers, R. W. (2003). Number of thiol groups rather than the size of aggregates determines the hardness of cold set whey protein gels. *Food Hydrocolloids, 17*, 469-479.

Bauer, R., Carrotta, R., Rischel, C., & Ogendal, L. (2000). Characterisation and isolation of intermediates in ß-lactoglobulin heat aggregation. *Biophysical Journal, 79*, 1030-1038.

C. Baldasso, T.C. Barros, & Tessaro, I. C. (2011). Concentration and purification of whey proteins by ultrafiltration. *Desalination, 278*(1-3), 381-386.

Chanasattru, W., Jones, O. G., Decker, E. A., & McClements, D. J. (2009). Impact of cosolvents on formation and properties of biopolymer nanoparticles formed by heat treatment of β-lactoglobulin–Pectin complexes. *Food Hydrocolloids, 23*(8), 2450-2457.

ChemBK. (2017). DL-Dithiothreitol.

Retrieved from http://www.chembk.com/en/chem/L-DTT

Chen, L., Remondetto, G. E., & Subirade, M. (2006). Food protein-based materials as nutraceutical delivery systems. *Trends in Food Science & Technology, 17*(5), 272-283.

Chen, L., & Subirade, M. (2005). Chitosan/ß-lactoglobulin core -shell nanoparticles as nutraceutical carriers. *Biomaterials, 26*, 6041-6053.

Creamer, L. K. (1995). Effect of sodium dodecyl sulfate and palmitic acid on the equilibrium unfolding of bovine β-lactoglobulin. *Biochemistry 1995*(34), 7170-7176.

Donald, A. M. (2007). Why Should Polymer Physicists Study Biopolymers? *Journal of Polymer Science: Part B: Polymer Physics, 45*, 3257-3262.

Donato, L., Schmitt, C., Bovetto, L., & Rouvet, M. (2009). Mechanism of formation of stable heat-induced ß-lactoglobulin microgels. *International Dairy Journal, 19*, 295-306.

Gilbert, R. M. (1984). Caffeine consumption. *Prog Clin Biol Res, 158*, 185-213.

Giroux, H. J., & Britten, M. (2011). Encapsulation of hydrophobic aroma in whey protein nanoparticles. *Journal of Microencapsulation (Micro and Nano Carriers), 28*(5), 337-343.

Giroux, H. J., Houde, J., & Britten, M. (2010). Preparation of nanoparticles from denatured whey protein by pH-cycling treatment. *Food Hydrocolloids, 24*, 341-346.

Gulseren, I., Fang, Y., & Corredig, M. (2012). Whey protein nanoparticles prepared with desolvation with ethanol: characterisation, thermal stability and interfacial behavior. *Food Hydrocolloids, 29*, 258-264.

Gunasekaran, S., Ko, S., & Xiao, L. (2006). Use of whey proteins for encapsulation and controlled delivery applications. *Journal of Food Engineering, 83*, 31-40.

Hansted, J. G., Wejse, P. L., Bertelsen, H., & Otzen, D. E. (2011). Effect of protein-surfactant interactions on aggregation of ß-lactoglobulin. *Biochimica Et Biophysica Acta, 1814*, 713-723.

Havea, P., Singh, H., & L.K., C. (2001). Characterization of heat-induced aggregates of β-lactoglobulin, α-lactalbumin, and bovine serum albumin in a whey protein concentrate environment. *Dairy Research, 68*(3), 483-497.

Huppertz, T., & de Kruif, C. G. (2008). Structure and stability of nanogels particles prepared by internal cross-linking of casein micelles. *International Dairy Journal, 18*, 556-656.

Jauregi, P., & Welderufael, F. (2010). Added-value protein products from whey extraction, fractionation, separation, purification. *Nutrafoods, 9*(4), 13-23.

Jones, O. G., Lesmes, U., Dubin, P., & McClements, D. J. (2010). Effect of polysaccharide charge on formation and properties of biopolymer nanoparticles created by heat treatment of ß-lactoglobulin-pectin complexes. *Food Hydrocolloids, 24*, 374-383.

Khazaeli, P., Pardakhty, A., & Shoorabi, H. (2007). Caffeine-loaded niosomes: characterisation and *in vitro* release studies. *Drug Delivery, 14*, 447-452.

Kibatake, N., & Kinekawa, Y. (1998). Digestibility of bovine milk whey protein and ß-lactoglobulin in vitro and in vivo. *J. Agric. Food Chem., 46*, 4917-4923.

Ko, S., & Gunasekaran, S. (2006). Preparation of sub-100-nm ß-lactoglobulin (BLG) nanoparticles. *Journal of Microencapsulation, 23*, 887-898.

Krebs, M. R. H., Devlin, G. L., & Donald, A. M. (2009). Amyloid fibril-like structure underlies the aggregate structure across the pH range for ß-lactoglobulin. *Biophysical Journal, 96*, 5013-5019.

Li, B., Du, W., Jin, J., & Du, Q. (2012). Preservation of (-)-Epigallocatechin-3-gallate Antioxidant Properties Loaded in Heat Treated beta-Lactoglobulin Nanoparticles. *Journal of Agricultural and Food Chemistry, 60*(13), 3477-3484.

Livney, Y. D. (2010). Milk proteins as vehicles for bioactives. *Current Opinion in Colloid & Interface Science, 15*(1-2), 73-83. doi:10.1016/j.cocis.2009.11.002

Maccaferri, S., Klinder, A., Cacciatore, S., Chitarrari, R., Honda, H., Luchinat, C., Costabile, A. (2012). In vitro fermentation of potential prebiotic flours from natural sources: Impact on the human colonic microbiota and metabolome. *Molecular Nutrition&Food Research, 56*(8), 1342-1352.

Mehalebi, S., Nicolai, T., & Durand, D. (2008). Light scattering study of heat-denatured globular protein aggregates. *International Journal of Biological Macromolecules, 43*, 129-135.

Mills, D. J. S., Tuohy, K. M., Booth, J., Buck, M., Crabbe, M. J. C., Gibson, G. R., & Ames, J. M. (2008). Dietary glycated protein modulates the colonic microbiota towards a more detrimental composition in ulcerative colitis patients and non-ulcerative colitis subjects. *Journal of Applied Microbiology, 105*, 706-714.

Mills, O. E. (1976). Effect of temperature on tryptophan fluorescence of beta-lactoglobulin B. *Biochim Biophys Acta, 434*(2), 324-332.

Moitzi, C., Donato, L., Schmitt, C., Bovetto, L., Gillies, G., & Stradner, A. (2011). Structure of ß-lactoglobulin microgels formed during heating as revealed by small-angle X-ray scattering and light scattering. *Food Hydrocolloids, 25*, 1766-1774.

Mudgal, P., Daubert, C. R., & Foegeding, E. A. (2011). Kinetic study of ß-lactoglobulin thermal aggregation at low pH. *Journal of Food Engineering, 106*, 159-165.

Nicolai, T., Britten, M., & Schmitt, C. (2011). ß-lactoglobulin and WPI aggregates: formation, structure and applications. *Food Hydrocolloids, 25*, 1945-1962.

Pham, T. T., Jaafar-Maalej, C., Charcosset, C., & Fessi, H. (2012). Liposome and niosome preparation using a membrane contactor for scale-up. *Colloids and Surfaces B-Biointerfaces, 94*, 15-21.

Qin, B. Y., Bewley, M. C., Creamer, L. K., Baker, H. M., Baker, E. N., & Jameson, G. B. (1998). Structural basis of the Tanford transition of bovine ß-lactoglobulin. *Biochemistry, 1998b*(37), 14014-14023.

Qin, B. Y., Creamer, L. K., Baker, E. N., & Jameson, G. B. (1998). 12-Bromododecanoic acid binds inside the calyx of bovine β-lactoglobulin. *FEBS Lett., 1998a*(438), 272-278.

Reynolds, J. A., & Tanford, C. (1970). Binding of Dodecyl Sulfate to Proteins at High Binding Ratios. Possible Implications for the State of Proteins in Biological Membranes. *National Academy of Sciences, 66*(3), 1002-1007.

Ron, N., Zimet, P., Bargarum, J., & Livney, Y. D. (2010). Beta-lactoglobulin-polysaccharide complexes as nanovehicles for hydrophobic nutraceuticals in non-fat foods and clear beverages. *International Dairy Journal, 20*(10), 686-693. doi::10.1016/j.idairyj.2010.04.001

Roy, V. K., Kumar, S., & Gurusubramanian, G. (2012). Protein-structure, properties and their separation by SDS polyacrylamide gel electrophoresis *Sicencevision 12*(4), 170-181.

Sakurai , K., Oobatake , M., & Goto, Y. (2001). Salt-dependent monomer–dimer equilibrium of bovine β-Lg at pH 3. *Protein Science 10*, 2325-2335.

Sarkar, A., Goh, K. K. T., Singh, R. P., & Singh, H. (2009). Behaviour of an oil-in -water emulsion stabilised by ß-lactoglobulin in an *in vivo* gastric model. *Food Hydrocolloids, 23*, 1563-1569.

Sawyer, L. (2002). Beta-Lactoglobulin: Properties, structure and function. *Journal of Dairy Science, 85*(Supplement 1), 50.

Schokker, E. P., Singh, H., Pinder, D. N., & Creamer, L. K. (2000). Heat-induced aggregation of ß-lactoglobulin AB at pH= 2.5 as influenced by ionic strength and protein concentration. *International Dairy Journal, 10*, 233-240.

Shpigelman, A., Cohen, Y., & Livney, Y. D. (2012). Thermally-induced ß-lactoglobulin-EGCG novehicles: loading, stability, sensory and digestive-release study. *Food Hydrocolloids, 29*, 57-67.

Sigma-Aldrich. (2017). 2-Mercaptoethanol ≥99.0% |Sigmaaldrich.com. Retrieved from 31 January 2017, http://www.sigmaaldrich.com/catalog/product/aldrich/m6250?lang=en&region=GB

Somogyi, L. P. (2010). Caffeine Intake by the U.S. Population.

Tauliera, N., & Chalikiana, T. V. (2001). Characterization of pH-induced transitions of β-lactoglobulin: ultrasonic, densimetric, and spectroscopic studies. *Journal of Molecular Biology 314*(4), 873-889.

Tumolo, T., Angnes, L., & Baptista, M. S. (2004). Determination of the refractive index increment (dn/dc) of

molecule and macromolecule solutions by surface plasmon resonance. *Analytical Biochemistry, 333*(2), 273-279.

Warren, J., & Gordon, J. (1966). On the Refractive Indices of Aqueous Solutions of Urea. *The Journal Of Physical Chemistry, 70*(1), 297-300.

Zeese, M., Huppertz, T., & Kelly, A. (2008). Effect of high-pressure treatment on in-vitro digestibility of ß-lactoglobulin. *Innovative Food Science and Emerging Technologies, 9*, 62-69.

Zimet, P., & Livney, Y. D. (2009). Beta-lactoglobulin and its nanocomplexes with pectin as vehicles for omega-3 polyunsaturated fatty acids. *Food Hydrocolloids, 23*(4), 1120-1126. doi:10.1016/j.foodhyd.2008.10.008

CHAPTER THREE

Characterisation of resveratrol-β-lactoglobulin nanoparticles and thermal stability

ABSTRACT

Resveratrol, a phenolic antioxidant which widely distributed in many plants, is proved to exhibits many health benefits properties such as anti-inflammatory, antioxidant and antimicrobial activities. However, low solubility and instability of resveratrol are main impediments to achieve its bioavailability. Beta-lactoglobulin (ß-Lg), the major whey protein, is believed to play an important role to transport small hydrophobic molecules. The solubility of resveratrol was determined as 5-7mg/100ml by total phenolic content (spectrophotometric and Folin method). Production of resveratrol-beta-lactoglobulin nanoparticles was produced according to the method (pH 6 and 75°C, 45 min) developed by the previous study. The size of resveratrol-ß-Lg nanocomplexes was 181.8 nm, and the concentration of resveratrol had no influence on the size of nanoparticles. During heating, a thermal degradation and isomerization happened, and resveratrol-ß-Lg nanoparticles exhibited an improved antioxidant activity even though the fluorescence measurement confirmed that native ß-Lg have stronger binding ability than nanoparticles form. The binding of resveratrol and native ß-Lg was following a Stern-Volmer model; binding constant was $1.67x10^5$, and the binding number is 1.33. No binding model was found to fit Resveratrol-ß-Lg nanoparticles. Resveratrol-ß-Lg nanoparticles maintained the antioxidant activity level under Pasteurisation. Therefore, Beta-lactoglobulin has the potential to protect the antioxidative properties of

resveratrol under thermal processing and could be utilised for food applications.

Keywords: Resveratrol, Beta-lactoglobulin, Nanoparticles, Antioxidant activity.

3.1. Introduction

Nowadays, consumers are attracted to dietary supplements instead of drugs to improve health and oral administration is the most convenient and commonly applied method to develop new nutraceutical. Based on many studies, the predominant problem of nutraceuticals is poor bioavailability due to their low aqueous solubility which, affects over 40% of the new chemical entities produced by high throughput screening processes (Lipinski, 2002). Several reasons contribute to the solubility problem: 1) high Molecular weight; 2) high Log of the octanol-water partition coefficient (log P), which is a measure of a drug's lipophilicity. In order to improve the aqueous solubility, numerous researchers have developed many approaches such as particle size reduction, crystal engineering, salt formation, solid dispersion and use of surfactant, complexation (Savjani, Gajjar., & Savjani, 2012). New techniques like nanoparticles, nanotubes, nanosuspensions and nanocomplexes are employed to improve the solubility of poorly soluble drugs and nutraceuticals (Rabinow, 2004; Tran, Tran, & Lee, 2013). Proteins like zein, whey proteins, soy proteins and other natural polymers like cyclodextrins have been applied not only in pharmaceutical but also in food applications (Duarte et al., 2015; Gorji et al., 2015; Pujara, Jambhrunkar, Wong, McGuckin, & Popat, 2017). Empirically, the nutraceuticals have similar benefits as pharmaceuticals but without all of the side effects. Therefore, in the food industry, the concept of “General Recognised As Safe” (GRAS) has been

applied to nutraceuticals supplements since 1958 (Burdocka & Carabin, 2004). Simple and safe carrier candidates, which meet the GRAS qualification and possibly have essential health benefits, should be investigated to improve aqueous solubility of bioactives.

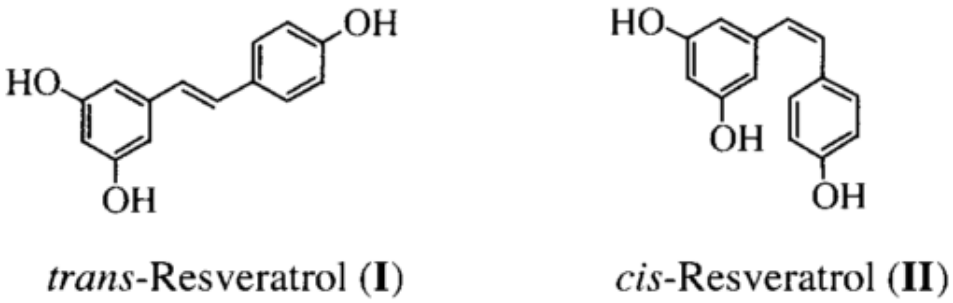

trans-Resveratrol (**I**) *cis*-Resveratrol (**II**)

Figure 3.1: the chemical structure of Trans-Resveratrol and cis- Resveratrol (Burns et al., 2002).

Resveratrol (3,5,4'-Trihydroxystilbene), is a typical non-flavonoid phenol that belongs to the stilbene family and has various properties including antioxidant, anti-cancer, anti-inflammatory, and antineoplastic (Bhat & Pezzuto, 2002; Jang et al., 1997; Soleas, Diamandis, & Goldberg, 1997). Resveratrol is thought to be one of the main contributors to the famous “French paradox”: despite the French people’s high-fat intake, a low cardiovascular diseases incidence was found. It has been ascribed partly to the red wine consumption (Catalgol, Batirel, Taga, & Ozer, 2012). Since then, the studies of resveratrol have been carried out broadly in the food and pharmacy field. There are 72 different natural resources which contain resveratrol, especially grapes, peanuts and blueberries (Burns et al., 2002; Jimenez-Garcia et al., 2012; Limmongkon et al., 2017; Lyons et al., 2003). Even though resveratrol is widely distributed in various plants and

fruits, there are some pharmacokinetic limitations, which led to low bioavailability: The low water solubility, labile properties, and rapid metabolism (Amri, Chaumeil, Sfar, & Charrueau, 2012; Database, 2017; Pund, Joshi, & Patravale, 2016). The low solubility of resveratrol in oral administration is due to the chemical structure of resveratrol: two phenolic rings bonded together by a double styrene bond, which contributes two isometric cis- and trans-forms of resveratrol (Figure 3.1) (Gambini et al., 2015). It is believed that the trans-isomeric form is more abundant than cis-resveratrol, while the trans-isomer is able to transform into cis-isomer under light exposure and heating. Light exposure allows a rapid isomerization of trans-resveratrol, especially in the ultraviolet radiation at 366nm or at low concentration (Flieger, Tatarczak-Michalewska, & Blicharska, 2017; Frkmont, 2000; Gambini et al., 2015; Trela & Waterhouse, 1996). Heating not only leads to increasing of solubility but also results in degradation, isomerization and reduction of antioxidant activity. The effect of heating on resveratrol can be complex depending on temperature (Flieger et al., 2017; Lee et al., 2014). In order to overcome its low solubility and low stability hence to achieve bioavailability, encapsulation might be a solution to handle these limitations of resveratrol. The encapsulation of resveratrol with a number of biopolymers has been investigated including chitosan and γ-poly (Jeon, Lee, & Lee, 2016), soy protein isolate (Pujara et al., 2017), milk protein (Gorji et al., 2015) and zein (Penalva et al., 2015) and β-lactoglobulin (Zhang et al., 2014). The main whey protein, β-lactoglobulin, plays an interesting role in transporting retinol molecules and has binding properties of small hydrophobic molecules. Resveratrol has been found to be bound to the surface of the hydrophobic

pocket of β-lactoglobulin (Liang & Subirade, 2010; Liang, Tajmir-Riahi, & Subirade, 2008). Thus, β-lactoglobulin can be an attractive candidate as a carrier to offer a solution to both, poor solubility and low stability to processing /storage conditions such as heating and light exposure.

In Chapter two, β-lactoglobulin nanoparticles were found to complex with caffeine (Guo, Harris, Kaur, Pastrana, & Jauregi, 2017). Higher binding affinity for caffeine in nanoparticles form rather than in the native form was found. The aim of the present work is to apply this method to produce resveratrol-β-lactoglobulin nanoparticles, investigate the effect of these nanoparticles and native β-lactoglobulin on the solubility and stability of resveratrol under different thermal processing conditions. In addition, fluorescence measurements were carried out to gain an insight into the interactions between these two molecules. Moreover, the stability of resveratrol to light is investigated. The results of this study might be useful in the investigation of future carriers for stabilisation and delivery of resveratrol.

3.2. Materials and methods

3.2.1. Material

98% w/w trans-resveratrol is supplied by HPLC from Evolva RES140332

β-Lactoglobulin from bovine milk ≥ 85.0 % (PAGE), lyophilized powder L2506 is purchased from Sigma

Folin-Ciocalteu reagents: Folin-Ciocalteu (F9252), and Sodium carbonate BioXtra, ≥99.0% (S7795) is purchased from Sigma

Reagents of ABTS method: 2,2'-Azino-bis(3-ethylbenzothiazoline-6-sulfonic acid) diammonium salt (ABTS) ≥98.0 % (HPLC) (A1888), Potassium persulfate (K2S2O8) ACS reagent, ≥99.0% (216224)；(±)-6-Hydroxy-2,5,7,8-tetramethylchromane-2-carboxylic acid (Trolox), 97% (238813), and ethanol, ≥99.8% (GC) (32221) are purchased from Sigma-Aldrich

Reagents of the ferric reducing antioxidant power (Frap) method reagents：

TPTZ (2,4,6-Tris(2-pyridyl)-s-triazine) (T1253)； Ferric Chloride Hexahydrate(207926) are purchased from Sigma-Aldrich.

3.2.2. Determination of resveratrol solubility in water solution

A series of resveratrol solutions/suspensions were prepared from 1mg/100ml, 3mg/100ml, 5mg/100ml, 7mg/100ml, 8mg/100ml, and 9ml/100ml to determine the solubility of resveratrol. All the solutions/suspensions were covered by tissue paper and were stirring with a magnetic stirrer at room temperature for 2 hours before any measurements. Two methods were applied to determine resveratrol solubility in water

solution: the direct spectrophotometric method and total phenolic content by Folin-Ciocalteu method.

The direct spectrophotometric method: The Lambda max value of resveratrol aqueous solution (2mg/100ml) was determined by using a Lambda 20 spectrophotometer (Perkin-Elmer®) and scanning UV absorption from wavelength 190nm to 600nm with 1 nm spectral bandwidth. The absorbance of resveratrol solutions/suspensions was measured at the maximum wavelength by the Spectrophotometers (Ultrospec ® 1100 pro) using a quartz cuvette with a path length of 1cm and deionized water was used as the blank. The solubility of resveratrol at room temperature was determined from the plot of the absorbance against concentration as the concentration after which no further significant increases were observed.

Folin-Ciocalteu method: The total phenolic content of all concentrations of resveratrol solutions/suspensions was measured by Folin- Ciocalteu method at 760nm, which was adapted from L.Singleton, Orthofer, and M.Lamuela-Raventós (1999). In general, 0.2 ml of resveratrol solution was added to around 6.0ml of deionized water into a 10ml volumetric flask. Folin-Ciocalteu reagent (0.5ml) was added and mixed. After 1 minute and no longer than 8 minutes, 1.5 ml 20% sodium carbonate solution was added and the volume adjusted to 10ml. After 2 hours incubation in the dark, the absorbance was recorded at 760nm using a UV-Vis Spectrophotometer (Ultrospec ® 1100 pro). Deionised water was used as the blank. All the experiments were carried out in triplicates, and the results were expressed in gallic acid equivalents (GAE; mg/L) using a gallic acid (10-120mg/L) standard curve. The solubility of resveratrol was determined as the

concentration at which the GAE value reached a peak and remained constant afterwards.

3.2.3. The stability to light of Resveratrol standard solutions

Resveratrol solutions/suspensions were exposed to overhead light (Philips, TL-D 840, 70w, and distant was 1 meter) in the laboratory during 0, 1, 3, 6 and 12 hours. The total phenolic content was measured at 303nm by a spectrophotometer (Ultrospec ® 1100 pro) and the Folin-Ciocalteu method as described above. The total antioxidant capacity of samples was measured by ABTS as described above. All the samples were determined in duplicate.

3.2.4. The preparation of resveratrol-β-lactoglobulin nanoparticles

Native β-lactoglobulin powder (0.01g) was added into 5ml resveratrol standard solutions /suspensions of varying concentrations in a 7ml Sterile container. Then the pH of the sample was adjusted to 6.0 using a pH meter (Mettler Toledo, Switzerland) with 0.1M HCl and 0.1M NaOH. After this, the sample was introduced into a water bath (Grant Instrument Ltd., Cambridge, United Kingdom) that have been previously heated at 75 °C. The sample was kept for 45 minutes at this temperature; it must be noted that the temperature of the sample reached the set temperature after about 13 minutes. On completion of the incubation time, samples were transferred to an ice bath for 10 minutes to terminate incubation. After 10 minutes in the ice bath, the pH of the sample was measured. The particle size was determined by dynamic light scattering (DLS).

3.2.5. The effect of heating and native β-lactoglobulin and β-lactoglobulin nanoparticle on the stability of resveratrol

After determination of solubility of resveratrol, all the following studies were carried out in a range of concentrations of resveratrol at the solubility or below. A set of resveratrol aqueous solutions in the range of solubility were used as a control and compared against samples of the same concentration of resveratrol that underwent different treatments. There were three different treatments: heating (see details below), the addition of native β-lactoglobulin (details below) and β-lactoglobulin nanoparticles (in 3.2.3).

When studying the effect of heating, all varying concentrations of resveratrol solutions/suspensions were heated at 75°C in a water-bath for 45 minutes and moved to an ice bath for 10 minutes afterwards. Then, samples were taken for analysis.

When exploring the effect of adding native β-lactoglobulin, 0.01g native β-lactoglobulin powder was added to 5ml resveratrol standard solutions/suspensions of varying concentrations in a 7ml Sterile container. Then samples were ready to carry out the further study.

The effect of heating, adding native β-lactoglobulin and β-lactoglobulin nanoparticles on the stability of resveratrol were determined by total phenolic content and the total antioxidant activity. For the total phenolic content, the Folin-Ciocalteu method mentioned above was applied, and when measuring the samples with native β-Lactoglobulin and β-Lactoglobulin nanoparticles, the interference of protein was eliminated by subtracting the GAE value of protein from the GAE value of samples. All the samples were prepared and determined in duplicate.

For the total antioxidant activity, the [2,2'-Azinobis(3-Ethylbenzothiazoline-6-Sulphonic Acid)] (ABTS) Free Radical Scavenging Activity Assay and Ferric ion Reducing Antioxidant Power assay (Frap) were used. In detail:

ABTS method: The total antioxidant activity of all samples was measured by ABTS assay at 734nm, which was modified from Re et al. (1999). In general, the $ABTS^{\bullet+}$ stock solution was prepared by mixing solution 5ml ABTS solution (7mM, 50ml volume, stored in an amber flask and kept under refrigeration at 0-4°C up to one month) and 88µl Potassium Persulfate ($K_2S_2O_8$) solution (140mM, 10ml volume, stored in an amber flask and dark place at room temperature up to one month) together. Then the mixture was kept in the dark and room temperature for at least 16h prior to use. For the study of phenolic compounds, the working solution of the $ABTS^{\bullet+}$ was obtained by diluting the $ABTS^{\bullet+}$ stock solution with phosphate buffered saline (PBS pH 7.4) to an absorbance of 0.70±0.02 at 734nm. 20µl of samples was added into 2ml $ABTS^{\bullet+}$ working solution, and the mixture was homogenised by 1mins vortex. The mixture was then incubated in the dark for 6 minutes, and the absorbance (ABS_{sample}) was recorded at 734nm using a UV-Vis Spectrophotometers (Ultrospec ® 1100 pro). The absorbance of $ABTS^{\bullet+}$ working solution was measured at the same wavelength and used as control ($ABS_{control}$). The PBS was to blank the spectrophotometer. The percentage of scavenging activity of each sample on $ABTS^{\bullet+}$ was calculated as the inhibition% (I%) using the following equation (Shah & Modi, 2015): Eq.(1)

$$\mathbf{I\%} = \frac{(\mathbf{ABScontrol} - \mathbf{ABSsample})}{\mathbf{ABScontrol}} \times \mathbf{100} \quad \textbf{(1)}$$

When measuring the samples with native β-Lactoglobulin and β-Lactoglobulin

nanoparticles, the interference of protein was eliminated by subtracting the I% of protein from the I% of samples. All the samples were prepared and determined in duplicate.

Frap method: The total antioxidant activity of all samples was also assessed by Frap method at 595nm, which was modified from Benzie and Strain (1996).In principle, The stock solution of Frap method included: 300 mM Acetate buffer (pH 3.6, 2.699 g sodium acetate trihydrate and 16ml (16.8g) glacial acetic acid dissolved in 1L deionised water), 2,4,6-tripyridyl-s-triazine (TPTZ) (10mM) in 10ml HCl (40mM), and 20mM Ferric Chloride Hexahydrate aqueous solution. The Frap reagent was mixed with the 25ml Acetate buffer, 2.5ml TPTZ and 2.5ml Ferric chloride solutions. Then ten µl of the sample/standard was added into 300µl Frap reagent in a microcentrifuge tube and vortexed for 10 seconds. Then 100µl of this mixture, in triplicates, was transferred into the microwell plate (96well, NUNC, FB) and absorbance was measured at 595nm by a computer controlled Tecan Microplate reader. Results were express as the ascorbic acid equivalents (AAE) using an ascorbic acid (0.001761mg/ml-0.1761mg/ml) standard curve. Increased absorbance of the reaction mixture indicated greater reduction capability. When measuring the samples with native β-Lactoglobulin and β-Lactoglobulin nanoparticles, the interference of protein was eliminated by subtracting the AAE value of protein from the AAE value of samples. All the samples were prepared and determined in triplicate.

3.2.6. The protective effects of native β-lactoglobulin and β-lactoglobulin nanoparticle on resveratrol under pasteurisation condition

Different concentrations of resveratrol standard solutions/suspensions, resveratrol-native β-lactoglobulin solutions and resveratrol-β-lactoglobulin nanoparticles solutions prepared using the methods above were incubated at Pasteurisation conditions, 63°C for 30 minutes. Then the total phenolic content was determined by Folin-Ciocalteu method. The total antioxidant capacity of samples was measured by the ABTS method. All the samples were determined in duplicate.

3.2.7. Fluorescence measurement of resveratrol-β-lactoglobulin solutions

The concentrations of resveratrol solutions were 0.23mg/100ml, 0.46mg/100ml, 0.92mg/100ml, 1.84mg/100ml, and 2.48mg/100ml.The protein concentration of resveratrol-native β-Lg solutions and resveratrol-β-Lg nanoparticles solutions was kept constant at 0.2% w/v. The degree of β-Lg conformational changes was determined based on fluorescence emission of tryptophan (Trp), which was measured by fluorescence spectrophotometer with the temperature controller (Varian Cary Eclipse, United Kingdom). Fluorescence spectra were obtained after excitation at 295nm, scanning an emission wavelength range between 300 nm to 510 nm, using 5nm excitation and emission slits wavelength. The data was collected by Cary Eclipse software version 2 (Varian Cary Eclipse, United Kingdom) and samples were analysed in at a constant temperature of 20°C. According to Liang and Subirade (2012), the fractional residual fluorescence or relative fluorescence intensity (**$RFI=F_{max}/F_0\times100$**) was

the fraction of the total protein fluorescence that was not quenched, and thus the fraction of β-Lg not bound to the ligand; where, F_0 is fluorescence intensity of pure β-Lg; F_{max} is the intensity at the emission maximum (λ_{max}). A low ratio of RIF demonstrated a strong binding of the ligand, while a ratio of 100% indicated no binding.

For the calculation of binding constant and binding number, the fluorescence quenching data were analysed by fitting to the Stern-Volmer equation (Liang et al., 2008) in dynamic quenching. Eq. (2):

$$\mathbf{F0/Fmax = 1 + Kq \times \tau 0 \times [Resveratrol] = 1 + K \times [resveratrol]} \quad \textbf{(2)}$$

F_0 and F_{max} are the fluorescence emission intensities without and with resveratrol; **[resveratrol]** is resveratrol concentration; K_q is the fluorescence quenching rate constant; τ_0 is the fluorophore fluorescence lifetime without quencher, and **K** is Stern-Volmer quenching constant.

For the static quenching, the binding constant K_s and binding number **n** can be calculated according to the double logarithmic equation(He et al., 2016). Eq. (3):

$$\mathbf{\log [(F0 - Fmax)/Fmax]) = logKs + n \log[resveratrol]} \quad \textbf{(3)}$$

3.2.8. Statistical analysis

Figures were plotted using MS Excel, MS Office 2013 (Microsoft Corporation, Redmond, WA, USA). The results were statistically analysed by analysis of variance using IBM® SPSS® Statistics version 20.0. Means and standard deviations from at least two measurements carried out on two samples repeated. The significance level was set at 0.05. Data fitting of experimental data to models was performed with Excel MS Office

2013 (Microsoft Corporation, Redmond, WA, USA)

3.3. Results and discussion

3.3.1. The solubility of resveratrol in aqueous solution

The solubility of resveratrol in water solution was determined by measuring total phenolic content using the direct spectrophotometric method and Folin-Ciocalteu method.

In the direct spectrophotometric method, the Lambda max of 2mg/100ml resveratrol aqueous solution was determined as 303 nm. Therefore, a plot of the absorbance at this wavelength against concentration was established. The absorbance of resveratrol reached a peak and levelled off at resveratrol concentration 7mg/100ml after an approximately linear increase (Figure 3.2). Results from Folin-Ciocalteu method showed the same trend, and at 7mg/100ml the GAE also remained constant at about 35.5 mg/L. Both these results indicated that 7mg/100ml corresponded to the limit of solubility of resveratrol in water. Surprisingly, it was in disagreement with the reported solubility value (3mg/100ml), but this was determined by high-performance liquid chromatography (HPLC) (Jeon et al., 2016; Pujara et al., 2017; SantaCruzBiotechnology, 2017). Moreover, the solubility value reported by Camont et al. (2009) using the UV spectrophotometric method was 6.85 mg/100ml, but they claimed that this increased solubility was due to sonication that helped to dissolve resveratrol. Another possible explanation of this different result was that, in our method, samples were not filtered prior to absorbance measurements, so any insoluble particles of resveratrol in

suspension could have led to an overestimation of the solubility. However, filtration was not still an option in this study due to the reasons below: filtration of aqueous solutions of resveratrol with a 0.45µm Polyethersulfone (PES) membrane proved to be very difficult as all resveratrol was retained (results obtained by HPLC but not shown here). Only the 0.22 µm Polypropylene (PVDF) filters showed high permeability for resveratrol but still, a reduction (7.69%) in absorbance observed. Moreover, high retention for β-Lg nanoparticles (about 80%) of 0.22 µm PVDF filter existed. Therefore, filtration was not applied in this work. Indeed, as mentioned before, the insoluble resveratrol particles might influence the total phenolic determination by direct absorbance measurement, however, particularly in the Folin assay, 0.5 ml samples were taken to carry out the assay and 20 times dilution was applied so any interferences by suspended particles would be minimal.

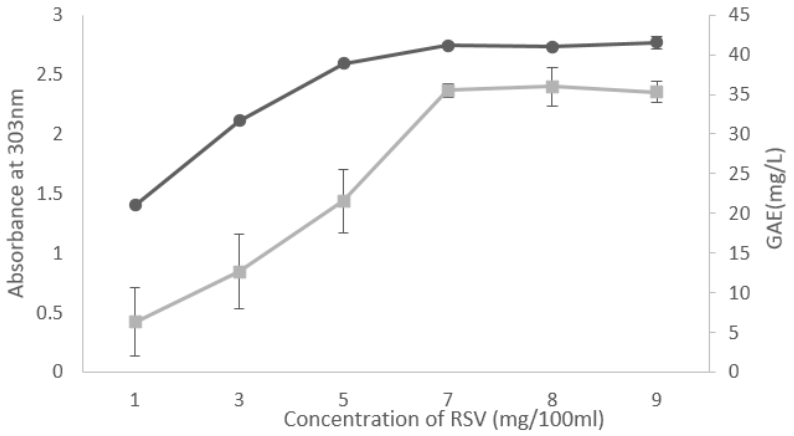

Figure3.2: The solubility of resveratrol in aqueous solution. ● Results of the direct spectrophotometric method ■ Results of Folin-Ciocalteu method.

To sum up, in this study, the solubility of resveratrol in deionized water at room temperature was 7mg/100 ml. As our solubility result was higher than some of the

reported values, it was assumed that at 7ml/100 ml, a nearly saturated solution of resveratrol was obtained. Therefore, the rest of experiments were carried out at the range of 1mg/100ml to 7mg/100ml.

3.3.2. The effect of light on resveratrol solubility and stability

For the stability to light, the resveratrol suspensions were exposed to the lab light for 12 hours. Based on the measurement of the direct spectrophotometric method, the concentration of resveratrol had an increasing trend with one exception at 1mg/100ml (Fig 3.3). Also, according to Figure 3.3, there was a reduction of GAE value at 1mg/100ml, but no significant difference at 3mg/100ml-7mg/100ml during 12 hours light exposure with a wide variance. Corresponding to the total phenolic content, inhibition% had the same increasing trend at 3mg/100ml-7mg/100ml. A significant positive correlation between total phenolic content (the direct spectrophotometric method) and total antioxidant capacity was observed as Pearson value was 0.844. Therefore, it was concluded that the resveratrol solution was not stable when exposed to lab light. Simimalrly, Pinelo, Rubilar, Sineiro, and Núñez (2005) found that resveratrol solution achieved maximum antioxidant activity at 22°C in water bath after three days.

Also, according to Orgován, Gonda, and Noszál (2017), the trans-resveratrol is more lipophilic than its isomer. Moreover, they also found that the cis-resveratrol has over ten times more solubility than trans-resveratrol. Another potential explanation could be that at high concentration, the trans-resveratrol converted to cis-resveratrol under the light condition and more cis-resveratrol dissolved in the solution leading to an increase

in antioxidant activity.

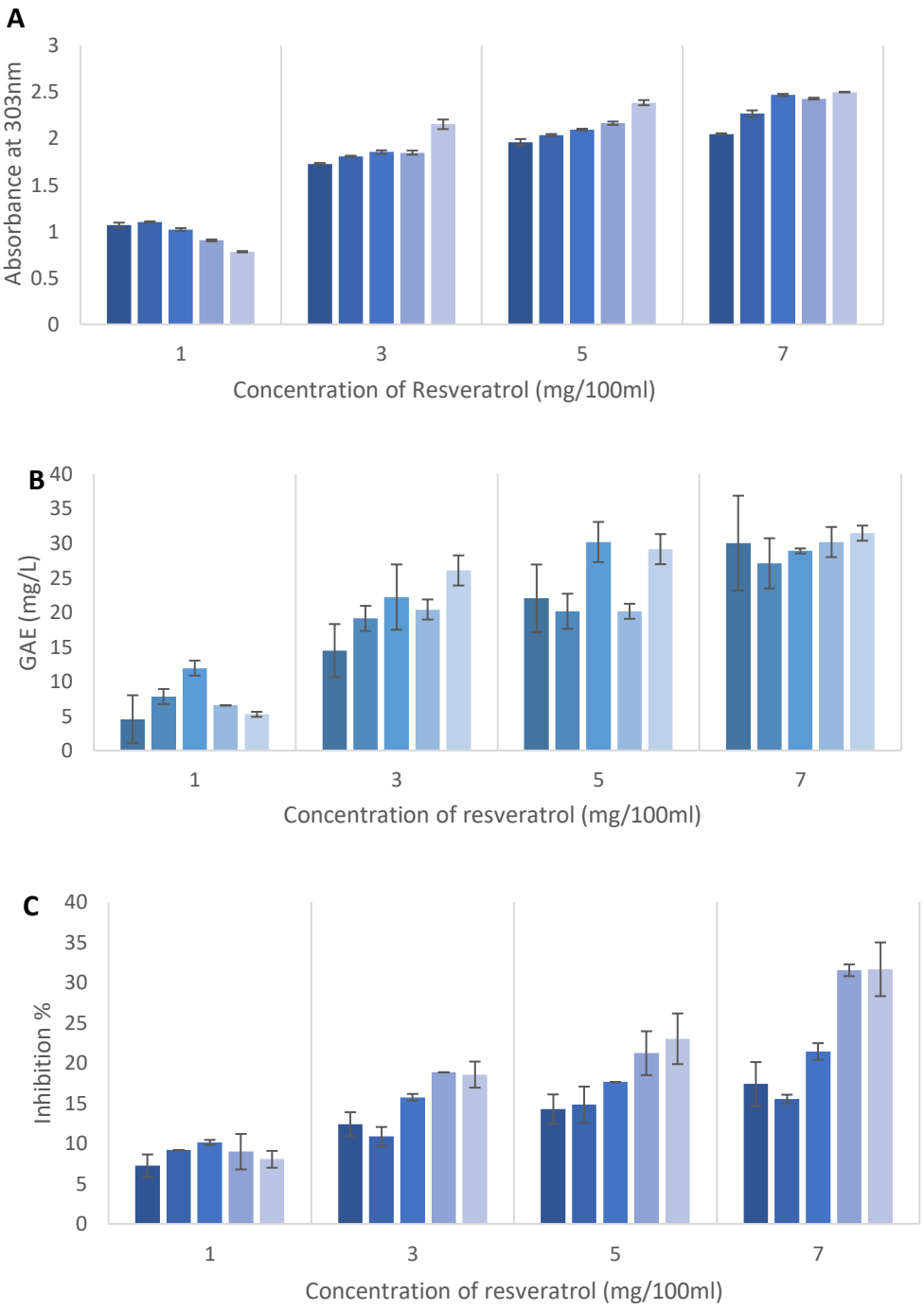

Figure 3.3: the stability of resveratrol to light by total phenolic content at 303nm (A), total phenolic content by Folin-Ciocalteu method (B) and total antioxidant capacity by ABTS (C). 0h 1h 3h 6h 12h.

3.3.3. The characterization of resveratrol-ß-lactoglobulin nanoparticles

After heating the mixture of resveratrol and ß-lactoglobulin (0.2%w/v) to form nanoparticles, the size of nanoparticles was measured by dynamic light scatting. The average size of resveratrol-ß-lactoglobulin nanoparticle was 181.80 nm±1.48 nm with polydispersion index 0.048 (in Figure 3.4). The nanoparticle size was close to Fonseca, Khalil, and Mainardes (2017) work (175nm), which encapsulation resveratrol with bovine serum albumin nanoparticles by desolvation method with ethanol. There was no significant difference in size among different concentrations of resveratrol nanoparticles and nanoparticles alone. It manifested that the nanoparticles around 200nm have been produced and the concentrations of resveratrol will not influence the size of nanoparticles. On the other hand, the size of nanoparticle was smaller than the nanoparticles we produced in previous work due to the lack of hydration step at 4 °C overnight. The reason why no hydration appiled was possibly unstable of resveratrol during storage .

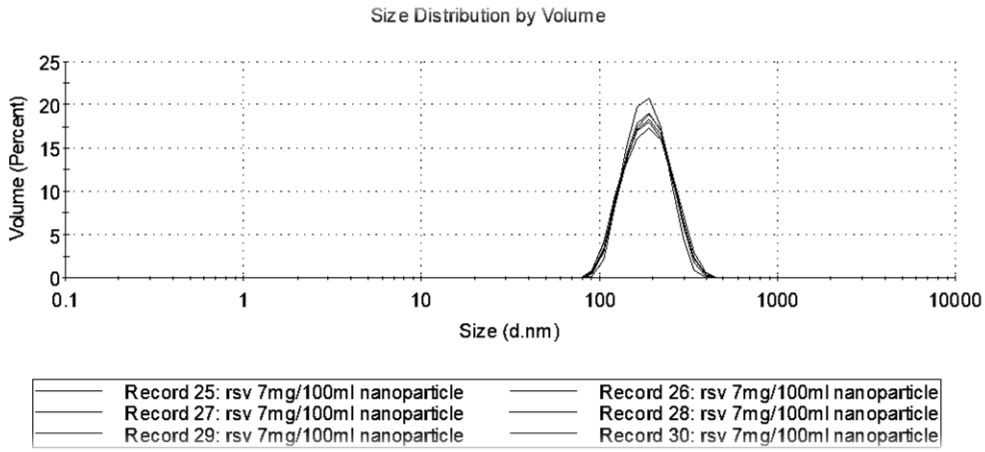

Figure 3.4: The example of the size distribution of resveratrol- ß-lactoglobulin nanoparticle by DLS.

3.3.4. Effect of heating, native ß-lactoglobulin, and resveratrol-ß-lactoglobulin nanoparticles on the stability of resveratrol

The effect of heating was investigated under the same conditions as those used in the ß-lactoglobulin nanoparticles preparation: heating at 75°C for 45 mins. After heating, 10 minutes in the ice bath allowed rapid reduction of samples temperature to room temperature. The concentration of native ß-lactoglobulin added to the resveratrol solution was the same as that used in the preparation of nanoparticles. The stability of resveratrol after the heating, protein addition and nanoparticles treatments was assessed by comparing the total phenolic content (Folin-Ciocalteu method), and total antioxidant activity (ABTS method and the Frap method) of treated samples with those of the control (resveratrol aqueous solution 1mg/100ml-7mg/100ml).

3.3.4.1. Total phenolic content by Folin-Ciocalteu method

According to Figure 3.5, results revealed a clear increment of GAE value after heating at all concentrations, indicating that the heating has a significant influence on resveratrol. Even though heating could improve the solubility of resveratrol in water dramatically (Filipa et al., 2003) as in this study all samples were subjected to an ice bath after heating, the increase of solubility due to heating would have been reduced or eliminated. So the increase in GAE observed at all concentrations, particularly those below the solubility (< 7 mg/100 ml) could be due to chemical changes in the molecule which resulted in changes in its oxidative status and/or oxidation power and led to enhanced blue colour production. However, at 7 mg/ 100 ml, the big increase in GAE from 30.01 to 81.46 mg/L

may also be partly due to an increase in solubility since near saturation might have been reached at this concentration of resveratrol. Flieger et al. (2017) pointed out that when the temperature reached 75°C or above, heating could induce the isomerization of resveratrol from trans-resveratrol to cis-resveratrol even without light. Also, Orgován et al. (2017) found that the solubility of cis-resveratrol was over ten times more than that of trans-resveratrol in water as trans-resveratrol was more lipophilic than its isomer. Thus, a possible explanation for the increase in GAE observed here could be that some of the trans-resveratrol isomerized to cis-resveratrol and that led to an increase in solubility.

When adding native ß-lactoglobulin, an increase in total phenolic content happened, while this increase was not significant ($P>0.05$) compared with to control sample at all concentrations. The interference of protein on total phenolic content has been eliminated by subtracting the GAE value corresponding to the protein from results (see Methods in 3.2.3). So any increases in GAE as a result of protein addition may be due to interactions between native ß-lactoglobulin and resveratrol that could lead to an increase in GAE, this is particularly the case for resveratrol concentration 3 and 5 mg/100ml, which are below and about the solubility of resveratrol.

Moreover, according to Figure 3.5, the samples of resveratrol with ß-lactoglobulin nanoparticles had the largest increment in phenolic content among these three treatments, and it was around three times the phenolic content of the control sample at all concentrations. Interestingly, the nanoparticles (combined the effect of heat and the addition of protein) led to a much higher increase than the heating alone for those

concentrations of RSV below solubility whereas for the highest concentration it had almost the same effect than heating alone.

Overall these results suggested that heating enhanced resveratrol and ß-lactoglobulin interactions as well as inducing isomerisation thus, these combined effects led to an increase in total phenol content. For the highest resveratrol concentration which was about saturation point, this increase in total phenols can be also translated into an increase in solubility.

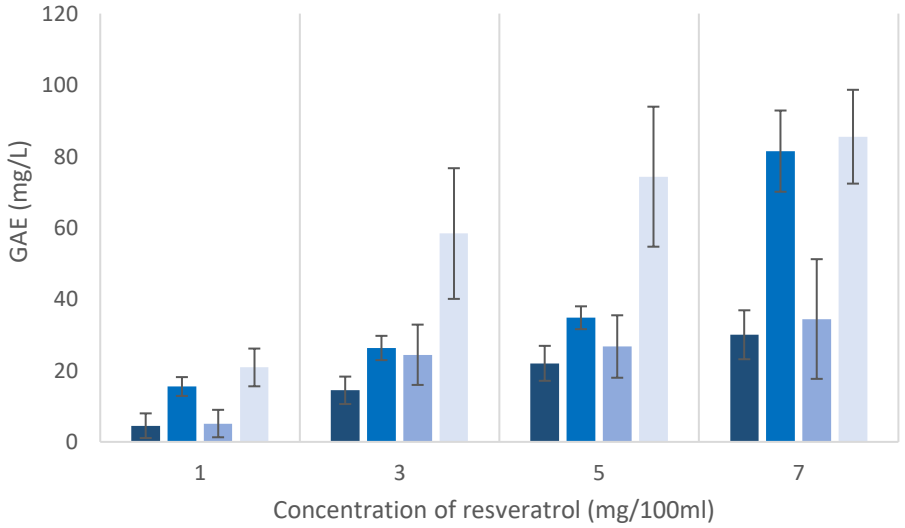

Figure 3.5: The total phenolic content results by Folin-Ciocalteu method of resveratrol, heated resveratrol and resveratrol-native ß-lactoglobulin, and resveratrol-ß-lactoglobulin nanoparticles. (Results were expressed at Gallic Acid Equivalents GAE mg/L) Standard RSV Heated RSV RSV+Native ß-Lg RSV+Nanoparticles of ß-Lg

3.3.4.2. Total antioxidant activity by ABTS method and Frap method

Besides total phenolic content, the total antioxidant capacity was another important property of resveratrol. Changes in this as a result of the different treatments were used to assess the stability of resveratrol. In this work, two methods were applied to measure antioxidant capacity: ABTS method and Frap method. Results in Figure 3.6 demonstrated a reduction of antioxidant activity measured as inhibition% after heating ($P<0.05$) at all concentrations. According to Mikulski, Gorniak, and Molski (2010), trans-resveratrol was a stronger antioxidant than cis-isomer due to the planar conformation; this conformation would ensure the main parameters contributing to antioxidant activity: favourable spin and unpaired electron distribution. Therefore, reduced antioxidant activity confirmed that trans-resveratrol might change to cis-isomer during the heating as also suggested by total phenols results above (section 3.3.3.1).

The addition of native ß-lactoglobulin led to no significant changes in antioxidant activity when compared against the control samples, indicating that the antioxidant activity would not be masked by ß-lactoglobulin.

On the other hand, the resveratrol-ß-lactoglobulin nanoparticles had higher activity than heated samples ($P<0.05$) at 1-5 mg/100ml. So the reduction in activity due to heating was counteracted by the interactions of resveratrol with the nanoparticles which led to similar or higher activity than control. This suggests a protective effect of ß-lactoglobulin nanoparticles against heat-induced loss of antioxidant activity. Interestingly, at 7ml/100ml, the difference in antioxidant activity between the heated sample (14.52%) and resveratrol-ß-lactoglobulin nanoparticle samples (21.31%) was not statistically

significant (0.072). At 7 mg/100 ml, the heating led to two counteracting effects, improving solubility which would increase activity and isomerization which would result in reduced activity, this is why both the heating effect and the nanoparticles did not have a significant impact on antioxidant activity.

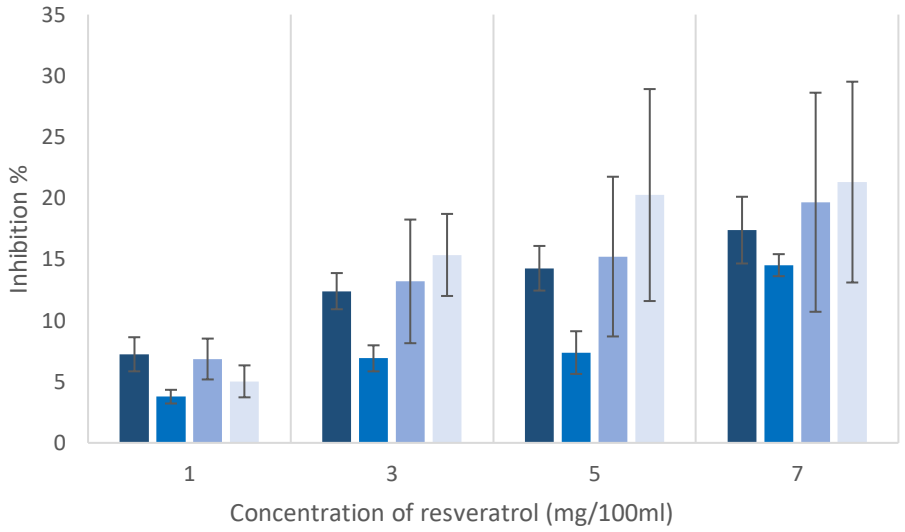

Figure 3.6: The total antioxidant activity results by ABTS method of resveratrol, heated resveratrol and resveratrol-native ß-lactoglobulin, and resveratrol- ß-lactoglobulin nanoparticles. Results were expressed as inhibition% (I%) Standard RSV Heated RSV RSV+Native ß-Lg RSV+Nanoparticles of ß-Lg.

Another antioxidant activity measuring method, Frap, was also applied to study the effects of different treatments on resveratrol. In Fig 3.7, the antioxidant activity results by Frap method were express in AAE (mg/ml). It was noted that there was no significant difference ($P<0.05$) of activity between 5mg/100ml and 7mg/100ml of control samples, which might suggest that solubility of resveratrol in water was 5mg/100ml instead of 7

mg/100ml.

A reduction in activity due to heating was observed for samples up to 5mg/100ml in agreement with ABTS measurements (Fig 3.6). Surprisingly, and contrary to what was observed by the ABTS method, a sharp increase was observed at 7mg/100ml. This phenomenon could be explained by an increase in solubilized resveratrol in the form of cis-resveratrol as a result of heating. Therefore, both trans-resveratrol and cis-resveratrol contributed to the antioxidant activity. These results also supported that the solubility of resveratrol in water might be below 7mg/100ml.

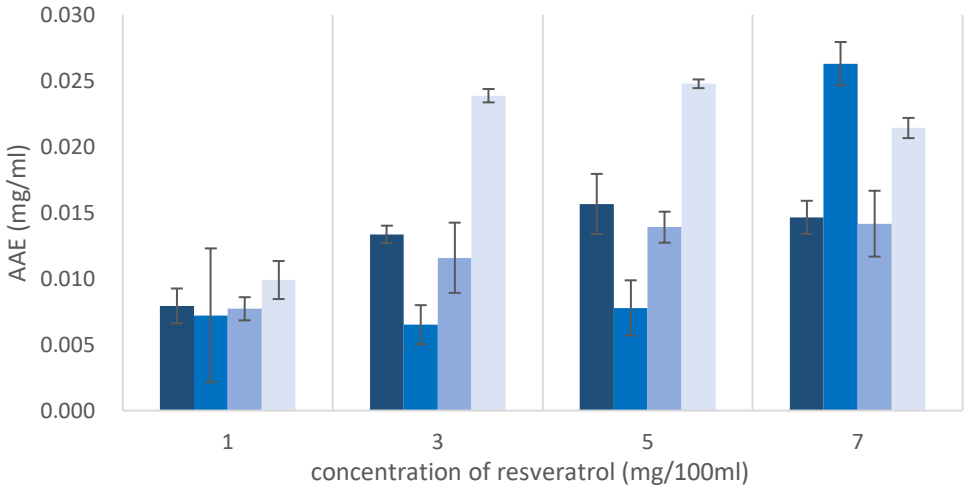

Figure 3.7: The total antioxidant activity results by Frap method of resveratrol, heated resveratrol and resveratrol-native ß-lactoglobulin, and resveratrol-ß-lactoglobulin nanoparticles.Results were expressed as Ascorbic Acid Equivalents (AAE mg/ml)

Standard RSV Heated RSV RSV+Native ß-Lg RSV+Nanoparticles of ß-Lg.

Moreover, the resveratrol-ß-lactoglobulin nanoparticles had the highest AAE value at all concentrations among all treatments (except heated sample at 7mg/100ml), whilst resveratrol with native ß-lactoglobulin samples had the same antioxidant activity as the

control samples (P>0.05). These results are in agreement with ABTS results. It was noted that the increase in AAE value of resveratrol-ß-lactoglobulin nanoparticles compared with the AAE value resveratrol-native ß-lactoglobulin was a significant difference, which was not observed by ABTS method. This was probably related to the different mechanisms of these two antioxidant activity measuring assays. In principle, blue/green $ABTS^{\bullet+}$ chromophore produced by the reaction between ABTS and potassium persulfate was measured spectrophotometrically at 734 nm, and this radical cation converted back to its colourless neutral form after reacting with antioxidants (Gülçin, 2010; Re et al., 1999). In this study, one of the main limitations of ABTS method was that the radicals were generated at least 16 hours before the reaction of ABTS with potassium persulphate, but assays were carried out with radicals generated at different times (not exactly 16 hours). Thus, it led to $ABTS^{\bullet+}$ radicals with different activities and influenced stability and reproducibility of results. On the other hand, the principle of Frap method was based on the reduction of Fe^{3+} to Fe^{2+} ions which results in the formation of an intense blue colour. According to Gülçin (2010), both Frap and ABTS methods worked effectively to determine the antioxidant activity of resveratrol, but different results were obtained for the same antioxidant samples.

Nevertheless, the results of both antioxidant capacity methods indicated that ß-lactoglobulin nanoparticles had the ability to prevent the deterioration of resveratrol during heating and protected its antioxidant capacity. In addition, ß-lactoglobulin had a more effective protective effect in the nanoparticle than native form.

Therefore, in order to obtain an improved understanding of the interactions between ß-

lactoglobulin and resveratrol and binding mechanism, the fluorescence measurements were conducted.

3.3.5. Determination of ß-lactoglobulin-resveratrol interactions by fluorescence

The fluorescence measurements of resveratrol-β-lactoglobulin solutions were conducted with resveratrol concentrations from 0.23mg/100ml-2.5mg/100ml.

During heating, the tertiary structure of native β-lactoglobulin was broken, the protein conformation opened up and the more hydrophobic residues became more exposed which should promote hydrophobic interactions and hydrogen bonding between β-lactoglobulin and ligands. The shifted $\boldsymbol{\lambda_{max}}$ to a longer wavelength indicated that the heating exposed the previously buried Trp and Tyr residues (shifting of $\boldsymbol{\lambda_{max}}$ from wavelength 337.0 nm to 357.14 nm and 335.08nm to 377.89nm in Figure 3.8) and the shifting of nanoparticles was larger than that of native β-lactoglobulin, which indicated more exposure of the fluorophore groups due to changes in β-lactoglobulin conformation as a result of heating during nanoparticles production. In Table 3.1, the RFI value decreased as the concentrations of resveratrol increased with both native and nanoparticles. The RFI value of resveratrol-native β-lactoglobulin (22.87) was smaller than the value of resveratrol-β-lactoglobulin nanoparticles (46.67), which indicated stronger binding of Resveratrol with native β-lactoglobulin than with its nanoparticles. This result was in disagreement with our previous work with caffeine where nanoparticles showed higher binding affinity than native β-lactoglobulin (Guo et al., 2017).

Table 3.1: the fluorescence measurement of Resveratrol standard, Resveratrol with native β-Lg, Resveratrol-β-Lg nanoparticles at different concentrations.

Concentration (mg/100ml)	Resveratrol with native β-Lg		Resveratrol-β-Lg nanoparticles	
	Fluorescence Intensity (a.u.)	RFI (%)	Fluorescence Intensity (a.u.)	RFI (%)
0	370.30±0.46	100.00	196.57±0.20	100.00
0.23mg/100ml	328.77±0.09	88.78	164.53±0.48	83.70
0.46mg/100ml	258.36±0.54	69.77	163.41±0.08	83.64
0.92mg/100ml	172.25±0.04	46.52	162.54±0.25	82.69
1.84mg/100ml	119.73±0.57	32.33	128.76±0.02	65.50
2.48mg/100ml	84.69±0.28	22.87	91.72±0.12	46.67

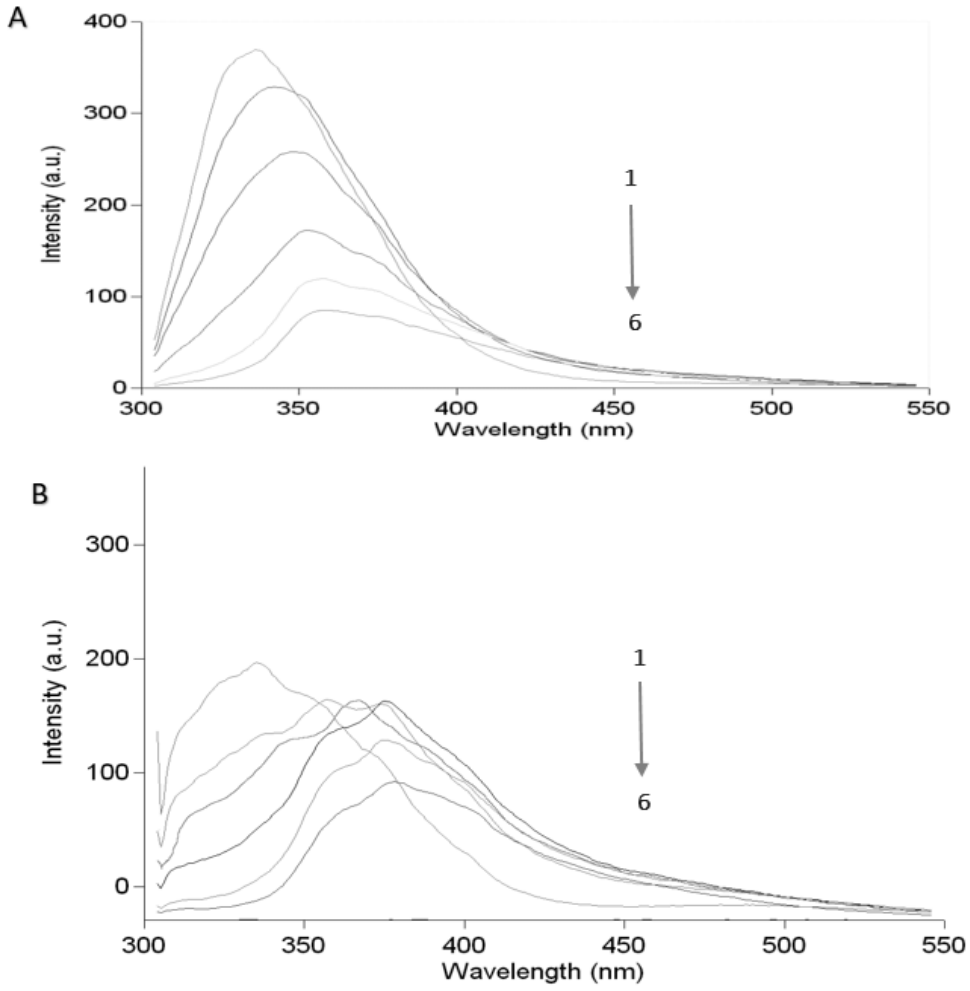

Figure 3.8: The fluorescence emission spectra of (A) resveratrol-native β-lg at 0mg/100ml-2.48mg/100ml (1-6); (B) resveratrol-β-lg nanoparticle at 0mg/100ml-2.48mg/100ml (1-6).

Furthermore, According to Eq (1), the Stern-Volmer equation constant, K of Resveratrol with native β-Lg was $3.18x10^4$ M^{-1} (R^2= 0.986) and since τ_0 is 1.28 ns for Trp of β-Lg (EricDufour, Genot, & Haertlé, 1994; Stojadinovic et al., 2013), K_q was $2.5x10^{13}$ $M^{-1}S^{-1}$, which was higher than the maximal dynamic quenching constant (1-2.0 × 10^{10} $M^{-1}S^{-1}$) and it suggested binding of resveratrol with β-Lg followed a static quenching mechanism. In this case, the fluorophore formed a stable complex with another molecule, and it was non-fluorescent. This result was in agreement with Liang and Subirade (2012); Liang et al. (2008), who confirmed that β-Lg fluorescence quenching induced by resveratrol is a static quenching. Thus, based on Eq. (2), the binding constant K_s was $1.67x10^5$ $M^{-1}$and the binding number was 1.33. This means 1.33 resveratrol molecules bind one β-Lg molecule and also K_s was in the range of 10^5 and 10^6 M^{-1}, which was in agreement with binding constants reported for native β-Lg and a range of substrates by Liang and Subirade (2010) (binding with folic acid: 4.3× 10^5M^{-1}), Shpigelman, Israeli, and Livney (2010a) (binding with EGCG: 1.05× 10^5M^{-1}), Liang et al. (2008) (binding with Resveratrol:10^4 ~10^5M^{-1}).

However, when applying the Stern-Volmer quenching equation to Resveratrol with β-Lg nanoparticles samples, K of Resveratrol with β-Lg nanoparticles was $9.1x10^3$, but the R^2 was 0.852. This indicated that the resveratrol to β-Lg nanoparticles binding did not follow the Stern-Volmer model. Moreover, the resveratrol-β-Lg nanoparticles did not fit the Langmuir-type model, either (data did not include here, but R^2 was 0.55).

To sum up, according to the fluorescence results, native β-Lg had higher binding affinity for resveratrol than its nanoparticles; the binding constant for native protein was

$1.67x10^5$, and the binding number was 1.33. However, no model was found to fit the binding of β-Lg nanoparticles with resveratrol. This is contrary to what was observed for caffeine and β-Lg in our previous work (chapter 2). According to Shpigelman et al. (2010) claimed a higher association of heated β-Lg with Epigallocatechin-3-gallate (EGCG) than native β-Lg, but Perez, Andermatten, Rubiolo, and Santiago (2014) demonstrated no significant difference in binding linoleic acid between native and heat-induced β-Lg aggregates. Therefore, the mechanism of interactions between different ligands and β-Lg should be different. The influence on binding properties of heat-induced β-Lg nanoparticles has different results depends on the ligand.

3.3.6. The effect on stability of resveratrol among different treatments under pasteurisation

Pasteurisation is a common commercial method to minimise health hazards from food pathogen and to extend shelf life for liquid food and drinks. Thus, it is important to examine the effect of pasteurisation on resveratrol stability and how would adding protein affect this. So here the aim is to apply the knowledge obtained in the experiments described above to an industrial thermal process. Firstly, as shown in figure 3.9 A, total phenolic content of resveratrol after pasteurisation showed the same results as the heating at 75 °C: dramatic increase of GAE value after pasteurisation. Secondly, it demonstrated that pasteurising resveratrol with native β-lactoglobulin had no significant difference in total phenolic content at all concentrations as compared to control. It was different with results when producing nanoparticles at 75°C, which showed a significant addition of total phenolic content. At this temperature, β-

lactoglobulin existed as a monomer in solution, and the tertiary structure started slightly changing (Blanpain-Avet et al., 2016). A possible reason could be that the interaction with β-lactoglobulin suppressed the chemical changes in resveratrol molecule at 63°C. Surprisingly, after pasteurisation of resveratrol-β-lactoglobulin nanoparticles, a reduction of total phenolic content happened at all concentrations.

On the other hand, the antioxidant activity (%inhibition) of standard resveratrol slightly reduced after pasteurisation at 1mg/100ml and 3mg/100ml but increased at 5mg/100ml and 7mg/100ml (Figure3.9 B). These results were different to results of heating at 75°C, which indicated that heating at 75 °C led to more degradation than at 63°C, and here samples were not put in an ice bath after Pasteurisation so solubility might increase by heating.

Our results were in agreement with those by Pinelo et al. (2005)'s work, who reported that an increase of the total antioxidant capacity of resveratrol solution (100mM) happened during heating at 60°C and the maximum value achieved at 6 hours. They explained that the initial increment on total antioxidant activity occurred in two steps of resveratrol oxidation. In the first period of storage, the weight of the polymerization pathway might be lower than that of the formation of the o-diphenol core, which gave more antioxidant activity. Also, the results of both native β-lactoglobulin and nanoparticles after pasteurisation resulted in an increment of total antioxidant activity. This suggested that during heating β-lactoglobulin denatured and this promoted interactions between the protein and resveratrol. Pasteurisation would enhance this interaction and lead to an increased antioxidant activity. It was noted that the activity

of resveratrol-native-β-lactoglobulin after pasteurisation was higher than the activity of resveratrol-β-lactoglobulin nanoparticle samples before pasteurisation. This may be due to the effect of heating on solubility. In addition, it also suggested that the heat-induced isomerisation was stronger at 75°C than at 63°C.

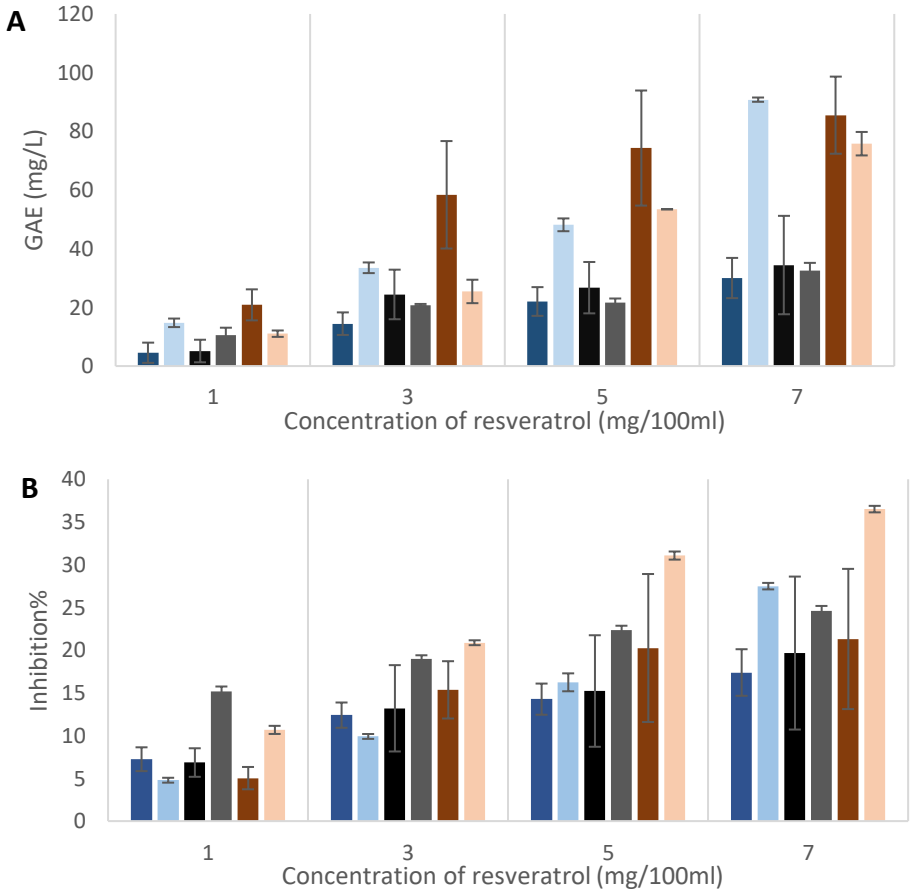

Figure 3.9: The total phenolic content (A) and the total antioxidant activity (B) of resveratrol, resveratrol with native β-Lg, Resveratrol-β-Lg nanoparticles before and after pasteurisation. RSV before pasteurisation RSV after pasteurization RSV+native β-Lg before pasteurisation RSV+native β-Lg after pasteurization RSV+ β-Lg nanoparticles before pasteurisation RSV+ β-Lg nanoparticles after pasteurisation.

3.4. Conclusions

In this work, the solubility of resveratrol in water was determined as 7mg/100ml by directly spectrophotometric and Folin-Ciocalteu method. However, it seemed that the solubility should be below this value based on the results of heated samples. Resveratrol was not stable to light, and light exposure resulted in higher phenolic content and total antioxidant capacity. Nanoparticles of β-lactoglobulin in the present of resveratrol were produced in size around 181.8nm, and the concentration of resveratrol was proved to have no significant difference in the size of nanoparticles. The thermal degradation and isomerization of resveratrol at 75°C led to reduced antioxidant capacity. Both native β-lactoglobulin and its nanoparticle form showed a protective effect on the antioxidant capacity of resveratrol against heat degradation. Moreover, the addition of β-lactoglobulin nanoparticles led to an increase in antioxidant activity. Surprisingly, according to fluorescence measurement, the results of RFI demonstrated that native β-lactoglobulin had stronger binding than its nanoparticles. Moreover, the binding constant of native β-lactoglobulin with Resveratrol is $1.67x10^{5,}$ and the binding number is 1.33 following Stern-Volmer model, but no model was found to fit the binding of resveratrol to nanoparticles. In summary, stronger interactions between native β-lactoglobulin and resveratrol than with its nanoparticles, despite the latter showing more protective effect. Therefore, β-lactoglobulin is a good candidate to improve the stability and antioxidative properties of resveratrol and could be used as an encapsulant to protect resveratrol during thermal processing. Our work gives solid evidence to prove that β-lactoglobulin nanoparticles could protect and enhance antioxidant activity of

resveratrol under pasteurisation conditions. Further studies should follow to investigate the stability of resveratrol during other industrial thermal processes like spray drying and ultra-heat treatment.

Acknowledgements

The trans-resveratrol powder was supplied by Evolva.

Special thanks to MSc student Napatsawan Wonggotwarin, who initiate this work.

Reference

Amri, A., Chaumeil, J. C., Sfar, S., & Charrueau, C. (2012). Administration of resveratrol: What formulation solutions to bioavailability limitations? *Journal of Controlled Release, 158*(2), 182-193.

Benzie, I. F. F., & Strain, a. J. (1996). The Ferric Reducing Ability of Plasma (FRAP) as a Measure of "Antioxidant Power": The FRAP Assay. *Analytical Biochemistry, 239*(1), 70-76.

Bhat, K. P. L., & Pezzuto, J. M. (2002). Cancer Chemopreventive Activity of Resveratrol. *Annals of the New York Academy of Sciences, 957*, 210-229.

Blanpain-Avet, P., André, C., Khaldi, M., Bouvier, L., Petit, J., Six, T., Jeantet, R., Croguennec. T., Delaplace, G. (2016). Predicting the distribution of whey protein fouling in a plate heat exchanger using the kinetic parameters of the thermal denaturation reaction of β-lactoglobulin and the bulk temperature profiles. *Journal of Dairy Science, 99*(12), 9611-9630.

Burdocka, G. A., & Carabin, I. G. (2004). Generally recognized as safe (GRAS): history and description. *Toxicology Letters, 150*(1), 3-18.

Burns, J., Yokota, T., Ashihara, H., Lean, M. E. J., & Crozier, A. (2002). Plant Foods and Herbal Sources of Resveratrol. *Food Chemistry, 50*(11), 3337-3340.

Camont, L., Cottart, C.-H., Rhayema, Y., Nivet-Antoinea, V., Djelidi, R., Collinc, F., Beaudeux, J., Bonnefont-Rousselot, D. (2009). Simple spectrophotometric assessment of the trans-/cis-resveratrol ratio in aqueous solutions. *Analytica chimica Acta, 634*(1), 121-128.

Catalgol, B., Batirel, S., Taga, Y., & Ozer, N. K. (2012). Resveratrol: French paradox revisited. *Front Pharmacol, 3*(141), 1-18.

Database, P. C. (2017). Pubchem.ncbi.nlm.nih.gov. Retrieved from https://pubchem.ncbi.nlm.nih.gov/compound/resveratrol#section=Top

Duarte, A., Martinho, A., Luís, A., Figueiras, A., Oleastro, M., Domingues, F. C., & Silva, F. (2015). Resveratrol encapsulation with methyl-ß-cyclodextrin for antibacterial and antioxidant delivery applications. *Food Science and Technology, 63*(2015), 1254-1260.

EricDufour, Genot, C., & Haertlé, T. (1994). β-lactoglobulin binding properties during its folding changes studied by fluorescence spectroscopy. *Biochimica et Biophysica Acta (BBA) - Protein Structure and Molecular Enzymology, 1205*(1), 105-112.

Filipa, V., Plockováa, M., Šmidrkala, J., Špičkováa, Z., Melzochb, K., & Schmidtc, Š. (2003). Resveratrol and its antioxidant and antimicrobial effectiveness. *Food Chemistry, 83*(4), 585-593.

Flieger, J., Tatarczak-Michalewska, M., & Blicharska, E. (2017). Characterization of the cis/trans Isomerization of Resveratrol by High-Performance Liquid Chromatography. *Analytical Letters, 50*(2), 294-303

Fonseca, D. P., Khalil, N. M., & Mainardes, R. M. (2017). Bovine serum albumin-based nanoparticles containing resveratrol: Characterization and antioxidant activity. *Journal of Drug Delivery Science and Technology, 39*, 147-155.

Frkmont, L. (2000). Minireview Biological effects of resveratrol *Life Sciences, 66*(8), 663-673.

Gambini, J., Inglés, M., Olaso, G., Lopez-Grueso, R., Bonet-Costa, V., Gimeno-Mallench, L., . . . Borras, C. (2015). Properties of Resveratrol: In Vitro and In Vivo Studies about Metabolism, Bioavailability, and Biological Effects in Animal Models and Humans. *Oxidative Medicine and Cellular Longevity, 2015*, 1-14.

Gorji, E. G., Rocchi, E., Schleining, G., Bender-Bojalil, D., Furtmüller, P. G., Piazza, L., . . . Toca-Herrera, J. L. (2015). Characterization of resveratrol-milk protein interaction. *Journal of Food Engineering, 167*(2015), 217-225.

Gülçin, İ. (2010). Antioxidant properties of resveratrol: A structure–activity insight. *Innovative Food Science and Emerging Technologies, 11*(1), 210-218.

Guo, Y., Harris, P., Kaur, A., Pastrana, L., & Jauregi, P. (2017). Characterisation of ß-lactoglobulin nanoparticles and their binding to caffeine. *Food Chemistry, 71*(2017), 85-93.

He, Z., Zhu, H., Xu, M., Zeng, M., Qin, F., & Chen, J. (2016). Complexation of bovine β-lactoglobulin with malvidin-3-O-glucoside and its effect on the stability of grape skin anthocyanin extracts. *Food Chemistry, 209*, 234-240.

Jang, M., Cai, L., Udeani, G. O., Slowing, K. V., Thomas, C. F., Beecher, C. W. W., . . . Pezzuto, J. M. (1997). Cancer Chemopreventive Activity of Resveratrol, a Natural Product Derived from Grapes. *Science, 275*(5297), 218-220.

Jeon, Y. O., Lee, J.-S., & Lee, H. G. (2016). Improving solubility, stability, and cellular uptake of resveratrol by nanoencapsulation with chitosan and -poly (glutamic acid). *Colloids and Surfaces B: Biointerfaces, 147*(2016), 224-233.

Jimenez-Garcia, S. N., Guevara-Gonzalez, R. G., Miranda-Lopez, R., Feregrino-Perez, A. A., Torres-Pacheco, I., & Vazquez-Cruz, M. A. (2012). Functional properties and quality characteristics of bioactive compounds in berries: Biochemistry, biotechnology, and genomics. *Food Research International, 54*(2013), 1195-1207.

L.Singleton, V., Orthofer, R., & M.Lamuela-Raventós, R. (1999). Analysis of total phenols and other oxidation substrates and antioxidants by means of folin-ciocalteu reagent. *Methods in Enzymology, 299*(1999), 152-178.

Lee, D.-U., Kim, H. M., Lee, D. G., Jeon, S.-H., Lee, J.-J., & Lee, S. (2014). Effects of Thermal Treatments on the Stability of trans-Resveratrol and Yeast Inactivation in trans-Resveratrol-Amplified Grape Juice. *Archives of Biological Sciences, 66*(1), 323-329.

Liang, L., & Subirade, M. (2010). Beta-Lactoglobulin/Folic Acid Complexes: Formation, Characterization, and Biological Implication. *The Journal of Physical Chemistry B, 114*(19), 6707–6712.

Liang, L., & Subirade, M. (2012). Study of the acid and thermal stability of ß-lactoglobulin–ligand complexes using fluorescence quenching. *Food Chemistry, 132*(4), 2023-2029.

Liang, L., Tajmir-Riahi, H. A., & Subirade, M. (2008). Interaction of β-Lactoglobulin with Resveratrol and its Biological Implications. *Biomacromolecules, 9*(1), 50-56.

Limmongkon, A., Janhom, P., Amthong, A., Kawpanuk, M., Nopprang, P., Poohadsuan, J., . . . Boonsong, T. (2017). Antioxidant activity, total phenolic, and resveratrol content in five cultivars of peanut sprouts. *Asian Pacific Journal of Tropical Biomedicine, 1*(1), 1-7.

Lipinski, C. (2002). Poor Aqueous Solubility—an Industry Wide Problem in Drug Discovery. *American Pharmaceutical Review, 5*(3), 82-85.

Lyons, M. M., Yu, C., R. B. Toma, Cho, S. Y., Reiboldt, W., Lee, J., & Breemen, R. B. V. (2003). Resveratrol in Raw and Baked Blueberries and Bilberries. *Journal of Agricultural and Food Chemistry, 51*(20), 5867-5870.

Mikulski, D., Gorniak, R., & Molski, M. (2010). A theoretical study of the structure–radical scavenging activity of trans-resveratrol analogues and cis-resveratrol in gas phase and water environment. *European Journal of Medicinal Chemistry, 45*(3), 1015-1027.

Orgován, G., Gonda, I., & Noszál, B. (2017). Biorelevant physicochemical profiling of (E)- and (Z)-resveratrol determined from isomeric mixtures. *Journal of Pharmaceutical and Biomedical Analysis 138*, 322-329.

Penalva, R., Esparza, I., Larraneta, E., Gonzalez-Navarro, C. J., Gamazo, C., & Irache, J. M. (2015). Zein-Based Nanoparticles Improve the Oral Bioavailability of Resveratrol and Its Anti-inflammatory Effects in a Mouse Model of Endotoxic Shock. *Journal of Agricultural and Food Chemistry, 63*(23), 5603-5611.

Pinelo, M., Rubilar, M., Sineiro, J., & Núñez, M. J. (2005). A thermal treatment to increase the antioxidant capacity of natural phenols: Catechin, resveratrol and grape extract cases. *European Food Research and Technology, 221*(3), 284-290.

Pujara, N., Jambhrunkar, S., Wong, K. Y., McGuckin, M., & Popat, A. (2017). Enhanced colloidal stability, solubility and rapid dissolution of resveratrol by nanocomplexation with soy protein isolate. *Journal of Colloid and Interface Science, 488*(2017), 303-308.

Pund, S., Joshi, A., & Patravale, V. (2016). Improving bioavailability of nutraceuticals by nanoemulsification. In A. M. Grumezescu (Ed.), *Nutraceuticals Nanotechnology in the Agi-Food Industry* (Vol. 4, pp. 481-534). London: Elsevier Inc.

Rabinow, B. E. (2004). Nanosuspensions in drug delivery. *Nature Reviews Drug Discovery 3*(9), 785-796.

Re, R., Pellegrini, N., Proteggente, A., Pannala, A., Yang, M., & Rice-Evans, C. (1999). Antioxidant activity applying an improved ABTS radical cation decolorization assay. *Free Radical Biology & Medicine, 26*(9-10), 1231-1237.

SantaCruzBiotechnology. (2017). Resveratrol | CAS 501-36-0.

Savjani, K. T., Gajjar., A. K., & Savjani, J. K. (2012). Drug Solubility: Importance and Enhancement Techniques. *International Scholarly Research Notices: Pharmaceutics, 2012*, 1-10.

Shah, P., & Modi, H. A. (2015). Comparative Study of DPPH, ABTS and FRAP Assays for Determination of Antioxidant Activity. *International Journal for Research in Applied Science & Engineering Technology 3*(636-641).

Shpigelman, A., Israeli, G., & Livney, Y. D. (2010). Thermally-induced protein-polyphenol co-assemblies: Beta-lactoglobulin based nanocomplexes as protective nanovehicles for EGCG. *Food Hydrocolloids, 24*, 735-743.

Soleas, G. J., Diamandis, E. P., & Goldberg, D. M. (1997). Resveratrol: A Molecule Whose Time Has Come? And Gone? *Clinical Biochemistry, 30*(2), 91-113.

Stojadinovic, M., Radosavljevic, J., Ognjenovic, J., Vesic, J., Prodic, I., Stanic-Vucinic, D., & Velickovic, T. C. (2013). Binding affinity between dietary polyphenols and ß-lactoglobulin negatively correlates with the protein susceptibility to digestion and total antioxidant activity of complexes formed. *Food Chemistry, 136*(3-4), 1263-1271.

Tran, P., Tran, T., & Lee, B. (2013). Enhanced solubility and modified release of poorly water-soluble drugs via self-assembled gelatin–oleic acid nanoparticles. *Pharmaceutical nanotechnology, 455*(1-2), 235-240.

Trela, B. C., & Waterhouse, A. L. (1996). Resveratrol: Isomeric Molar Absorptivities and Stability. *Journal of Agricultural and Food Chemistry, 44*(5), 1253-1257.

Zhang, J., Liu, X., Subirade, M., Zhou, P., & Liang, L. (2014). A study of multi-ligand beta-lactoglobulin complex formation. *Food Chemistry, 15*, 256-261.

CHAPTER FOUR

Further study of β-lactoglobulin nanoparticles and production of whey protein nanoparticles

ABSTRACT

In this chapter, the stability of β-lactoglobulin nanoparticles produced by the heat-induced method has been examined under different processing and treatment conditions. Ethanol is a common solvent for hydrophobic compounds and it is widely used in food products. Adding ethanol reduced the charge of solution leading to a smaller zeta potential, therefore, larger aggregates were produced at increased ethanol content. Sedimentation of nanoparticles happened when centrifugation was applied at high speed (>863g) thus, less protein concentration remained in the supernatant. Freeze-drying had no significant influence on particle size when compared freshly made samples with redispersion freeze-dried samples; however, the latter had higher PDI indicating reduced sized distribution uniformity. On the other hand, whey protein nanoparticles were produced with the same method. The size of whey protein nanoparticle was in a range of 150 to 350nm and the size depended on the concentration of protein. However, the aggregation yield of whey protein nanoparticles was lower than with β-Lg (maximum obtained was 85% whilst it was 93% with β-Lg). Nevertheless, these results showed that whey protein nanoparticles can be prepared with this method. It is practical to use whey, a cheaper and abundant source to prepare nanoparticle in the food industry. Further studies are necessary to investigate proteins interactions in the nanostructure of whey protein nanoparticles.

4.1. Introduction

In the last two chapters, β-lactoglobulin nanoparticles in a range of 200nm-300nm have been produced by simple and robust heat-induced method, and intermolecular non-covalent interactions (hydrogen bonding and hydrophobic interactions) were proved to be the predominant interactions responsible for the microstructure of the nanoparticles. Applications including encapsulation of caffeine and resveratrol have been successfully developed. Numerous bioactives have low water solubility, thus, when encapsulating these nutraceuticals, organic solvents are applied in order to dissolve these compounds. Ethanol is the most common, and it is classified as generally recognised as safe (GRAS) solvent, but up to a concentration limit. The concentration of ethanol in food reported as GRAS was around 3% (FDA, 2017a, 2017b, 2017c) and it depends on the type of food. Ethanol has an influence on the charge of protein, organisation of dipolar moments, the secondary structure of the protein, and even the binding properties (Mousavi, Chobert, Bordbar, & Haertle, 2008). Also, Gulseren et al. (2012) developed a method to produce whey protein isolate (WPI) and β-lactoglobulin nanoparticles around 100nm with desolvation method using ethanol. On the other hand, in Chapter three, when entrapping resveratrol, there was a proposal that ethanol was used to dissolving the resveratrol (details were discussed in Chapter Five). Therefore, it is interesting to study the effect of ethanol on the β-lactoglobulin nanoparticle. Meanwhile, centrifugation is a common step in food processing for solids separation from the liquid. Some of the studies use high-speed centrifugation to separate encapsulated bioactives from free bioactives to determine the encapsulation efficiency of nanoparticles product

(Gülserena et al., 2012; Pujara et al., 2017; Patricia Zimet & Yoav D. Livney, 2009). In detail, the free bioactives floated in the supernatant after centrifugation, and the particles (pellet) sedimented at the bottom with entrapped bioactives. Thus it is interesting to investigate the influence of centrifugation on the nanoparticles. Also, freeze drying is a common approach to extend the shelf life of the product by reducing the moisture content, and it is especially applied to heat sensitive bioactives.

Moreover, whey protein is more economical than pure β-lactoglobulin to produce nanoparticles and more convenient to use particularly for industrial applications. , As β-lactoglobulin is the main protein in whey (about 50% of total protein in whey). Here the method applied for β-lactoglobulin is applied to produce whey protein nanoparticles.

The aim of this chapter is, as an extension of the studies presented in chapters two and three, to explore the effects of ethanol, centrifugation and freeze drying on the stability of β-lactoglobulin nanoparticles and to examine the feasibility of applying the method developed for β-lactoglobulin to produce whey protein nanoparticles.

4.2. Materials and methods

4.2.1. Materials

β-Lactoglobulin from bovine milk ≥85% (PAGE), lyophilized powder L2506 is purchased from Sigma

Ethanol absolute, ≥99.8% (GC) (32221-M) is purchased from Sigma

Bicinchoninic Acid solution (B9643-1L) and Copper sulphate solution (C2284) are

purchased from Sigma

4.2.2. The effect of ethanol on nanoparticles

The β-Lg nanoparticles were prepared following the method 2.2.1 at pH 6.0 with different concentration of ethanol ranged from 0%, 7%, 14%, and 28%. The particle size was measured by Dynamic light scattering (Malvern Instruments Inc., Malvern, United Kingdom) at room temperature. The measurement was determined by considering the refractive index of β-Lg as 1.45, and that of the dispersant medium (deionised water) as 1.33 and the refractive index of ethanol was 1.34-1.35 based on the value from Belda, Herraez, and Diez (2005), Refractometer.pl (2017). Zeta potential was measured by measured by Zetasizer Nano Z in Electrophoretic Light Scattering mode (Malvern Instruments Inc., Malvern, United Kingdom). A folded capillary cell (DTS1070) was used to measure the zeta potential. The cell was washed with Ethanol and Deionised water before each measurement.

4.2.3. The effect of centrifugation on nanoparticles.

The β-Lg nanoparticles were prepared following the method 2.2.1 at pH 6.0. The samples were centrifuged at 863*g* (2000rpm), 5400*g* (5000rpm) with Heraus Multifuge 3SR+ centrifugation machine (Thermo Scientific, Waltham, USA) and 9788*g* (9600rpm) with MiniSpin (Eppendorf). After centrifugation, the supernatant was taken to carry out the Bicinchoninic acid assay to measure the total protein concentration, and the size of the supernatant was measured by DLS. Briefly, 0.1 ml of the sample was added to 2 ml of BCA working reagent (bicinchoninic acid and copper (II) sulphate pentahydrate),

followed by incubation at 37°C for 30 min. The reaction solution was measured at 562 nm in an Ultrospec ® 1100 PRO UV-vis spectrophotometer (United Kingdom), and a calibration curve was established using β-Lg nanoparticles ranged from 0-1000 μg/ml. A β-Lg nanoparticles sample without centrifugation was used as the control group.

4.2.4. The effect of freeze drying on particle size

The β-Lg nanoparticles were prepared by the method mentioned at 2.2.1 at pH 6.0. Then, 3ml of the sample was transferred to 7 ml Sterile container and covered with lab tissue paper, which was fastened by tape. Then, the container was put into Freeze Dryer (VirTis SP Scientific Sentry 2.0) and samples were freeze drying for three days. Then, the samples were resuspended in the same volume of deionized water and the particle size of both nanoparticles and redissolving samples were measured by DLS

4.2.5. Whey protein nanoparticle preparation

4.2.5.1. Preparation of sweet whey

Sweet whey was prepared by the modified method described in Welderufael, Gibson, and Jauregi (2012). Pasteurised skimmed milk was purchased from the local Tesco shop and heated in a water bath (Grant Instrument Ltd., Cambridge, United Kingdom) at 37^{O}C. Then commercial rennet was added at the concentration of 0.3mL/L into 500ml of milk sample with 2mins stirring. The milk was incubated for 60mins, and then the casein coagulum was cut vertically (25 X 25 mm) by a knife and then, incubation was allowed to prolong for 20 min after which the whey was collected from the vessel and filtered

using cheese cloth. Then whey solution was transferred into 50ml Falcon tube and carried out centrifugation at 2212*g* (3200rpm) for 30 min, using a Heraus Multifuge 3SR+ centrifuge (Thermo Scientific, Waltham, USA). Additionally, the sweet whey was filtered using microfiltration syringe membrane of 0.45µm pore size to remove any remaining casein curds. The collected whey was stored at -20^{o}C until used for further experiments.

4.2.5.2. Protein concentration determination of sweet whey

Protein concentration in sweet whey was determined by bicinchoninic acid method (BCA) based on the method **2.2.4**. For protein samples with unknown concentration, the selected dilutions (10-fold, 20-fold, and 50-fold dilution) of sweet whey were prepared to ensure the concentration was within the linear range of 200-1000µg/ml. Experiments were performed in triplicates.

4.2.5.3 Sweet whey nanoparticle and its particle size measurement

After determination of protein content in sweet whey, solutions with different protein concentrations (% w/v) were prepared; 0.2, 0.3, 0.5, and 1.0 % w/v. 200ppm Sodium azide (200ppm) was added to stock whey solutions to prevent microbial growth, and the solutions were stored at fridge (4^{o}C). Then, the method described in 2.2.1 for production of β-Lg nanoparticles was applied to produce the whey protein nanoparticles, and the particle size was measured by the DLS method (refer to the section). All experiments were carried out in triplicate. The yield of whey protein aggregation was determined by separating the denatured whey nanoparticles from native whey using centrifugal ultrafiltration Vivaspin® 20 (Sartorius Stedim Biotech, Germany) with 50kDa weight cut-

off PES (Polyethersulfone) membrane. To quantify the amount of native and aggregated whey protein, 5ml of the whey nanoparticles solution was centrifuged at 863*g* (Heraus Multifuge 3SR+ centrifuge, Thermo Scientific, Waltham, USA) for 15 minutes to separate the nanoparticles and native proteins. The retentate and permeate volumes were determined by weight, and the protein concentration in permeate was determined by BCA method in **2.2.4.** The percentage of protein aggregated was determined by measuring the total protein in permeate and by applying a mass balance of protein as shown in Eq. (1):

$$\boldsymbol{Yield\ of\ whey\ nanoparticle}\% = \frac{\textbf{Protein mass in feed} - \textbf{Protein mass in permeate}}{\textbf{Protein mass in feed}} \quad \textbf{(1)}$$

4.3. Results and discussion

4.3.1. The effect of ethanol on nanoparticles

Compared with water, ethanol was far less polar, and when adding ethanol, the hydrogen-bonded water molecule will be replaced by the hydrogen-bonded ethanol in the protein-solvent interaction. Moreover, the tertiary and secondary structure of the protein has changed reversibly (Dufour, Bertrand-Harb, & Haertle´, 1993; Mousavi et al., 2008). As shown in Figure 4.1, a clear increase in particle size with ethanol concentration was observed; on the contrary, the polydispersion index (PDI) reduced (0.1-0.063). On the other hand, the zeta potential of nanoparticles decreased dramatically with the addition of ethanol, as expected, which indicated that ethanol reduced the charge of protein and electrostatic repulsion among β-Lg and this possibly promoted further aggregation of protein into larger particles. According to Bhattacharjee (2016),

guidelines classifying nanoparticle-dispersions with zeta-potential values of ± 0–10 mV, ± 10–20 mV, ± 20–30 mV and > ± 30 mV as highly unstable, relatively stable, moderately stable and highly stable, respectively. Therefore, adding ethanol resulted in changes in stability of nanoparticles from highly stable with zeta potential -41.3mV to relatively stable with zeta potential -18.8 mV. According to Gulseren et al. (2012) and Gülserena et al. (2012), they produced whey protein nanoparticles around 100nm by ethanol desolvation method with a further dilution to achieve low ethanol concentration (around 1%). However, they still found that these nanoparticles at neutral or alkaline pH had low stability, and acidification to pH 3 was necessary to maintain the size of particles. It might indicate that ethanol desolvation was not able to stabilise of the dispersion.

In summary, adding ethanol resulted in a reduction of zeta potential, thus, the charge of particles and led to the occurrence of large particles.

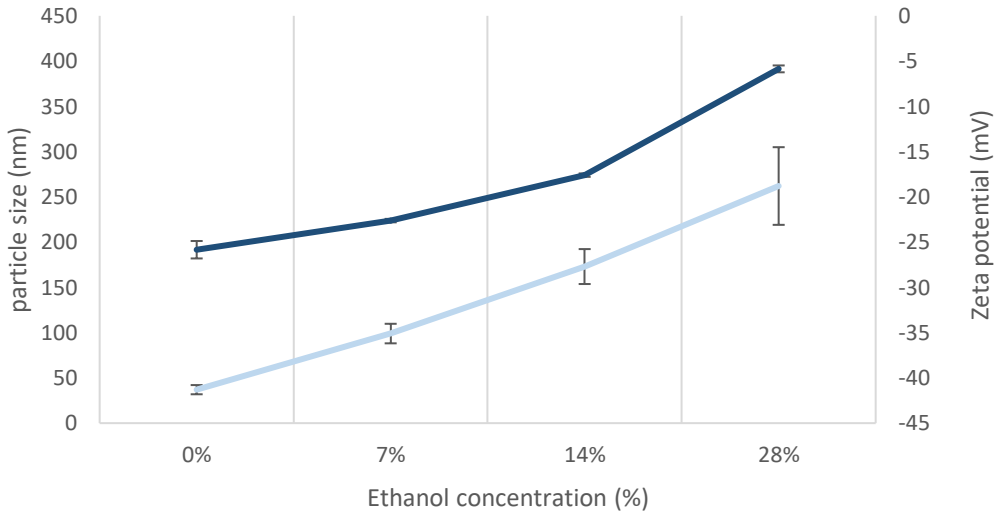

Figure 4.1: The particle size and zeta potential of ß-Lg nanoparticles with different concentration of ethanol (0-28%).(Dark blue represents the particle size and light blue represents zeta potential)

4.3.2. The effect of centrifugation on nanoparticles

The influence of centrifugation on nanoparticles was assessed by the protein concentration of the supernatant and particle size supernatant. According to Table 4.1, there was a slight reduction in protein concentration in the supernatant of samples centrifuged at 863*g* and none-centrifuged, while little protein remained in the supernatant after centrifuging at 9788*g*, which revealed that sedimentation of the nanoparticles happened due to the centrifugal force that disrupted the colloidal stability. Figure 4.2 demonstrated the effect of centrifugation on the particle size. There was no significant difference in particle size of nanoparticles in supernatant before and after centrifugation at 863*g*. At 5400*g* and 9788*g*, the particle size reduced dramatically (190.6 nm and 131.7 nm, respectively) which was in agreement with the decrease in protein in the supernatant of these samples. Based on these results centrifugal speed 863g was chosen as on optimum centrifugal force in terms of colloidal stability of the nanoparticles. This was an important finding as if high speed of centrifugation was applied, the colloidal stability of particles would be disrupted and would also lead to a reduction in encapsulation efficiency.

Table 4.1: The results of protein concentration in the centrifugated supernatant by BCA method.

	UV [562nm]	% of absorbance of none-centrifugation samples
None-centrifugation nanoparticles	0.825±0.018[a]	100.00
863g (2000 rpm)	0.763±0.008[b]	92.54±0.96
5400g (5000 rpm)	0.327±0.006[c]	39.60±0.08
9788g (9600 rpm)	0.028±0.001[d]	3.40±0.10

Data were expressed as mean ± standard deviation for triplicate tests. Different superscripts in the same column indicate significant differences at P<0.05

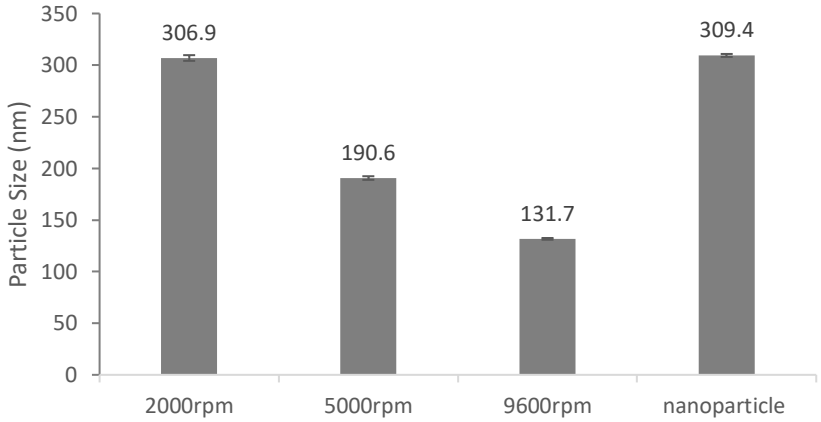

Figure 4.2: The particle size of samples after different speed centrifugation.

4.3.3. The effect of freeze drying on the nanoparticles

As the moisture content was eliminated during freezing drying, the ice formation led to oppression of particles away from frozen areas, thus, increasing the particle concentration and inducing a large particles agglomeration (Deville, Saiz, Nalla, & Tomsia, 2006). Interestingly, when the effect of freeze drying on the particle size was assessed by comparing the particle size of freeze dried nanoparticles that had been resuspended

and freshly made nanoparticles no significant differences were observed, only a slight increase of the PDI. (Fig 4.3). Vries, Gomez, Jansen, Linden, and Scholten (2017) produced whey protein nanoparticles of around 150 nm by heating at 85 °C for 15 min at pH 5.7. A homogenization step was induced to break the weak gel into small aggregates in their work. They also found that freeze drying did not affect the particle size and therefore it was applied in order to eliminate moisture from the nanoparticles.

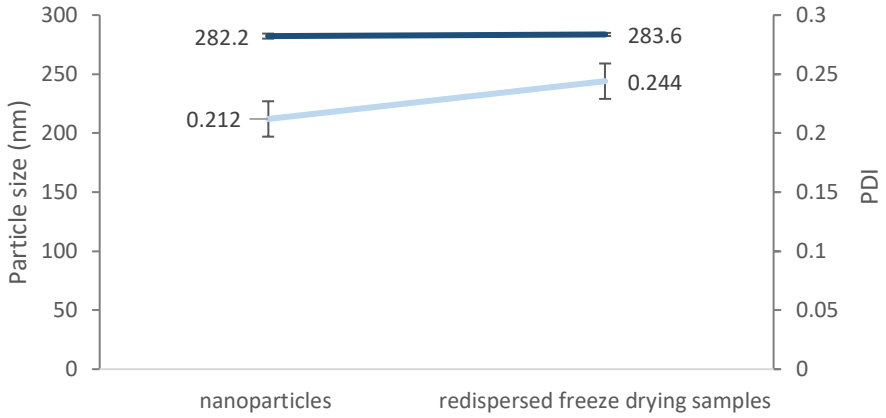

Figure 4.3: The particle size of nanoparticles and redispersed freeze drying samples. (Dark blue represents the particle size and light blue represents PDI)

4.3.4. Whey protein nanoparticles

Compared with β-Lg, it is more economical and practical to use whey proteins to produce nanoparticles. In this work, sweet whey was used to generate nanoparticles. The protein concentration in sweet whey was determined as 11.0mg/ml (1.1% w/v), which corresponds to the value given by Boland (2011). The size of whey nanoparticles increased with the concentration of protein in samples. Interestingly, the particles size of the 0.2% w/v whey was around 150 nm, which was smaller than the β-Lg

nanoparticles at the same protein concentration. The size of 0.5% w/v whey samples was close to the size obtained with 0.2% w/v β-Lg. β-Lg is around 50% of total protein in whey. Thus, these results might indicate that β-Lg concentration in whey protein might have the main influence on the particle size and characteristics. Surprisingly, the PDI of 1%w/v whey protein nanoparticles increased to 0.69, and a bimodal size distribution occurred, indicating nonuniformity of particle size and existence of larger aggregates exceeding the nanometer scale. Moreover, the unheated whey protein showed particle size above 100nm, which was not observed with native β-Lg (below 10 nm as a dimer). In sweet whey, some large proteins like Immunoglobulin G (150kDa) existed, and possibly oligomers of large proteins may be formed during the sweet whey processing *(*heating at 37°C). Sats et al. (2014) also found the particles over 100nm with high PDI in bovine colostrum whey, which contained more Immunoglobulin G. This might reflect that an ultrafiltration with proper molecule weight cut off membrane was necessary to eliminate the large whey proteins before the nanoparticle preparation.

Table 4.2: Effect of protein concentration on the size of whey nanoparticles (Heat load, 75^{o}C 45mins; pH, 6)

Protein concentration (%w/v)	Particle size (nm)	Polydispersity	Yield of whey protein nanoparticle (%)
0.2	150.85 ± 1.21^{d}	0.18±0.02^{b}	72.75±1.38% ^{a}
0.3	170.20 ± 3.69^{c}	0.15±0.01^{b}	74.33±2.96% ^{a}
0.5	231.07 ± 11.68^{b}	0.18±0.02^{b}	80.52±1.74% ^{b}
1	351.90 ± 14.34^{a}	0.69±0.17^{a}	84.66±2.17% ^{c}

Data were expressed as mean ± standard deviation for triplicate tests. Different superscripts in the same column indicate significant differences at P<0.05

Moreover, the yield of whey protein nanoparticle was calculated according to equation (1) (Table .4.2). It increased corresponding to protein concentration, but even the highest yield (85%) obtained at the highest concentration (1 mg/ml), it was still lower than the yield obtained with β-lactoglobulin nanoparticles (93%). This suggested that some of the whey protein did not contribute to the nanoparticle formation. Moreover, according to Ramos et al. (2017), there are complex protein-protein interactions, for example, the interaction between β-Lg and α-La. Therefore, the predominant interactions/forces to establish the three-dimensional network of the whey nanoparticles should be investigated.

4.4. Conclusions

In this chapter, the stability of β-Lg nanoparticles was investigated under several processing conditions. Adding ethanol reduced the zeta-potential of nanoparticles and led to large aggregates. Centrifugation at high speed resulted in sedimentation of nanoparticles and reduction of protein concentration in supernatant. Surprisingly, redispersion of freeze-dried samples had no significant effect on particle size. Lastly, whey protein nanoparticles were successfully produced with size in the range of 150 to 350nm by applying the same method as that developed for β-Lg nanoparticles. However, the aggregation yield was lower for whey (maximum obtained was 85%) than with β-Lg (93%). Nevertheless, these results were promising and showed that particles of similar size can be obtained starting from whey, which is cheaper and more practical to use for industrial applications. Further studies need to be carried out to explore proteins

involved in the nanostructure of whey protein nanoparticles and characterization of these nanoparticles should be considered in terms of stability, storage and other food processing conditions.

References

Belda, R., Herraez, J. V., & Diez, O. (2005). A study of the refractive index and surface

tension synergy of the binary water/ethanol: influence of concentration. *Physics and Chemistry of Liquids, 43*(1), 91-101.

Bhattacharjee, S. (2016). DLS and zeta potential – What they are and what they are not? *Journal of controlled release, 235*(2016), 337-351.

Boland, M. (2011). Whey proteins. In G. O. Phillips & P. A. Williams (Eds.), *Handbook of Food Proteins* (pp. 30-55). Oxford Cambridge Philadelphia New Delhi: Woodhead Publishing Limited.

Deville, S., Saiz, E., Nalla, R. K., & Tomsia, A. P. (2006). Freezing as a Path to Build Complex Composites. *Science, 311*(5760), 515-518.

Dufour, E., Bertrand-Harb, C., & Haertle´, T. (1993). Reversible effects of medium dielectric constant on structural transformation of ß-Lg and its retinol binding. *Biopolymer, 33*(4), 589-598.

FDA. (2017a). Agency Response Letter GRAS Notice No. GRN 000371. Retrieved from https://www.fda.gov/Food/IngredientsPackagingLabeling/GRAS/NoticeInventory/ucm267323.htm

FDA. (2017b). Food Additive Status List-Ethyl Alcohol (Ethanol). Retrieved from https://www.fda.gov/food/ingredientspackaginglabeling/foodadditivesingredients/ucm091048.htm#ftnE

FDA. (2017c). GRAS Notification for Ethanol. Retrieved from https://www.fda.gov/downloads/Food/IngredientsPackagingLabeling/GRAS/No

ticeInventory/ucm268080.pdf

Gulseren, I., Fang, Y., & Corredig, M. (2012). Whey protein nanoparticles prepared with desolvation with ethanol: characterisation, thermal stability and interfacial behavior. *Food Hydrocolloids, 29*, 258-264.

Gülserena, İ., Fang, Y., & Corredig, M. (2012). Zinc incorporation capacity of whey protein nanoparticles prepared with desolvation with ethanol. *Food Chemistry, 135*(2), 770-774.

Mousavi, S. H.-A., Chobert, J.-M., Bordbar, A.-K., & Haertle, T. (2008). Ethanol Effect on the Structure of ß-Lactoglobulin B and Its Ligand Binding. *Journal of Agricultural and Food Chemistry, 56*(18), 8680-8684.

Pujara, N., Jambhrunkar, S., Wong, K. Y., McGuckin, M., & Popat, A. (2017). Enhanced colloidal stability, solubility and rapid dissolution of resveratrol by nanocomplexation with soy protein isolate. *Journal of Colloid and Interface Science, 488*(2017), 303-308.

Ramos, O. L., Pereira, R. N., Martins, A., Rodrigues, R., Fucinos, C., Teixeira, J. A., . . . Vicente, A. A. (2017). Design of whey protein nanostructures for incorporation and release of nutraceutical compounds in food. *Food science and nutrition, 57*(7), 1377-1393.

Refractometer.pl. (2017). Refractive index of ethanol solutions Retrieved from http://www.refractometer.pl/refraction-datasheet-ethanol

Sats, A., Mootse, H., Pajumägi, S., Pisponen, A., Tatar, V., & Poikalainen, V. (2014). Estimation of Particle Size Distribution in Bovine Colostrum Whey by Dynamic

Light Scattering (DLS) Method. *Agronomy Research, 12*(3), 801-806.

Vries, A. d., Gomez, Y. L., Jansen, B., Linden, E. v. d., & Scholten, E. (2017). Controlling Agglomeration of Protein Aggregates for Structure Formation in Liquid Oil: A Sticky Business. *ACS applied materials & interfaces2017, 9*(11), 10136-10147.

Welderufael, F. T., Gibson, T., & Jauregi, P. (2012). Production of Angiotensin-I-Converting Enzyme Inhibitory Peptides from ß-Lactoglobulin- and Casein-Derived Peptides: An Integrative Approach. *Biotechnology progress, 28*(3), 746-755.

Zimet, P., & Livney, Y. D. (2009). Beta-lactoglobulin and its nanocomplexes with pectin as vehicles for u-3 polyunsaturated fatty acids. *Food Hydrocolloids, 23*(4), 1120-1126.

CHAPTER FIVE

Conclusions and future works

5.1. Conclusions

The emerging trend of novel delivery systems of bioactive compounds has already attracted extensive attention from the scientific community. In the present work, the aim was to explore if it was feasible to produce nanostructures from β-Lg in a consistent and reproducible manner by a simple heat-induced denaturation method. In particular, it was interesting to investigate if β-Lg nanoparticles play an effective role in bioactives encapsulation. On the other hand, it was worth studying if similar type of nanoparticles could be produced by the same method using whey.

In the first part of the study, the main achievement was that β-Lg nanoparticles were produced by the heat-induced denaturation method at optimum conditions of pH (6.0) and heat load (heating at 75 °C for 45 mins), which were found to be key operating parameters (Chapter 2). Nanoparticles were around 200-300 nm with a monodisperse size distribution and with colloidal stability (this was due to their high negative charge as measured by zeta potential -37.42mV). High yield (93%) of aggregation of β-Lg was achieved. An improved insight of their formation was obtained where the main forces responsible for the protein aggregation and stabilisation of the nanoparticles were hydrogen bonding and hydrophobic interactions based on their lack of stability to urea and SDS, respectively. The exposure of buried hydrophobic parts of the protein upon unfolding of β-Lg due to heat denaturation was confirmed by the fluorescence

measurements. Consequently, all these results show that a robust and reproducible method was successfully developed to produce β-Lg nanoparticles by a simple heat-induced denaturation method. Compared with the desolvation method which uses organic solvents, our method only needed pH adjustment and heat denaturation, which met the GRAS requirements. This facile method provides an innovative approach that can be applied to food products and has potential to be developed at industrial scale.

In order to study the applicability of these nanoparticles to food bioactives, the encapsulation of the amphiphilic alkaloid caffeine was investigated (chapter 2). Caffeine-loaded β-Lg nanoparticles (~350 nm) were significantly larger than the nanoparticles only, and maximum encapsulation efficiency was 13.54% at 50:1 caffeine to β-Lg molar ratio. The binding of caffeine to protein (both of native β-Lg and heat denatured β-Lg) followed a Langmuir type isotherm. Heating of β-Lg unfolded the previously buried and more hydrophobic parts of the protein which led to more binding of caffeine. β-Lg nanoparticles exhibited a rapid peptic degradation at SGF conditions as shown by a dramatic particle size reduction, however, limited release of caffeine (36.4%) was observed, which suggested that binding of caffeine was not dependent on the microstructure but relied mainly on interactions with the unfolded protein. The full release of caffeine happened after the small intestinal digestion phase. These findings suggested the potential capacity of β-Lg nanoparticles for the encapsulation of bioactives and their enteric release.

Moreover, another application of the β-Lg nanoparticles focused on Resveratrol (Chapter 3) because of its remarkable health-benefit properties including antioxidant, anti-cancer,

anti-inflammatory, and antineoplastic (Bhat & Pezzuto, 2002; Catalgol et al., 2012; Filipa et al., 2003). At the same time, there was a potential cooperation opportunity and funding from Evolva; they needed to explore a solution to increase the resveratrol solubility in water from 3mg/100ml to 3mg/ml. It seemed to be difficult to achieve this target without adding some organic solvent. However, the influence on the structure and binding properties of β-Lg were unclear and different depending on the types of solvents. Therefore, β-Lg nanoparticles were applied to encapsulate the resveratrol without adding organic solvent first. The solubility of resveratrol was firstly determined by total phenolic content at between 5mg/100ml-7mg/10ml and resveratrol was not stable to light but exhibited a higher phenolic content and total antioxidant capacity after 12 hours light exposure at room temperature. There was an obvious thermal degradation happening when heating at 75°C since the loss of antioxidant capacity occurred as determined by both ABTS and Frap methods. Isomerization of trans-resveratrol to cis-resveratrol might happen under these conditions. A protective function of β-Lg on the antioxidative properties of resveratrol was observed during heat degradation, and resveratrol-β-Lg nanocomplexes exhibited a higher total antioxidant activity than the control (resveratrol only), even though the binding of resveratrol by β-Lg nanoparticles was lower than native β-Lg. M. Li, Ma, and Ngadi (2013) also reported an improved antioxidant activity upon binding of curcumin to β-Lg. However, the fluorescence measurements demonstrated a clear interaction between these two molecules, but surprisingly, the RFI indicated that the binding between native β-Lg and resveratrol (22.87%) was stronger than resveratrol-β-Lg nanocomplexes (46.67%). This was

opposite to what was observed for caffeine binding. Moreover, interestingly, Shpigelman et al. (2010b) claimed a higher association of pre-heated β-Lg with Epigallocatechin-3-gallate (EGCG) than native, while Perez et al. (2014) reported no significant differences in binding linoleic acid between native and heat-induced β-Lg aggregates. Also, Shpigelman, Shoham, Israeli-Lev, and Livney (2014) found that β-Lg-naringenin complexes exhibited no significant effect on the binding stoichiometry and no impact on the efficacy of crystallisation suppression of naringenin. Therefore, it seems that β-Lg and β-Lg nanoparticles exhibited different binding ability with different ligands, and this might relate to binding sites, and the way ligands interacted with proteins. Also, binding of resveratrol to native β-Lg followed a Stern-Volmer model with binding constant $1.67x10^{5,}$ and the binding number is 1.33 but no model was found to fit resveratrol-β-Lg nanoparticles. On the other hand, both resveratrol-native β-Lg and resveratrol-β-Lg nanocomplexes expressed higher antioxidant activity under Pasteurization conditions compared to resveratrol standard.

Lastly, the stability of β-Lg nanoparticles was examined under different laboratory processes and conditions (chapter 4), which might relate to the further study of industry applications. Linked with resveratrol study, ethanol was tested as a possible solvent to improve resveratrol's solubility. The addition of ethanol led to larger aggregates and reduction of the charge of particles (zeta-potential). Application of high-speed centrifugation resulted in the sedimentation of nanoparticles and loss of protein concentration in supernatant. Moreover, it was found that there was no difference in the particle size of resuspended freeze dried samples and freshly prepared samples.

Meanwhile, whey nanoparticles were produced by the same method developed for β-Lg using sweet whey made from skimmed milk. The size of whey nanoparticles at 0.5% w/v protein concentration was similar to that obtained with 0.2% β-Lg (~250nm). Overall, in this study, it has been shown that a simple and robust heat-induced denaturation method has been developed to produce β-Lg nanoparticles and similar nanoparticles can be produced by whey. Nanoparticles were applied to encapsulate caffeine and resveratrol to form nanocomplexes with denatured β-Lg. It was highlighted that encapsulation of bioactives with β-Lg nanoparticles can result in their controlled release and can have a protective effect. These nanoparticles may find an application to improve delivery caffeine in the intestinal tract. In the case of resveratrol, potentially β-Lg can protect it from light and heat degradation, therefore can be used in the formulation of resveratrol during thermal processing or storage. To conclude, given the growing interest towards health promoting food products, the β-Lg/whey protein nanoparticles produced in this study contributed to a possible solution for food nanodelivery of nutraceuticals and has contributed with useful knowledge in the bioactive compounds protection. It is believed these β-Lg/whey protein nanoparticles have the potential for applications in food products with health benefits.

5.2. Limitations of the current study and suggestions for further work

In this work, a robust and reproducible method to produced β-Lg nanoparticles was developed, and it was applied to caffeine and resveratrol encapsulation. Indeed, some limitations existed in this study, and further research can be carried out. The section below mainly discussed the limitations of this work and suggestions for future work.

The size of β-Lg nanoparticle was 200nm-300nm, which was larger than nanoparticles produced by desolvation method (around 100nm) (Gulseren et al., 2012; S. Ko & S. Gunasekaran, 2006). In the beginning, the target was around or below 100nm to meet the strict definition of nano size (0-100nm). However, nanoparticles produced at pH 6.3 or above showed low reproducibility, even though the size was smaller and within the nano range. Sometimes, a bimodal distribution was obtained with high PDI (>0.3) (Figure 5.1) and sometimes no nanoparticles above 10nm were obtained. It might indicate that the intermolecular interactions among β-Lg molecules were not sufficient to form 100nm nanoparticles. Some approaches were applied, for example, adding different ions to change the ionic strength and change the net charge of protein to promote interactions or cross-linking between ions and protein molecules. Some divalent ions (Calcium and magnesium) induced aggregation via electrostatic interactions, ion/hydrophobic interactions and cross linking with negatively charged carboxylic groups of neighbouring protein molecules. Giroux et al. (2010) produced 100-200nm whey protein nanoparticles by adding 2.5mM Calcium using pH-cycling treatment method, and Phan-Xuan et al. (2014) achieved 100nm-400nm denser microgels in the presence of Ca^{2+} at neutral pH. However, it is also noted that adding ions may influence the binding

properties of the protein and this is ill-defined. Therefore it is interesting to carry out investigation the influence of ions in nanoparticles formation, size and binding properties.

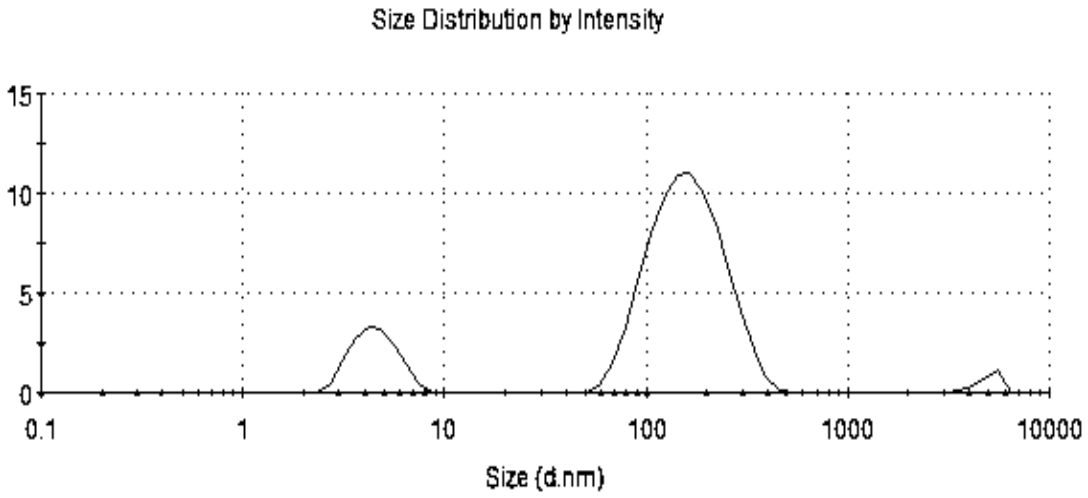

Figure 5.1: An example of the multi-size distribution of 0.2%w/v β-Lg solution at pH 7.5 for 75°C for 45mins.

On the other hand, the nanoparticles produced in the present study were mainly stabilised by hydrogen bonding and hydrophobic interactions, not by the disulphide bonds. This is mainly due to the acidic conditions and the low protein concentration used in the method developed here. Therefore, it might be the reason why rapid particle degradation and high burst effect of caffeine release in simulated gastric fluid was found. Meanwhile, even though the maximum encapsulation efficiency (13.54%) was relatively low, a sensory experiment could be conducted to examine the masking of bitterness by encapsulation of caffeine. The caffeine has a detection threshold at 1.2Mm, and there was a specific concentration (6 mM), where bitter taste can be perceived and could be differentiated (Keast & Roper, 2007). Based on this concentration, the masking function of encapsulation could be investigated; it is worth noting that the ethical assessment

would need to be conducted carefully as the overdosage of caffeine could lead to poisoning.

In the resveratrol encapsulation study, the resveratrol could not be quantified by high-performance liquid chromatography due to the filtration limitation. Thus, the separation of free resveratrol and bound resveratrol could not be achieved, and the encapsulation efficiency could not be determined. In fact, there was a proposal to carry out encapsulation by dissolving resveratrol in ethanol since resveratrol could be filtered in ethanol. However, there was a concern that adding ethanol would lead to solubilisation of resveratrol in ethanol predominantly, which would hinder its encapsulation or complexation with β-Lg. Moreover, free resveratrol in 28% v/v ethanol/water solution had low permeability through ultrafiltration membrane (50KDa MWCO, Vivaspin® 20, Sartorius Stedim Biotech, Germany). Another idea was after dissolving resveratrol in ethanol and making nanoparticles, an evaporation step was applied to eliminate ethanol. However, even heating at 75°C for two hours, only limited ethanol was evaporated. Pujara et al. (2017) proposed that using reduced pressure in a rotary evaporator could eliminate ethanol. Nevertheless, β-Lg nanoparticles proved to have a protective function on the antioxidant activity of resveratrol under pasteurisation, and it might be helpful in improving the bioavailability of resveratrol. On the other hand, Circular dichroism spectra can be investigated to characterise the secondary structure of proteins due to the peptide bond absorption.

Lastly, whey protein nanoparticles were produced by our method and even a smaller particles size than β-Lg nanoparticles at the same protein concentration achieved.

Further characterization needs to be conducted to explore the predominant interaction to form the nanoparticles. Also, the yield of whey protein nanoparticle (72%-85%, depending on protein concentration) was relatively low compared with pure β-Lg nanoparticles (over 90%). An ultrafiltration step was suggested to be applied to eliminate the larger proteins from the whey and proteins which did not form the nanoparticles. Some encapsulation experiments like caffeine and resveratrol could be carried out with whey protein nanoparticles to make a comparison between β-Lg/whey protein nanoparticles.

References

Bhat, K. P. L., & Pezzuto, J. M. (2002). Cancer Chemopreventive Activity of Resveratrol. *Annals of the New York Academy of Sciences, 957*, 210-229.

Catalgol, B., Batirel, S., Taga, Y., & Ozer, N. K. (2012). Resveratrol: French paradox revisited. *Front Pharmacol, 3*(141), 1-18.

Filipa, V., Plockováa, M., Šmidrkala, J., Špičkováa, Z., Melzochb, K., & Schmidtc, Š. (2003). Resveratrol and its antioxidant and antimicrobial effectiveness. *Food Chemistry, 83*(4), 585-593.

Giroux, H. J., Houde, J., & Britten, M. (2010). Preparation of nanoparticles from denatured whey protein by pH-cycling treatment. *Food Hydrocolloids, 24*(4), 341-346.

Gulseren, I., Fang, Y., & Corredig, M. (2012). Whey protein nanoparticles prepared with desolvation with ethanol: characterisation, thermal stability and interfacial behavior. *Food Hydrocolloids, 29*, 258-264.

Keast, R. S. J., & Roper, J. (2007). A Complex Relationship among Chemical Concentration, Detection Threshold, and Suprathreshold Intensity of Bitter Compounds. *Chemical Senses, 32*(3), 245-253.

Ko, S., & Gunasekaran, S. (2006). Preparation of sub-100-nm ß-lactoglobulin (BLG) nanoparticles. *Journal of Microencapsulation, 23*, 887-898.

Li, M., Ma, Y., & Ngadi, M. O. (2013). Binding of curcumin to ß-lactoglobulin and its effect on antioxidant characteristics of curcumin. *Food Chemistry, 141*(2013), 1504-1511.

Perez, A. A., Andermatten, R. B., Rubiolo, A. C., & Santiago, L. G. (2014). ß-Lactoglobulin heat-induced aggregates as carriers of polyunsaturated fatty acids. *Food Chemistry, 158*(2014), 66-72.

Phan-Xuan, T., Durand, D., Nicolai, T., Donato, L., Schmitt, C., & Bovetto, L. (2014). Heat induced formation of beta-lactoglobulin microgels driven by addition of calcium ions. *Food Hydrocolloids, 34*, 227-235.

Pujara, N., Jambhrunkar, S., Wong, K. Y., McGuckin, M., & Popat, A. (2017). Enhanced colloidal stability, solubility and rapid dissolution of resveratrol by nanocomplexation with soy protein isolate. *Journal of Colloid and Interface Science, 488*(2017), 303-308.

Shpigelman, A., Israeli, G., & Livney, Y. D. (2010). Thermally-induced proteinepolyphenol co–assemblies: Beta-lactoglobulin based nanocomplexes as protective nanovehicles for EGCG. *Food Hydrocolloids, 24*, 735-743.

Shpigelman, A., Shoham, Y., Israeli-Lev, G., & Livney, Y. D. (2014). ß-Lactoglobulinenaringenin complexes: Nano-vehicles for thedelivery of a hydrophobic nutraceutical. *Food Hydrocolloids, 40*(2014), 214-224.